NASA Technical Memorandum 78668

AN INTRODUCTION TO SHUTTLE/LDEF
RETRIEVAL OPERATIONS: THE R-BAR
APPROACH OPTION

William M. Hall

·February 1978

TABLE OF CONTENTS

List of Figures

List of Figures (Cont'd)

List of Tables

Unit Conversion Table

The following table may be used to convert from the U.S. Customary
Units used in this report to the International System of Units (SI).

To convert from	to	multiply by
foot	meter	0.3048
inch	meter	0.0254
lbf (pound force, avoirdupois)	newton	4.4482
lbm (pound mass, avoirdupois)	kilogram	0.45359
foot/second^2	meter/second^2	0.3048
nautical mile (U.S.)	meter	1852
foot/second	meter/second	0.3048
degree (angle)	radian	0.017453

1.0 Introduction

The task of rendezvousing and station keeping with another orbiting body has never been simple. Nevertheless, considerable experience has been derived from the Gemini and Apollo programs. The scenario of systematic maneuvers has become somewhat standardized over the years.

In the final phase of a Gemini/Apollo rendezvous, the TPI (Terminal Phase Initiation) burn placed the chase vehicle on a collision course with the target vehicle. High rates of closure (approximately 30 feet per second at one mile) were utilized in order to minimize navigational dispersions. An orderly line of sight braking schedule provided a range rate gradient of approximately 5 feet per second per 1000 feet (See Figure 1-1.)

The final 5 fps of closing range rate was not scheduled to be dissipated until the station keeping range, R_S, was achieved. R_S was less than 100 feet. During the entire braking sequence the target vehicle suffered plume impingement from the chase vehicle's jets. The impingement imparted momentum to the target vehicle and contaminated its surfaces with exhaust products. Impingement consequences were not significant for two reasons: first, the target vehicle was not especially sensitive to contamination; and second, the imparted momentum, rotational and translational, caused minor perturbations of the target vehicle's motion To be sure, the ratio of the target vehicle mass to the chase vehicle mass was near unity; furthermore, the target vehicle usually had significant attitude control capability which could immediately dump any imparted angular momentum.

1

40

35

30

Maximum 25
Closing
Range Rate
(R̊),
ft./sec 20

15

10

5

0

0   0.5   1.0

R_s

Range (R), mi

0.08 mi (422 ft)
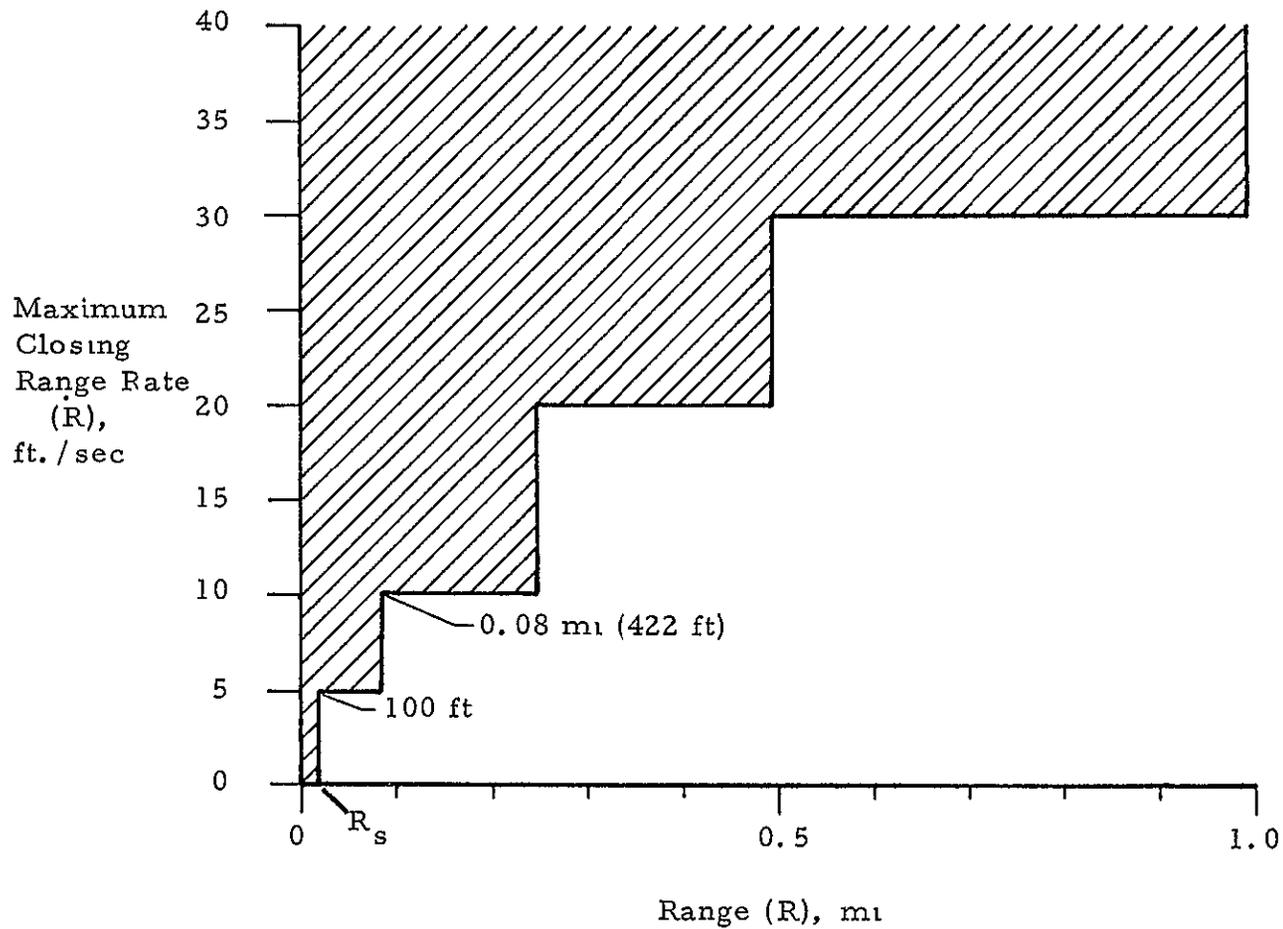
100 ft

R_S - Station Keeping Range ≈ 100 ft.

Figure 1-1.- Typical Apollo/Gemini Rendezvous Terminal Braking Schedule

With the advent of shuttle, the ratio of target vehicle mass to chase vehicle mass enters a new regime. In stark contrast to even the 18,000-pound LDEF, the Orbiter is essentially an order of magnitude heavier at approximately 180,000 pounds. Braking from 30 feet per second will require a significantly greater expulsion of thruster combustion products. Whether it is a long burn from small thrusters or shorter burns from larger thrusters, a large translational momentum must be dumped into thruster exhaust products.

Only a small percentage of the plume's momentum is transferred to the target vehicle. Nonetheless, simulations[1] have clearly demonstrated that if the Orbiter follows the direct approach used by Gemini/Apollo, the momentum transfer to the target vehicle can be significant. In the case of LDEF, for example, the sum of the magnitudes of the angular impulses imparted by the plume field exceeded 500 ft-lb-sec. (To place this into perspective, only 80 ft-lb-sec of net impulse about the LDEF pitch axis is capable of tumbling LDEF at 0.09° per second.) Although the vector sum of the imparted angular impulse could be considerably less, the vector sum is not a totally controllable parameter during an approach. Some simulated direct approaches, for example, caused the LDEF inertial rate to change as much as 0.3° per second. Yet, 0.1° per second relative to the Orbiter is thought to be the upper limit for grappling operations. A corollary to these findings is that the LDEF surfaces would suffer considerable contamination during a direct approach.

---

[1]Reference the PDRS III Shuttle Engineering Simulator Post Simulation Report, CG5-77-246, November 7, 1977.

All of this has precipitated a reassessment of the final approach strategy. One solution, which at this time appears to be very viable, is commonly known as the R-bar ($\bar{R}$) approach. To be sure, the $\bar{R}$ approach is but one of several proposals being developed and studied at JSC. But the $\bar{R}$ approach has one very distinguishing attribute – orbital mechanics forces are utilized to brake the final closing velocity as the target is approached. It is, therefore, theoretically possible to approach LDEF without any braking plume impingement.

Because the $\bar{R}$ approach is still in its infancy, descriptive documentation is sparse and scattered. The intent of this working paper is to give a general description of an LDEF rendezvous which incorporates the $\bar{R}$ approach.

For the uninitiated reader, plunging into a document on rendezvous operations can be a disaster. Terminology is foreign, orbital mechanics is foreign, and the pertinent aspects of the Orbiter system are foreign. To help alleviate this problem, Sections 2.0 through 7.0 are provided. First, a typical intercept trajectory is introduced in the familiar geocentric frame. Next, a new but very convenient coordinate system (the LVLH, or Local Vertical Local Horizontal Frame) is defined and used to show trajectory progress as the Orbiter nears LDEF. Third, the most relevant Orbiter cockpit instrumentation is introduced. Throughout these sections and the paper in general, an attempt is made to explain rendezvous operations in terms of pilot activity and the controls and instruments he uses.

4

Section 8.0, <u>Entering the Braking Schedule</u>, discusses how the pilot must dissipate his closing range rate before the resulting plume fields can significantly disturb LDEF. Then, sections 9.0, 10.0, and 11.0 explain the procedures for translating the Orbiter to a position below LDEF and setting up for the R-bar final approach.

Section 12.0, <u>The $\bar{R}$ Approach</u>, presents the most important aspects of Orbiter dynamics when operating along the LDEF radius vector. It is shown, for example, why orbital mechanics forces are always acting in a direction to drive the Orbiter away from LDEF or to decelerate the Orbiter during an approach to LDEF. In addition, equations are derived to describe Orbiter motion in the relative state domain of range rate versus range and in the time domains of range versus time and range rate versus time. Throughout the section, particular attention is given to providing physical explanations of the more useful and important equations of motion.

Section 13.0, <u>$\bar{R}$ Approach Sensitivity</u>, addresses an important reality of the $\bar{R}$ approach, namely, its exceptional sensitivity to Orbiter/LDEF relative state errors and/or imperfect Orbiter control. Respect for this characteristic is so important that the remainder of the paper is almost totally devoted to assessing state measurement errors and how they may be accommodated in a practical $\bar{R}$ approach strategy.

Section 14.0, <u>The Digital Auto Pilot</u>, explains how the Orbiter Attitude Control System (ACS) is configured to minimize plume impingement and provide fine ΔV control resolution during an $\bar{R}$ approach. Some

disadvantages of the approach configuration and the basic ACS design
are also presented.

Radar errors (which are introduced in Section 6.3) become unaccept-
able well before an $\bar{R}$ approach can be completed. The current solution
to the problem lies in using a COAS (Crewman Optical Alignment Sight)
from the Apollo Program. Sections 15.1 through 15.9 explain the errors
and limitations of this device in measuring the relative state of the
Orbiter with respect to LDEF. Perhaps to the surprise of many readers,
the design requirements for large painted targets on LDEF are developed
and optimized.

Section 16.0, Man-in-the-Loop Simulation Findings, gives a brief
overview of some important findings from simulated $\bar{R}$ approaches. It is
revealed, for example, that in spite of an apparent incompatibility of
state measurement errors with the $\bar{R}$ approach sensitivity, special
techniques have evolved which make the $\bar{R}$ approach workable. The
discovery of the aft payload bay television camera as a relative motion
sensor is shown to be especially fortuitous. Its use and limitations
are discussed in Section 17.0.

Finally, Section 18.0 coalesces $\bar{R}$ approach theory, state measure-
ment error analysis, and Orbiter control capability into a possible $\bar{R}$
approach strategy. A demonstration of the strategy in Section 19.0
reveals to the reader how imperfect state knowledge significantly
increases the approach time over that required for an optimal approach.
Then the use of Orbiter braking allowances near LDEF is shown to be a
trade-off between margin for state errors and reductions in approach time.

6

Although grappling operations per se are outside the scope of this paper, Section 20.0 provides an explanation of LDEF's dual grapple fixtures and station-keeping targets. The intent is to show that Orbiter attitude constraints during an $\bar{R}$ approach (a subject covered in Section 14.0) impact the LDEF design.

2.0 Pre-TPI (Terminal Phase Initiation) Maneuvers - After orbit insertion, the Orbiter, always behind and below LDEF, executes a series of maneuvers to catch up with and climb to LDEF. These maneuvers shape the Orbiter's orbit until it is essentially identical to the LDEF orbit but 10 nautical miles below it. They also adjust the phasing of the two orbits such that the proper TPI conditions (time and elevation angle) are achieved.

3.0 TPI - The TPI burn is the last burn performed with the 6000-pound-thrust OMS (Orbital Maneuvering System) rocket engines. The burn places the Orbiter on an intercept trajectory to LDEF. The TPI ΔV (typically 20 fps) is directed along the line of sight vector to LDEF and occurs when LDEF is at 27 degrees elevation with respect to the Orbiter local horizontal (See Figure 3-1).

The term "line of sight" in this case implies that the pilot is observing the LDEF during the burn. Indeed, if the lighting conditions were appropriate, the pilot could observe the LDEF through his front window since the Orbiter +X axis (body frame) would be pointed at LDEF during the burn. However, the TPI must be constrained to occur very close to the orbital midnight. This sophisticated task of timing that

7

LDEF

$\overline{V}$

$\overline{R}$

Line of Sight

-27°

Orbiter Local Horizontal

Δh = 10 n. mi

$\overline{R}$
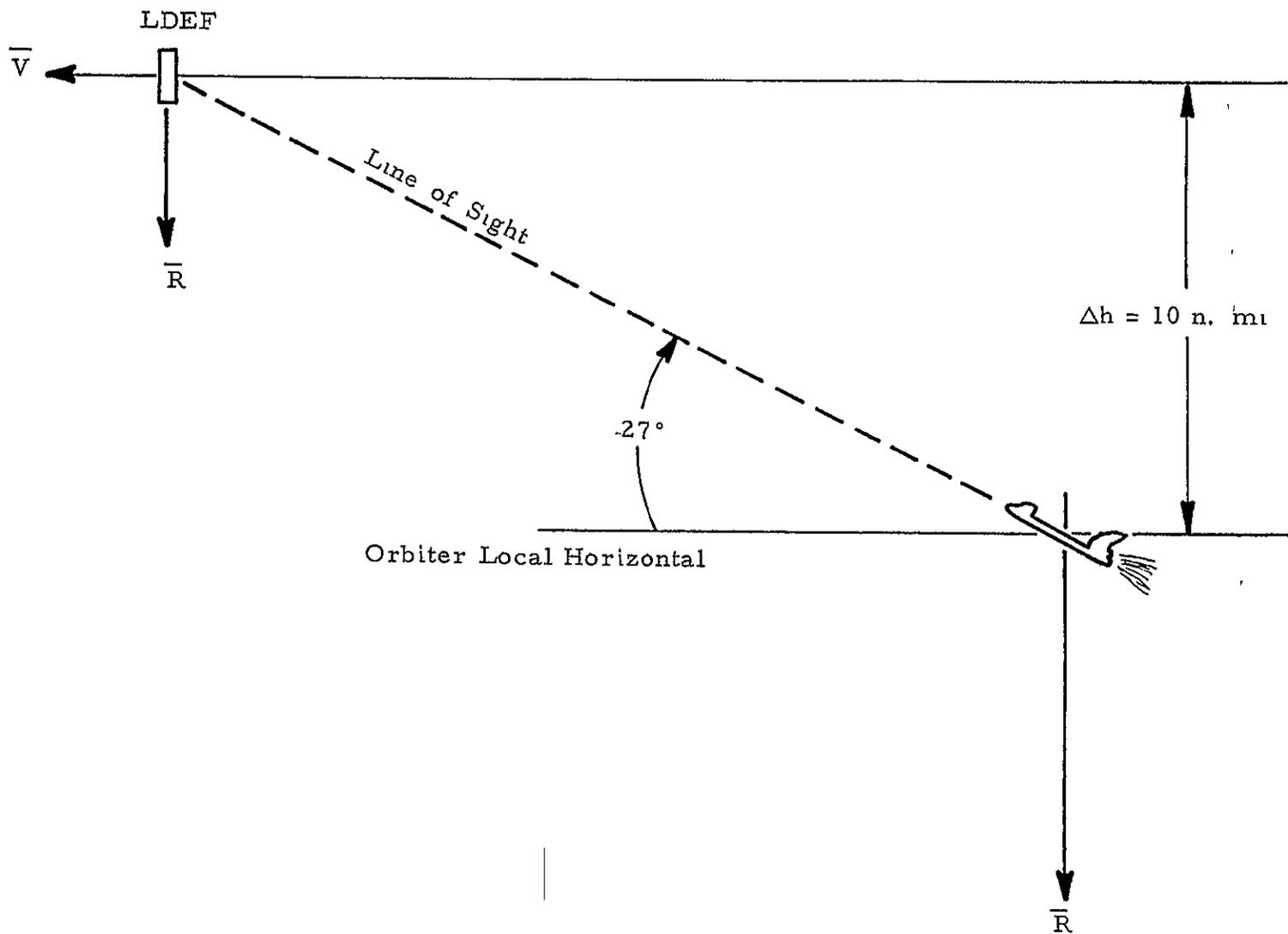
Figure 3-1.- Terminal Phase Initiation Burn

provides an elevation angle of 27 degrees at midnight was accomplished by the combined effect of the pre-TPI maneuvers. There are two reasons for this timing constraint. First, sunrise must occur in sufficient time to establish visual contact for final lateral corrections to the intercept trajectory. (No trajectory will be free of errors since all burns are with respect to the Orbiter's state vectors which are maintained through on-board, autonomous navigation). Second, sunset must not occur before the pilot can initialize the R-bar approach and rely on upward pointing payload bay flood lights to illuminate the LDEF. Although trajectory errors and the β angle (sun vector WRT orbit plane) will affect timing, sunrise typically occurs approximately 25 minutes after TPI.

4.0 Post-TPI

Immediately following the TPI burn, the Orbiter's Universal Pointing System (UPS) provides commands to the DAP (Digital Auto Pilot) such that the Orbiter's -Z axis (body frame) is directed along the best estimate of the LDEF LOS (line of sight). The commands cause the Orbiter to pitch down 90 degrees from the burn attitude. LOS to LDEF is now out the pilot's upper window at his aft station. The UPS also causes the Orbiter - Y axis to point along the orbital angular momentum vector, $\bar{H}$. This is provided by specifying to the UPS an Omicron of $0°$. (Omicron serves the basic purpose of defining a unique Orbiter attitude about a directed pointing vector).

The -Z body axis is sometimes referred to as the "Orbiter rendezvous axis." The COAS (crewman optical alignment sight) for rendezvous has its optical axis collinear with $-Z_B$. In addition, the Ku-band (micro-wave) doppler rendezvous radar antenna tracking angle limits are defined with respect to the Orbiter's -Z body axis.

Though rendezvous requires both radar and optical tracking of LDEF, contact after the TPI burn is established (in darkness) with the rendezvous radar. Since LDEF has no beacon transponder, the rendezvous radar is utilized in its passive mode. The range capability can be as short as 12 nautical miles for a minimal target, but LDEF's large cross section should increase this to TBD n. miles. (TPI occurs at a LOS range of approximately 23 miles).

It takes the Orbiter approximately 33 minutes from TPI to intercept LDEF (this time assumes no Orbiter braking). During this interval, the Orbiter flies through an orbital path of 130° (See Figure 4-1). Usually two small trajectory adjustments (TPM1 and TPM2) are made at approximately TPI+12 minutes and TPI+24 minutes. They are principally used to reduce in-plane dispersions.

At TPI plus 25 minutes the Orbiter passes through the LDEF radius vector but some 14,000 feet below the LDEF. The Universal Pointing System continues to point the Orbiter -Z axis along the best estimate of the LDEF LOS. About this time the LDEF and Orbiter begin to experience orbital sunrise and the pilot (now at his aft station) begins to visually scan his upper window ($-Z_B$ axis) and rendezvous COAS for the LDEF. The UPS should have the LDEF well within the COAS's 5 degree

10

LDEF Orbit

ORBITER
Orbit

Intercept

$\Omega_0 t = 130°$

LDEF at TPI

Sun
Vector

TPI

$\Delta h = 10$ n mi

0.27°

Earth
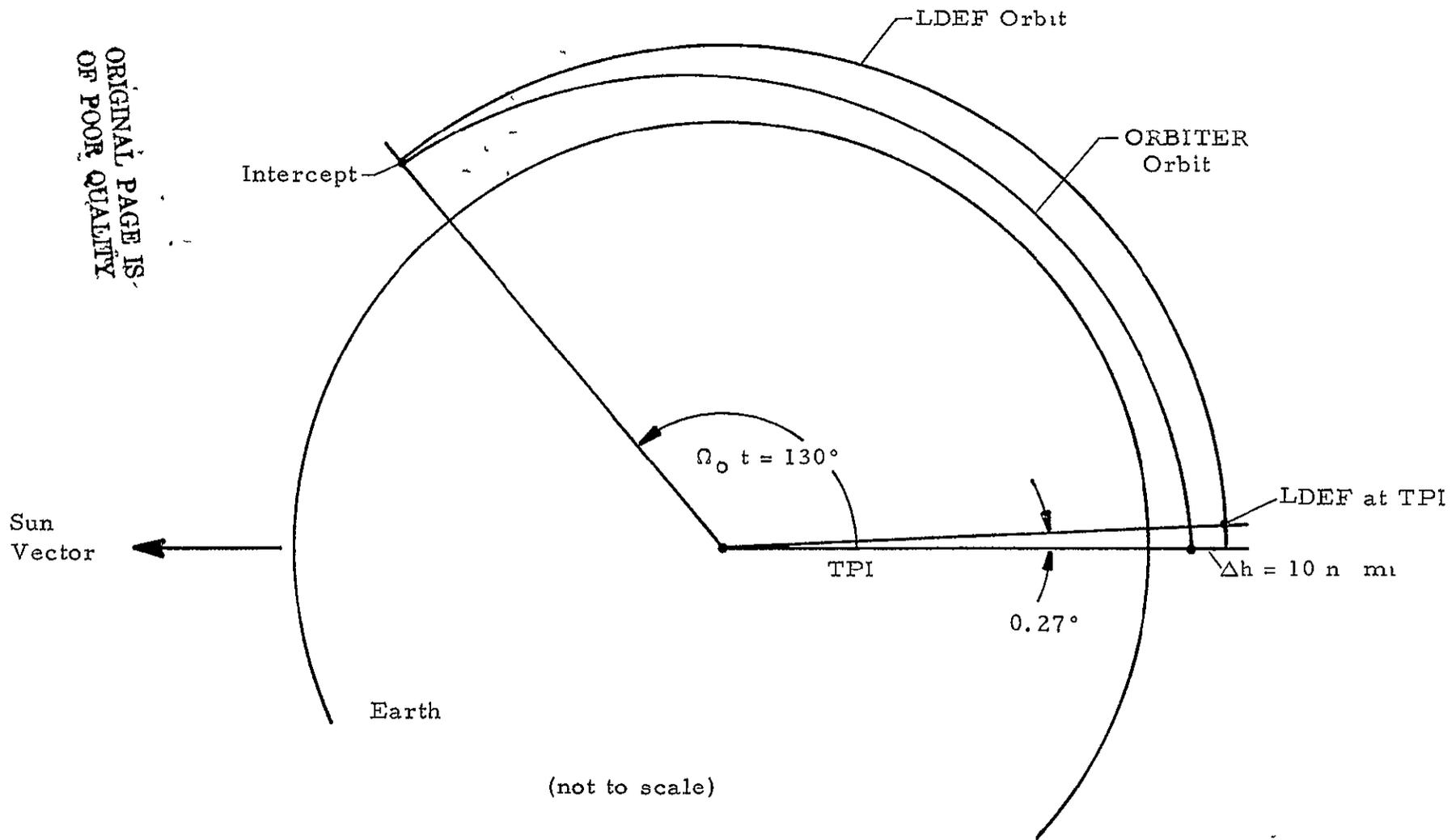
(not to scale)

Figure 4-1.- Post TPI Trajectory

11

half-cone angle field of view about the $-Z_B$.

5.0 The LVLH Coordinate System

It is convenient at this point to transfer one's reference from a geocentric coordinate system to an LDEF centered frame. This transformation facilitates a discussion of the relative orbital motion of LDEF and the Orbiter during the final stages of rendezvous. The new frame is shown in figure 5-1 and is commonly known as the LVLH (local vertical - local horizontal) Frame.

The LVLH coordinate frame is situated as follows: +Z axis directed toward the center of the earth, +Y axis perpendicular to the orbit plane with direction opposite the angular momentum vector, and +X axis positioned to complete the right-handed triad so that it is horizontal in the orbit plane, and in the direction of orbit travel. The frame rotates about the earth at a rate of Ω radians/second (referred to as "orb rate"). The position, altitude, etc. of the LVLH frame is a function of the gravitational force of the celestial body it is orbiting and can be defined completely by the parameter Ω. For example, an LVLH frame orbiting the earth at a constant 1.11 milliradians/second has an altitude of approximately 263 nautical miles.

The target spacecraft, LDEF, remains centered at (0, 0, 0) in the LVLH frame and the Orbiter position and velocity relative to LDEF is given by (X, Y, Z) and $(\dot{X}, \dot{Y}, \dot{Z})$, respectively.

For example, it was stated previously that at TPI+25 minutes the Orbiter passes through the LDEF radius vector but some 14,000 feet

12

+ Y

(X, Y, Z)
(0, 0, 0)

$\overline{V}$ ← +X

Direction of
Orbit Travel

$\overline{H}$

+ Z

$\overline{R}$

Earth

To Center of Earth
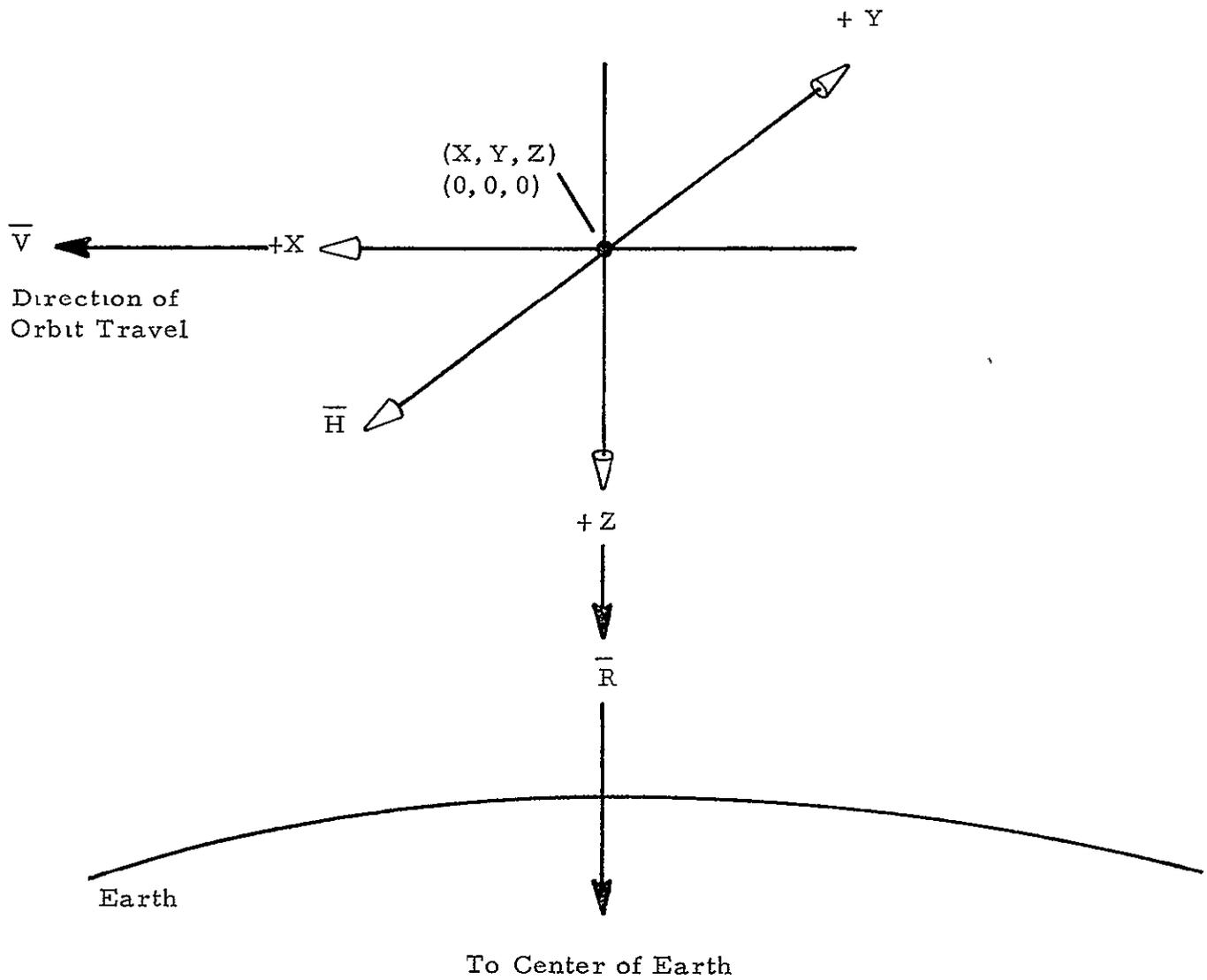
$\overline{V}$ - "V-Bar" - Tangential Velocity Vector (horizontal component)

$\overline{R}$ - "R-Bar" - Radius Vector

$\overline{H}$ - "H-Bar" - Orbital Momentum Vector

Figure 5-1.- LVLH Frame

13

$\overline{V}$ or $+$ X

NOTE:
View is along
$-\overline{H}$ or $+$ Y axis
into the page

TPI $+$ 25 min.
Elevation = 90°
Range = 14,000 ft.

Coordinates
(X, Y, Z) = (0, 0, 14000)
(Ẋ, Ẏ, Ż) = (16, 0, -33)

LOS at TPI
Elevation = 27°
Range = 125,000 ft

LOS at TPI $+$ 12 min.
Elevation = 47°
Range = 58,000 ft.

$\overline{R}$ or $+$ Z
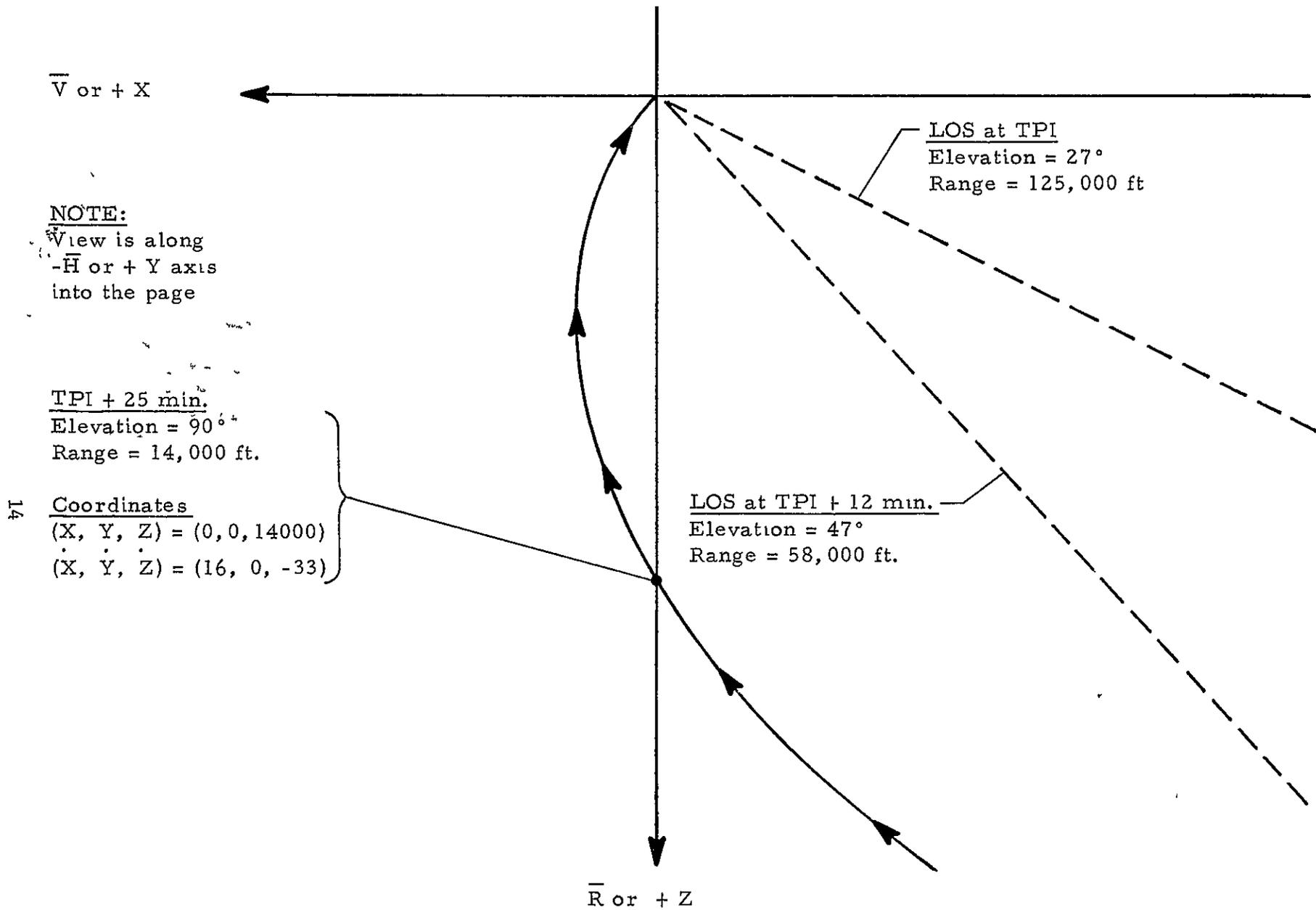
Figure 5-2.- Typical Intercept Trajectory in the LVLH Frame

14

below LDEF. The position in the LVLH frame is (0, 0, 14,000) in feet.
The corresponding velocity components are (16, 0, -33) in feet per
second. In other words, the Orbiter is rapidly climbing to LDEF and
moving ahead of LDEF. A typical LDEF intercept trajectory in the LVLH
frame is shown in figure 5-2.

One of the unique aspects of the intercept trajectory is the
rotation rate of the LOS vector. Note that any stationary line in the
$\bar{V}$ - $\bar{R}$ plane of the LVLH frame is actually rotating inertially at the
orb-rate, Ω; conversely, any inertially stationary line rotates clock-
wise at Ω in the LVLH frame. The latter describes what happens to the
LOS during the final phases of the approach trajectory. Within 22
minutes after TPI the inertial LOS rotational rate decreases from -0.8
milliradians per second to zero and remains essentially zero for the
remainder of the intercept trajectory. In the LVLH frame the trajectory
has the appearance of a spiral because the LOS is rotating clockwise
at Ω as the range is collapsing.

6.0 Some Important Cockpit Instrumentation

A discussion of the rendezvous scenario from the initial braking
phase to LDEF station keeping is more interesting and less enigmatic
if it includes descriptions of crew activities. However, a basic
understanding of some important cockpit instrumentation is a prerequisite
to such a discussion. To be sure, the pilot and co-pilot monitor and
react to numerous cockpit displays, but during the phases of interest
there are four instruments which receive "prime time". These are:

15

(1) the COAS, (2) the LOS Rate Needles, (3) Ku-band radar range and range rate displays, and (4) the ADI or "Eight Ball."

6.1   The Crewman Optical Alignment Sight (COAS) -

The COAS is a collimating device which is similar to an aircraft gun sight. The device is located in the pilot's aft station overhead window. It serves two purposes:

1.   It provides to the pilot a fixed line of sight attitude reference image which, when viewed through the rendezvous window, appears to be the same distance away as the target. The image is boresighted parallel to the Orbiter's $-Z_B$ axis and perpendicular to the Orbiter's X_B-Y_B plane.

2.   It provides a measurement of the target vehicle's subtended angle from which range and range rate information may be derived.

The COAS reference image is a reticle which consists of a 10-degree circle indexed in 10 degree increments, and vertical and horizontal cross hairs indexed in one degree increments (see figure 6.1-1). The image is projected on a rectangular piece of combining glass which resides at the forward edge of the window as shown in figure 6.1-2.

6.2   LOS Rate Needles

In addition to providing range and range rate information, the Ku-band radar system also measures components of the radar LOS inertial rotation rate. The data is presented on the LOS Inertial Rate Indicator shown in figure 6.2-1. The azimuth needle registers the component of radar LOS inertial angular rate along the Orbiter's -X body axis and the

16

$+X_B$

$+Y_B$

(View looking UP along
$-Z_B$ at Pilots Aft Station)

10°

Field
of
View
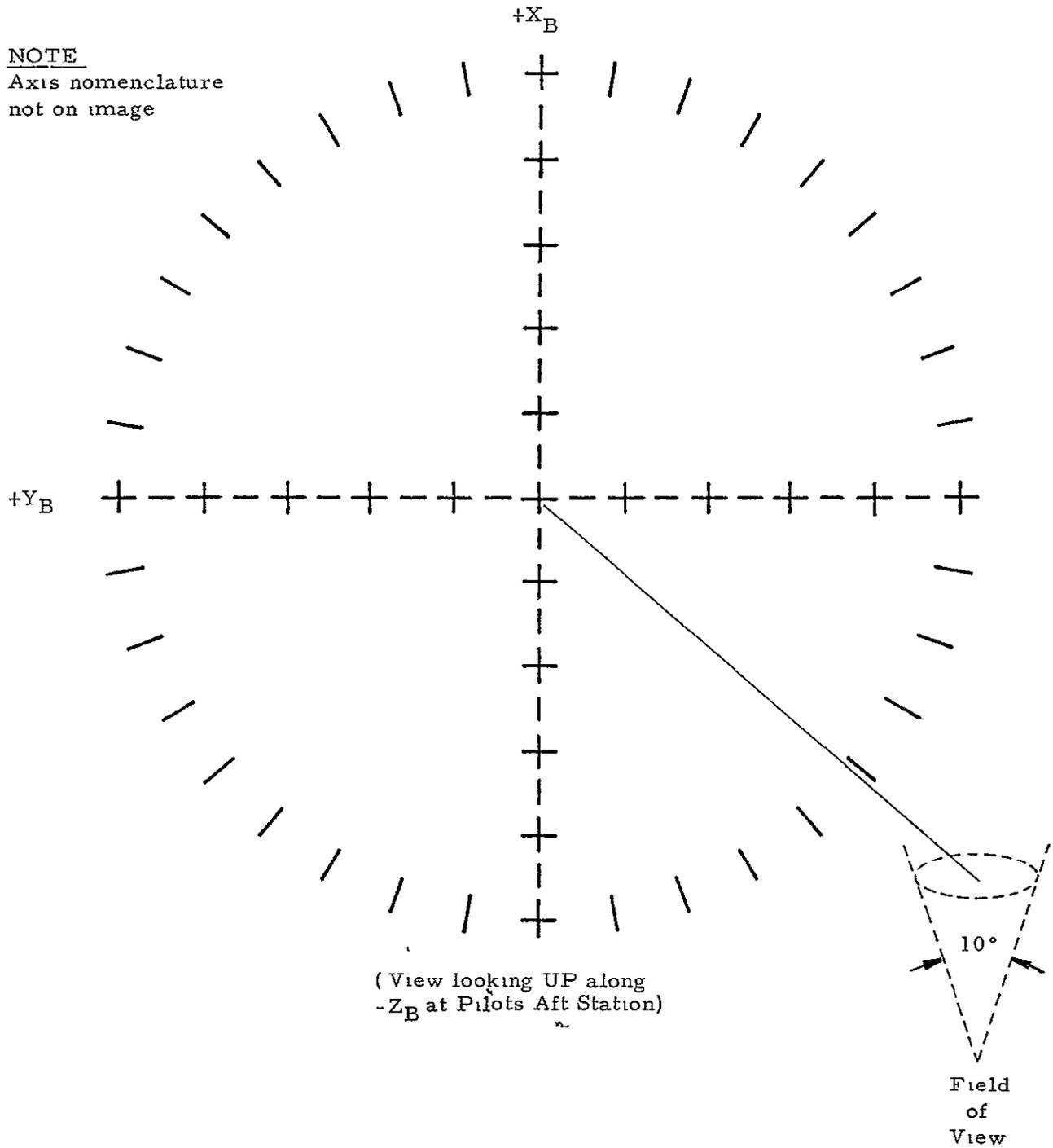
Figure 6.1-1.- COAS Reference Image (Crewman Optical Alignment Sight)

17
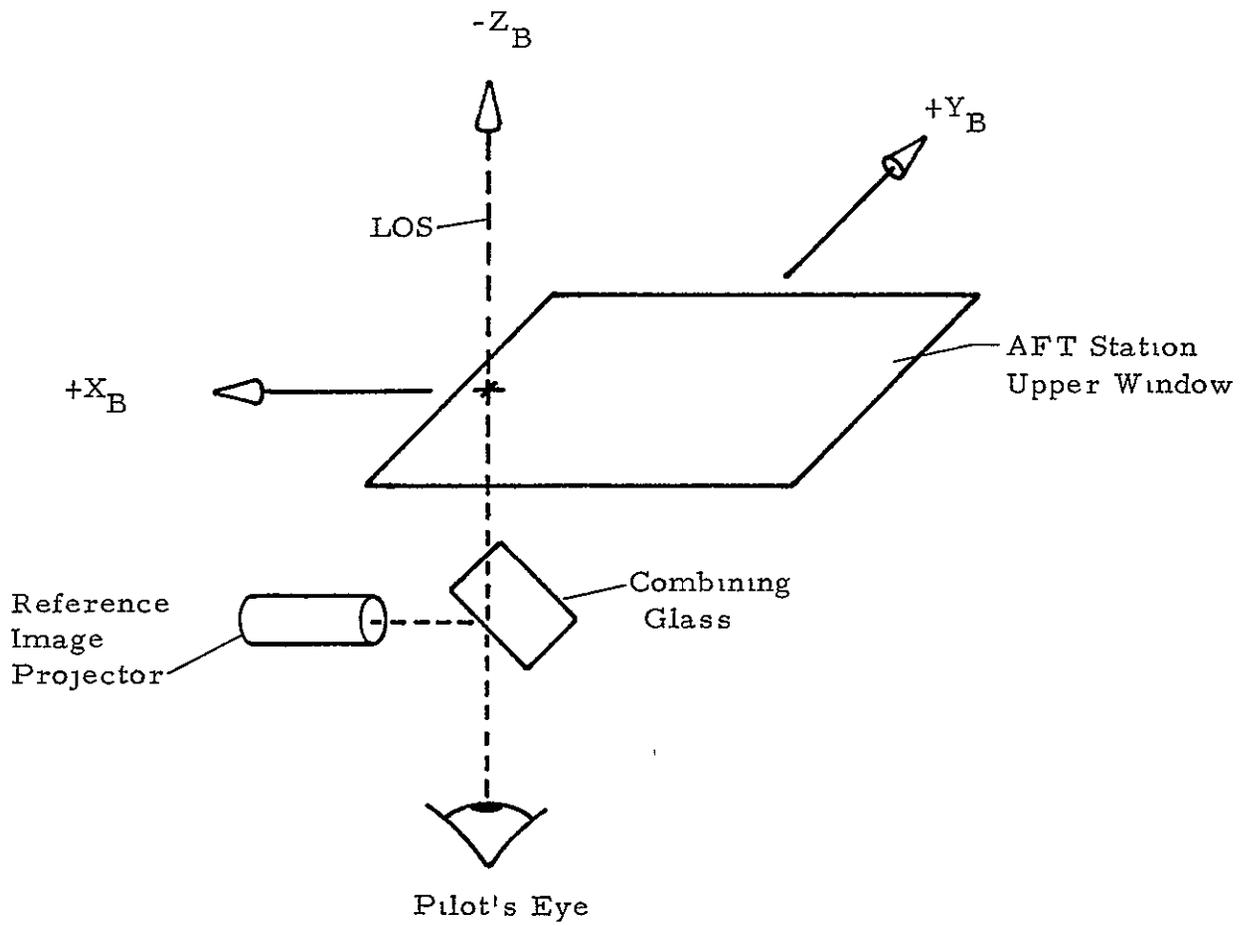
Figure 6.1-2.- COAS Schematic
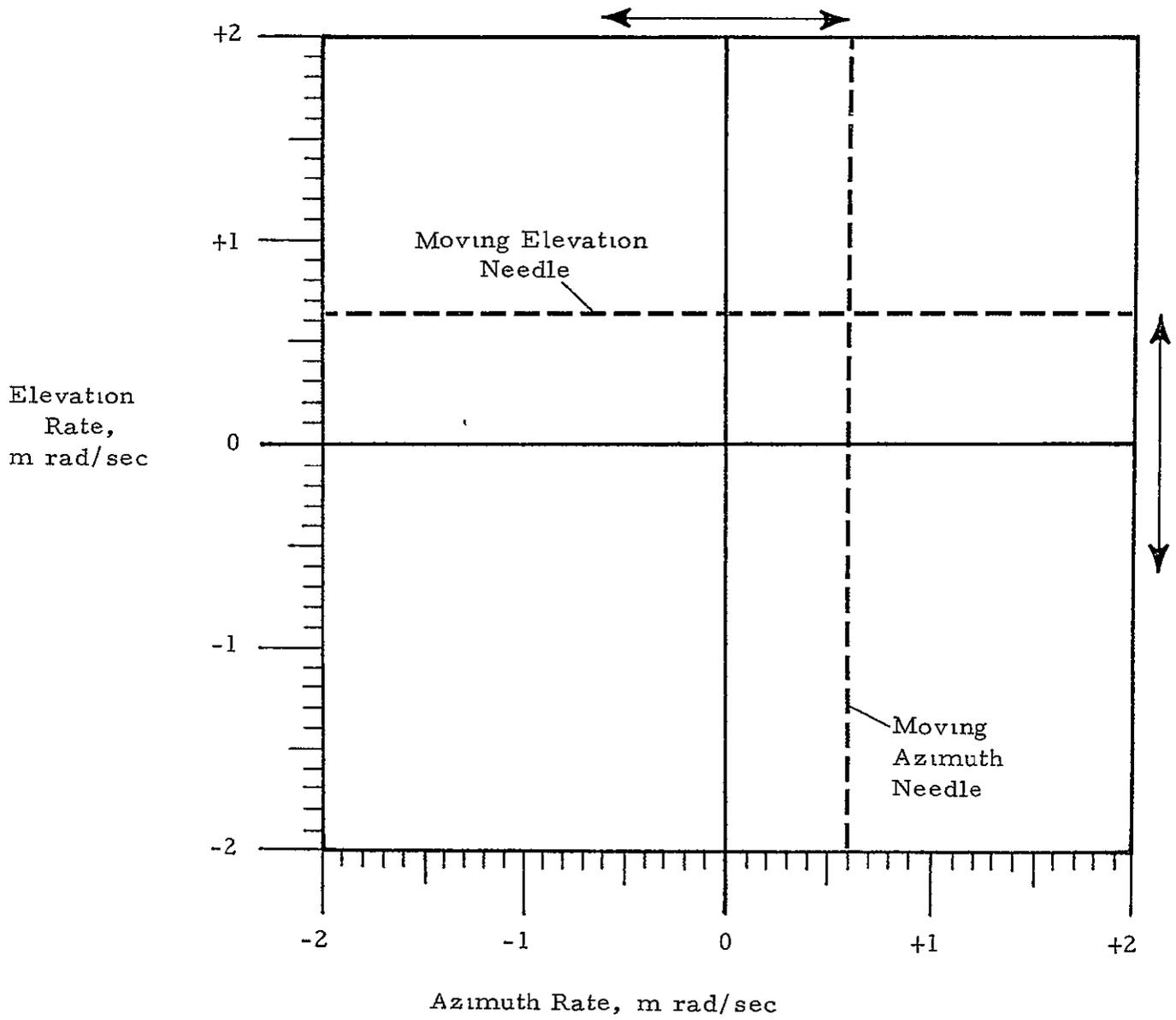
NOTE   Pilot may select a Readout Sensitivity of 1X   or 10X

Figure 6.2-1.- LOS Inertial Rate Indicator (Ku-Band Radar Antenna)

elevation needle registers the component of radar LOS inertial angular rate along the Orbiter's -Y body axis.

An appreciation of what the LOS rate data represents may be obtained through studying some examples. First, assume that the Orbiter is in perfect inertial attitude hold (no attitude limit cycling) and the target vehicle is centered in the COAS. If the position of the target vehicle in the COAS remains stationary, both LOS Rate Needles will register zero. If the target vehicle image starts moving toward the Orbiter's nose (along the X_B axis of the COAS), the elevation needle will read the angular rate of the radar LOS with respect to the inertially stationary COAS LOS. If the target vehicle image moves off center along the Y_B axis of the COAS, the azimuth needle will register the angular rate.

For a second example, assume once again that the Orbiter is in perfect inertial attitude hold and that the target is stationary in the COAS. Then assume that the pilot commands an Orbiter pitch rotation rate. In this case the target vehicle image will start moving in the COAS, but the LOS needles will remain zeroed. The result assumes of course that absolutely no increment of translational velocity was introduced into the Orbiter's motion by the pitch command. The important point is that Orbiter rotations do not affect the inertial angular rate of the radar LOS; they can, however, affect the components of the radar LOS inertial rate as presented by the LOS Rate Needles.

The final example is most relevant to rendezvous operations. Assume that the Orbiter is sitting on a runway at the Earth's equator

20

and the Orbiter's X_B axis is parallel to the equator. Further assume
that an appropriate radar target balloon (in the presence of no wind)
is above the Orbiter and on a 1000 foot tether line attached to the
Orbiter's cockpit. In this case the elevation rate needle will read
the Earth's sidereal rotation rate of approximately 15.04 degrees per
hour*, or the inertial angular sweep rate of the local vertical. The
balloon would be within the COAS field of view and its image stationary
with respect to the COAS reticles.

As a side note, the LOS Inertial Rate indicator is a "fly to"
type display. For example, if the elevation needle registers +1
milliradian per second, the pilot may null the rate by pushing the
aft station translational hand controller (THC)"UP."

6.3 Range and Range Rate

The LOS range and range rate data is simply presented by two
digital displays which are driven by the Ku-band radar system. The
uncertainties associated with this data greatly influence the
operational techniques employed in an $\bar{R}$ approach. The specified
uncertainties (as opposed to expected uncertainties in the flight
hardware) are as follows:

$\delta R = \pm 80$ ft. 3σ

$\delta \dot{R} = \pm 1$ ft/sec. 3σ

These uncertainties represent the scatter (or noise) about the mean. A
similar specification exists on any bias in the mean; however, bias is

------

*This rate is actually near or below the measurement threshold of the LOS
Rate Needles.

not considered an error source because it is assumed that it may be eliminated through compensation.

6.4 The Orbiter Attitude Director Indicator (ADI) -

The ADI, commonly known as the "Eight Ball" (see figure 6.4-1), is an instrument which constantly relates the pilot's line of sight attitude frame to a reference frame. Some definitions are required at this point.

• Line of Sight Attitude Frame - There are 3 LOS attitude frames in the Orbiter. They correspond to the 3 views available to the pilot from the cockpit, i.e., out the nose, out the payload bay bulkhead, and out the cockpit ceiling. The definitions of the 3 LOS frames with respect to Orbiter body axes are shown in figure 6.4-2. Loosely speaking, in each LOS frame the X axis is the pilot's LOS, the Y axis is out his right shoulder and the Z axis emerges from the soles of his feet.

• Reference Frame - The pilot has a choice of two reference frames, LVLH or inertial. The LVLH reference, as defined in Section 5.0, is used during the final phases of rendezvous.

• Rotation Sequence - The "eight ball" displays the attitude of the LOS frame in terms of pitch, yaw, and roll rotations (in that order) which are necessary to take the LOS frame from an initial alignment with the reference frame to the present attitude. The pitch, yaw, and roll rotations are rotations about the LOS's Y, Z and X axes, respectively. Sign convention is according to the right hand rule. The sequence and angle constraints, in summary,

22
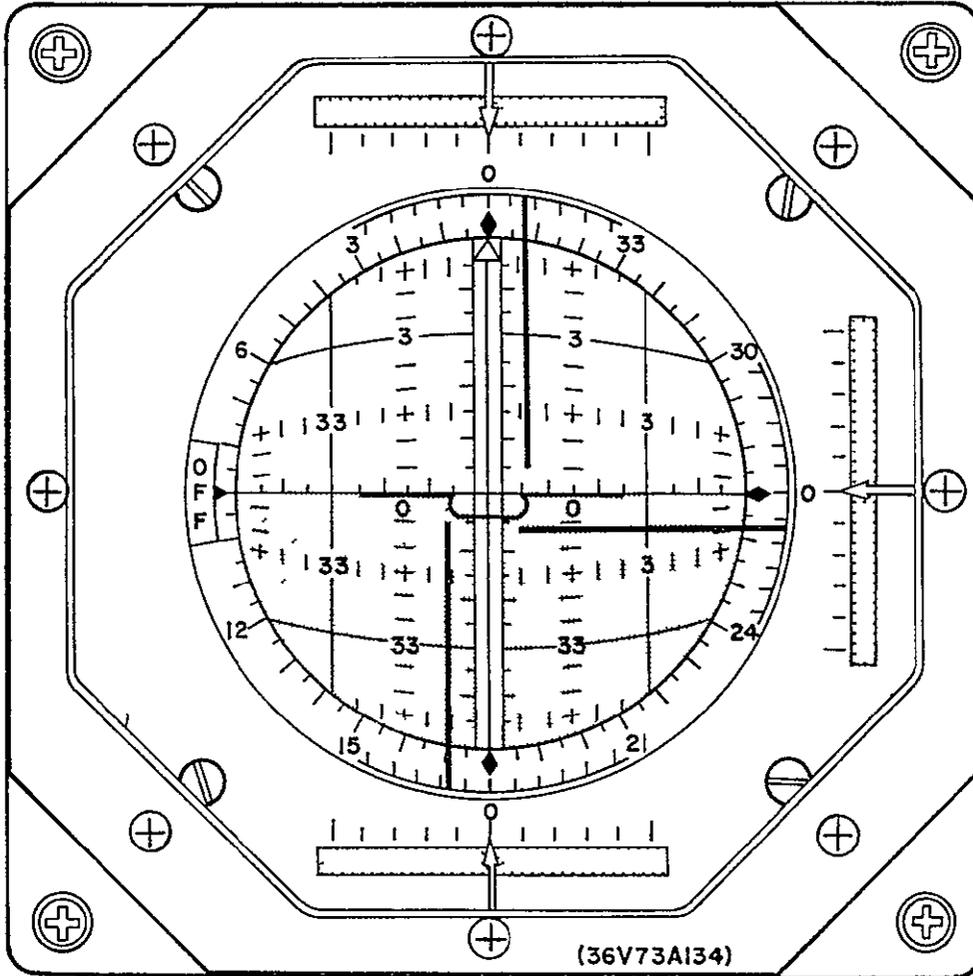
Figure 6.4-1.- The Attitude Director Indicator (ADI)

(36V73Al34)

23

Forward
LOS
Frame

Body
Frame

Forward LOS Frame	Body Frame
X	$+X_B$
Y	$+Y_B$
Z	$+Z_B$

Aft
LOS
Frame
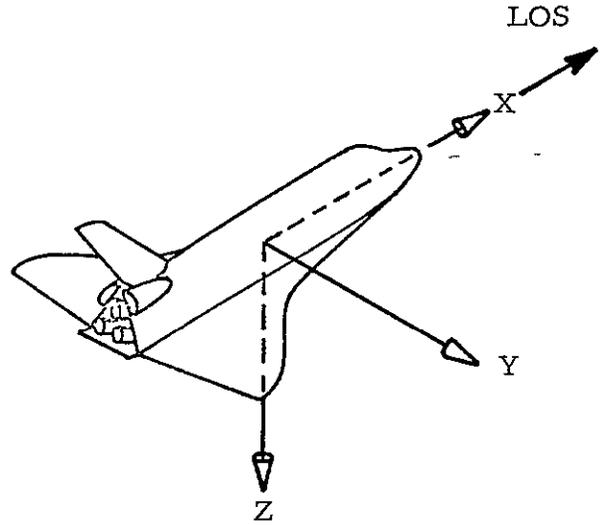
Body
Frame

Aft LOS Frame	Body Frame
X	$-X_B$
Y	$-Y_B$
Z	$+Z_B$

Upper
LOS
Frame
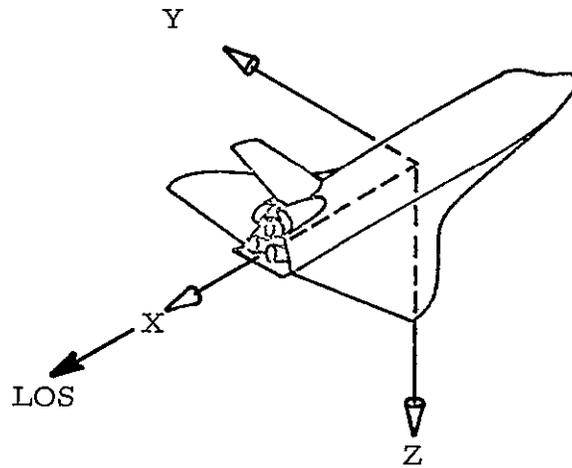
Body
Frame

Upper LOS Frame	Body Frame
X	$-Z_B$
Y	$-Y_B$
Z	$-X_B$
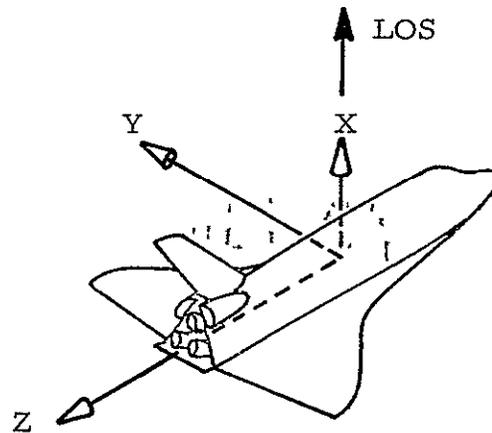
Figure 6.4-2.- The Three LOS Attitude Frames

24

1. Pitch-up (positive rotation about

>   LOS + Y axis) 0 to 360 degrees

2. Yaw right (positive rotation about

>   LOS + Z axis) 0 to +90 degrees

or

Yaw left (negative rotation about

>   LOS + Z axis) 0 to -90 degrees

3. Roll right (positive rotation about

>   LOS + X axis) 0 to +360 degrees

There are three "eight balls" in the cockpit. Two are located at the
forward station for the pilot and co-pilot; both display the attitude
of the forward LOS frame. The third is located at the pilot's aft
station and is switchable to display the attitude of either the aft
LOS frame (-X Sense Switch position) or the upper LOS frame (-Z Sense
Switch position). Though only the aft eight ball in the -Z Sense
Switch mode is used during the final stages of rendezvous, it is
frequently helpful (for explanatory reasons only) to compare the
readings at a given attitude.

Suppose that the Orbiter is oriented as follows:

> X_B along $\bar{V}$
>
> Y_B along $-\bar{H}$
>
> Z_B along $\bar{R}$

The forward eight ball will read:

>   Pitch   0
>
>   Yaw   0

25

Step #1
Pitch 180°

$-\overline{H}$
$+Y_B$

Pitch

$\overline{V}$
$+X_B$

Orbiter
Attitude

$+Z_B$
$\overline{R}$

Step #2
Roll 180°

Z

Y

X

Roll

LOS

X

Y

Aft LOS
Frame

Z
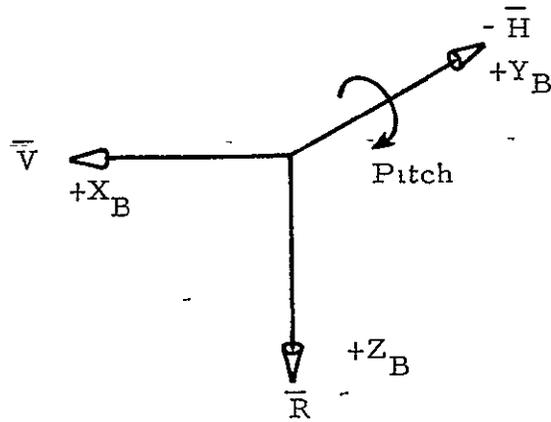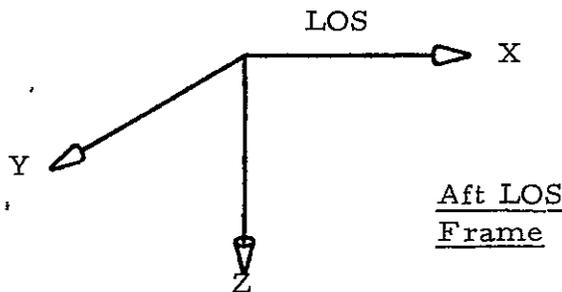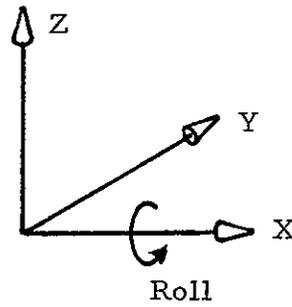
Figure 6.4-3.- Rotating to the Aft LOS Frame

26
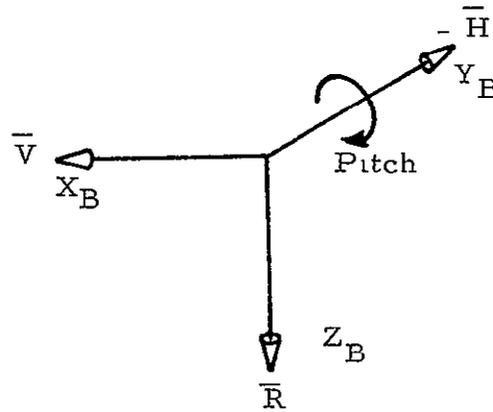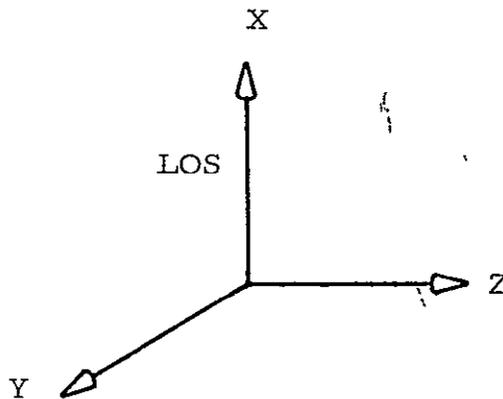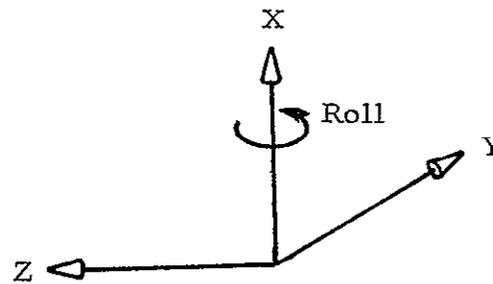
Figure 6.4-4.- Rotating to the Upper LOS Frame

Pitch = +135°

$\overline{V}$

LDEF

COAS
LOS

X

Orbiter

Upper LOS
Frame

Z

$\overline{R}$
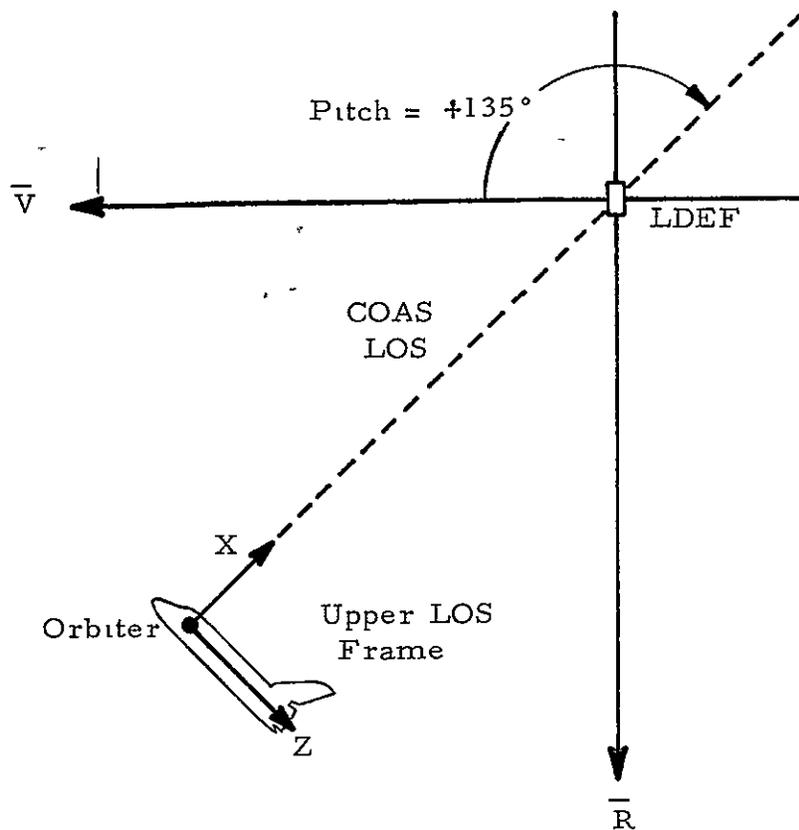
AFT EIGHT BALL READING
(Sense Switch to -Z)

Pitch	135
Yaw	0
Roll	180

(36V73AI34)
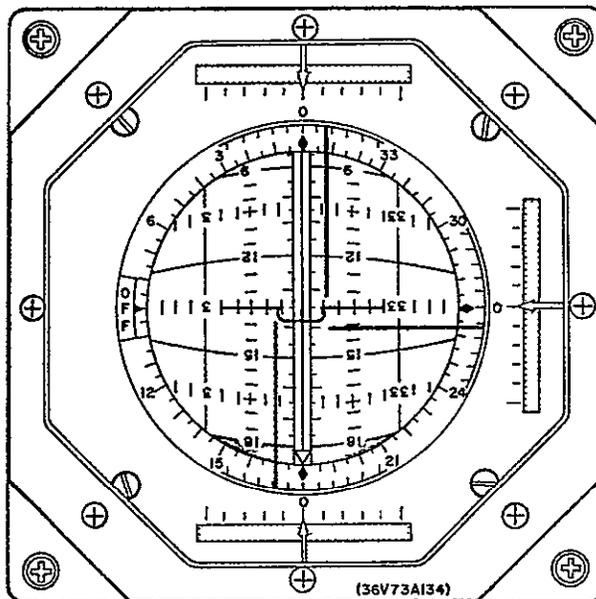
Figure 6.4-5.- Using the COAS and "Eight Ball" to Determine
Orbiter Approach Direction

28

Roll   0

The aft eight ball (with the Sense Switch in -Ẋ to display the aft LOS

frame attitude) will read:

                    pitch   180

                    yaw   0

                    roll   180

The rotation sequence is shown in figure 6.4-3.

     The AFT "eight ball" with the Sense Switch in -Z to display the

upper LOS frame attitude) will read:

                    pitch   90

                    yaw   0

                    roll   180

The rotation sequence is shown in figure 6.4-4.

     As a final example, assume that the pilot has LDEF centered in the

COAS as the Orbiter is closing on LDEF at a range of one mile. Further

assume that the aft "eight ball" (Sense Switch to -Z) is reading

                    pitch   135

                    yaw   0

                    roll   180

     An experienced pilot immediately knows that he is approaching LDEF

in the quadrant defined by $+\bar{V}$ and $+\bar{R}$. See figure 6.4-5.

7.0 Transferring to Visual LOS Navigation

     Somewhere between two and four miles from the target, the pilot

begins to rely on visual navigation and manual control of the Orbiter.

                                   29

Heretofore, the Universal Pointing System (UPS) was automatically

pointing the $-Z_B$ axis at the best estimate of the LDEF relative position.

But the pointing, as well as the trajectory, usually contains errors

which are derived from imperfect maintenance of the Orbiter's state

vectors. These errors are surprisingly small. Indeed, simulations

(which model error sources) typically show the target to be well within

one degree of the COAS center at four miles. Nonetheless, even small

errors, if allowed to propagate, can result in intercept "misses" of

up to two miles. It is, therefore, necessary to eliminate them.

Three possible cases may exist and are presented in figure 7-1.

In each case the Orbiter's attitude and path relative to the perfect

trajectory is shown at time t_1 and later at time t_2. In the perfect

trajectory, Case A, the LDEF is centered in the COAS and LDEF does not

move with respect to the star field behind it, i.e., the LOS direction

is inertially fixed. Case B shows the effects of an attitude error,

and Case C shows the effects of a trajectory error. Regardless of the

situation, the pilot first assumes that any error in the COAS is due to

a pointing or attitude error. The pilot reconfigures the DAP from the

"Auto Mode" (which was accepting UPS commands) to the "Manual Mode."

This immediately places the Orbiter in inertial attitude hold. Any

further pointing commands to the DAP are entered via the RHC

(rotational hand controller). (The UPS essentially had the Orbiter in

inertial attitude hold because the computed LOS direction at this point

is inertially fixed). The pilot, using the RHC, centers LDEF in the

COAS. When he releases the RHC, inertial attitude hold is resumed at

CASE A. IDEAL TRAJECTORY AND ATTITUDE
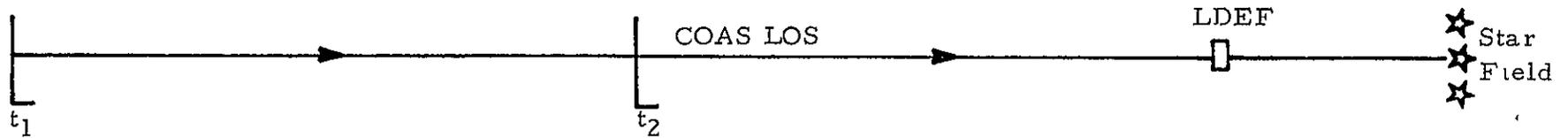
a. LDEF Stationary WRT Star Field
b LDEF Remains Centered in COAS

CASE B: IDEAL TRAJECTORY BUT ATTITUDE ERROR
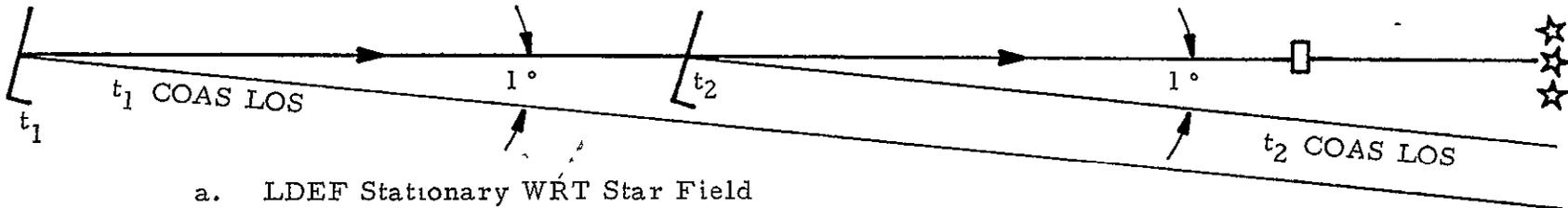
a. LDEF Stationary WRT Star Field
b. Constant LDEF Error of 1° in COAS
c. COAS LOS Stationary WRT Star Field

CASE C ATTITUDE ALINED TO TRAJECTORY BUT TRAJECTORY IN ERROR
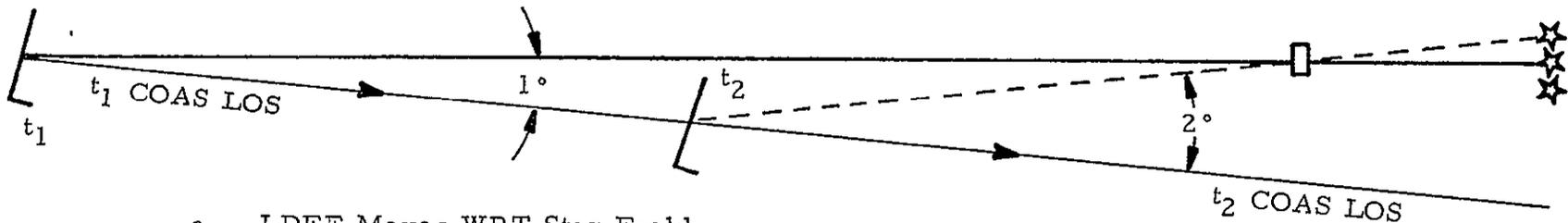
a. LDEF Moves WRT Star Field
b. LDEF Error in COAS increases from 1° to 2°
c. COAS Los Stationary WRT Star Field

7-1.- Initial Conditions at 2 to 4 miles prior to Commanding Attitude Hold

31

the new attitude. If LDEF remains centered in the COAS, the trajectory
is correct and an attitude error was just eliminated. If LDEF moves in
the COAS, the pilot, using the THC (translational hand controller),
drives the Orbiter onto a new trajectory defined by a COAS LOS centered
on LDEF. The THC is moved up, down, left, or right to position the
LDEF in the COAS. No RHC commands are used.

8.0 Entering the Braking Schedule

Braking the Orbiter velocity relative to LDEF is a manual opera-
tion. It is performed according to the schedule shown in figure 8-1.
The pilot relies on the Ku-band radar displays for range and range rate
information. The first "braking gate" occurs at 6,000 feet where the
closing range rate should not be greater than 25 fps. ($\dot{R}$ is
approximately 30 fps as this gate is approached.) The pilot can "kill"
5 fps of $\dot{R}$ by pulling back on the THC for 10 seconds as each gate is
approached, or he may anticipate the gates by removing the $\dot{R}$ in smaller
increments which would more closely approximate a linear deceleration.
The latter technique is generally used during the last phases of the
schedule because it minimizes plume impingement on the LDEF.

The typical braking schedule for Apollo/Gemini is also shown in
figure 8-1. The major difference is that braking must be completed
before the Orbiter enters an imaginary sphere (surrounding LDEF) in
which jet firings would have deleterious effects on LDEF, namely,
motion perturbations and contamination. The sphere's radius is commonly
denoted as R_{IMP} and is proposed to be at least 1000 feet for an LDEF
type payload.

Figure 8-1.- Proposed Orbiter Braking Schedule
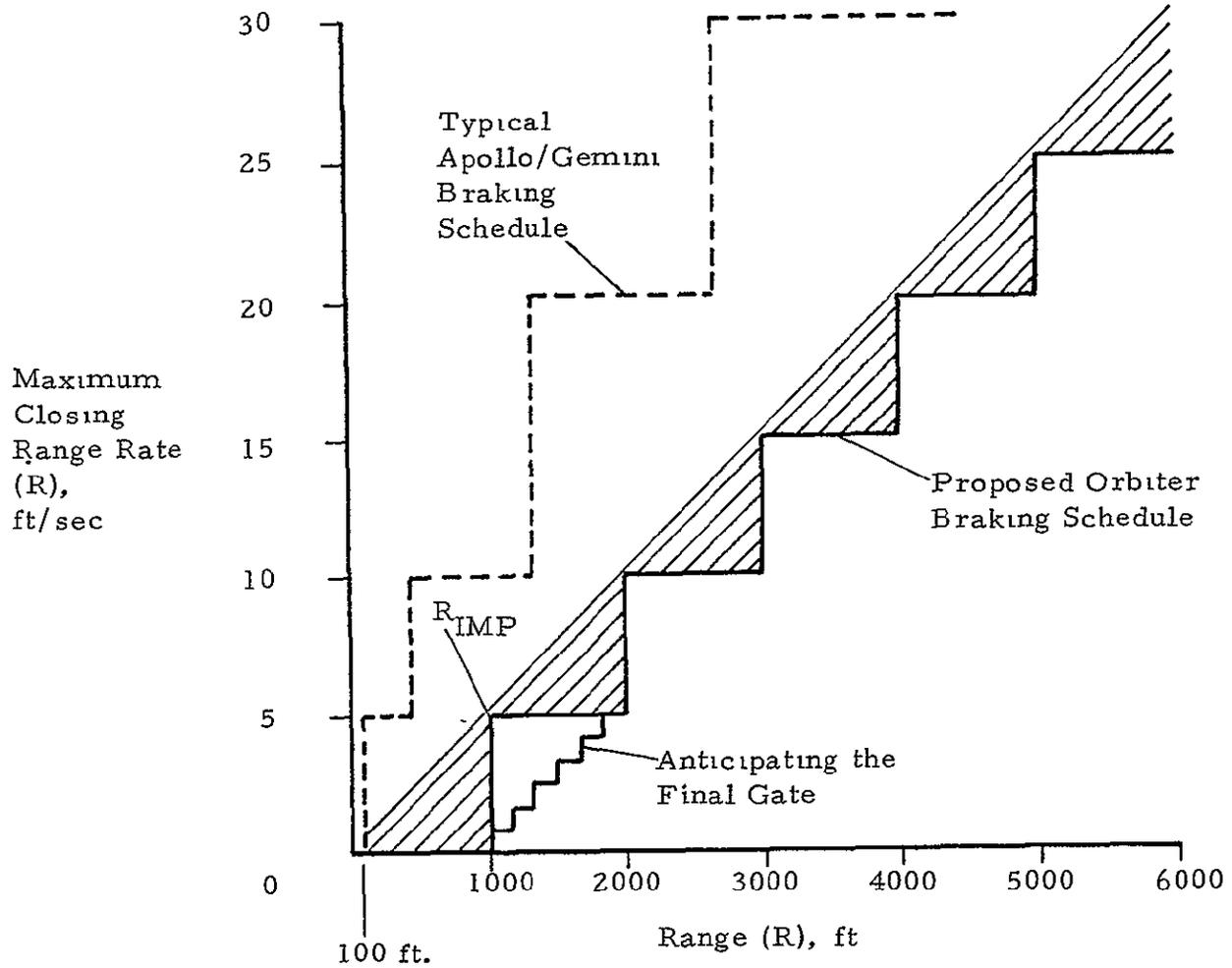
R_{IMP} - Minimum Range to Avoid Plume Impingement Effects

t_B + 715 sec   LDEF

⑥   — 66.47°

5 fps

⑤

t_B + 315 sec

1000

10 fps

2000

15 fps

t_B + 182 sec

④

20 fps

t_B + 102 sec

3000

③

25 fps

OS Angles

⑥   — 66.47°
⑤   — 40 47°
④   — 31 80°
③   — 26.60°
②   — 22.89°
①   — 20.00°

t_B + 44 sec

4000

②

5000

①

t_B

Range, ft

t_B — Time Braking Starts

t_B + XXX seconds (Assuming $\ddot{R}$ = constant)
                (Ref. only)

LOS Angles Measured from $\overline{R}$

LOS Angle = 20° + (t − t_B) Ω_{LDEF}

Ω_{LDEF} = LDEF Orbit Rate ≈ 0.065°/sec

6000

$\overline{R}$
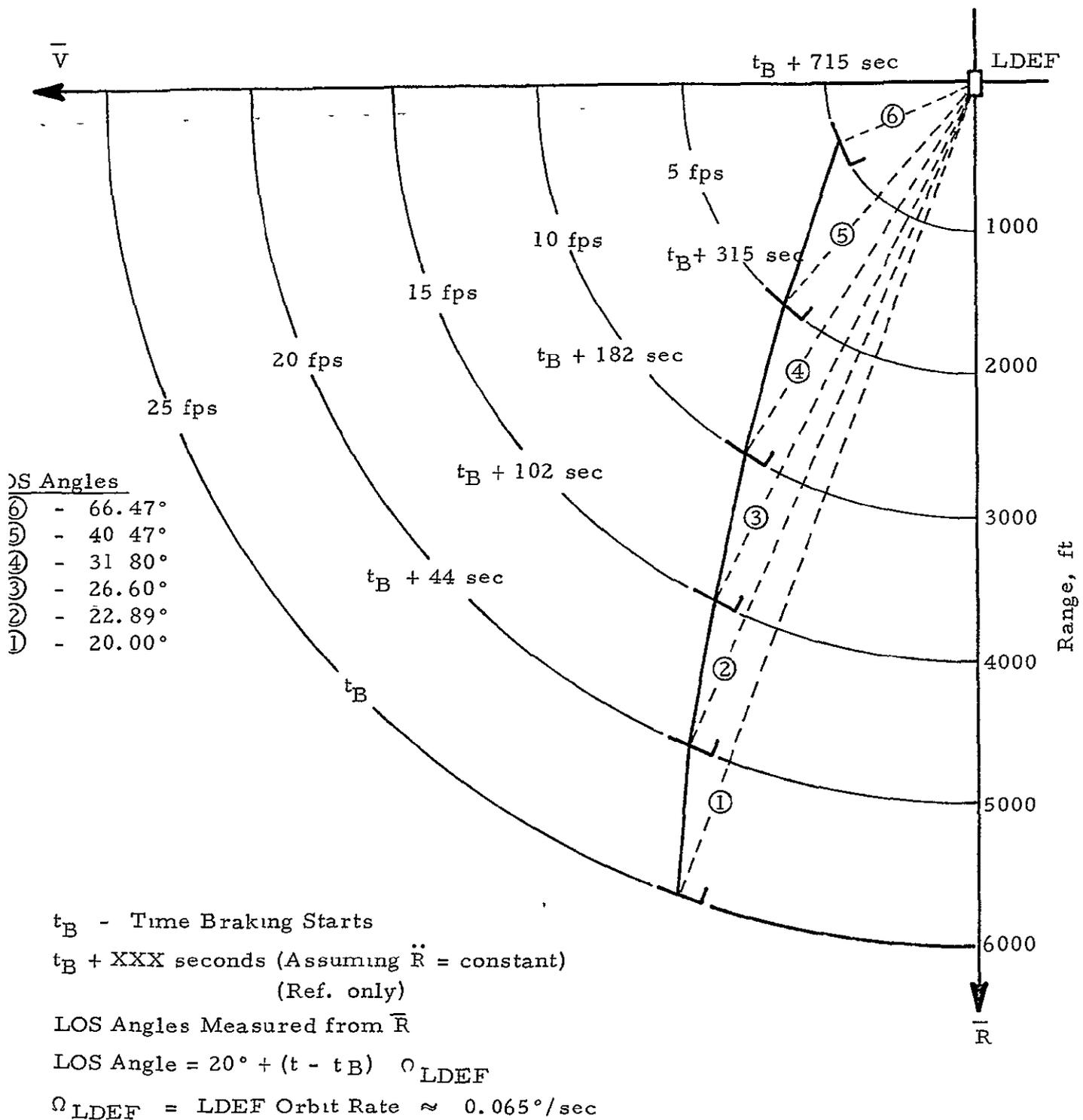
Figure 8-2.— Typical Orbiter Trajectory During Braking With an Inertially Stationary LOS

34

During braking the pilot continually maintains the LDEF centered in the COAS by using only the THC. This assures an LOS trajectory which greatly simplifies visual navigation and minimizes fuel usage. In addition, the pilot follows the braking schedule as closely as possible. Because of orbital mechanics effects, the braking perturbs the original intercept trajectory significantly. Getting ahead of the braking schedule worsens this situation and demands more fuel usage to maintain the LOS trajectory.

A typical trajectory during braking is shown in figure 8-2. The trajectory assumes a constant deceleration which just satisfies the braking schedule; in other words, the average velocity between any two consecutive gates is the mean of the two gate velocities. The LOS angle (measured from $\bar{R}$) rotates clockwise at the LDEF orb rate, Ω_L, because the direction of the trajectory is fixed in space. This trajectory ended at 66° at 1000 feet. But, because of trajectory errors before and during braking, the final position at 1000 feet could be anywhere in the quadrant defined by $+\bar{V}$ and $+\bar{R}$.

9.0 Updating the Orbiter's State Vectors

At the completion of the burn schedule, the state of the Orbiter may be updated. The LDEF state in the inertial frame is very accurately known (with respect to time) from many weeks of ground track data. When the Orbiter is within 1000 feet of LDEF, the LDEF state vectors more accurately reflect the Orbiter's position than the Orbiter's state vectors, which were maintained by autonomous on-board navigation. As a

35

result, the crew "dumps" the Orbiter's state and substitutes LDEF's state vectors.

10.0 Translating to $\bar{R}$

While the Orbiter was braking, the co-pilot was preparing a new load of directions for the Universal Pointing System. After the state vector update and the completion of braking the load is entered and the DAP is placed in the Auto Mode. In response, the UPS provides commands to the DAP which causes the Orbiter's $+Y_B$ to point at a celestial reference equivalent to LDEF's $-\bar{H}$ (negative orbital momentum vector). In addition, the UPS load commands a "open loop" rotation rate about the vector. This UPS configuration is commonly referred to as the "barbecue mode." The rotation rate is presently proposed to be twice the LDEF orb rate and in the negative direction (i.e., counter clockwise about $-\bar{H}$).

As the orbiter begins rotating the COAS LOS also starts rotating. The effect is that the LDEF image in the COAS begins moving off center and towards $-X_B$ or the Orbiter's tail. The pilot reacts to this by translating the Orbiter with the THC (firing his nose jets and moving aft). This action causes the LDEF image to move back to the COAS center. The pilot continues to pull back on the THC (firing the nose jets) until the radar LOS Needle Display indicates an elevation rate of +2.27 milliradians per second (or $+2\Omega_L$). But Needle Display has poor resolution at this rate and the pilot must concentrate on stopping and centering the LDEF image in the COAS. When this occurs, the COAS

LOS and the radar LOS vectors are synchronously rotating in space. The Orbiter's attitude and trajectory during this combined rotation and translation is shown in Figure 10-1.

Though the COAS LOS and radar LOS are rotating inertially at $2\,\Omega_L$, they are only rotating at Ω_L in the LVLH frame. As a consequence it takes

$$t = \frac{66\ \text{deg.}}{\Omega_L} = \frac{66\ \text{deg.}}{.065\ \text{deg/sec}}$$

or 1015 seconds to reach $\bar{R}$. During this time it is very important to maintain the range at 1000 feet as indicated by radar. Orbital mechanics are always accelerating the Orbiter away from the LDEF. This acceleration is non-existent on $\bar{V}$ and increases to a maximum at $\bar{R}$ even though the range is maintained at 1000 feet. Allowing the range to open as $\bar{R}$ is approached causes the effect to become even more pronounced and would result in a significant fuel expenditure to recover.

The pilot can monitor his progress to $\bar{R}$ by observing the Aft ADI (sense switch to $-Z_B$). The ADI is in the LVLH mode. Since the Orbiter state was updated, the ADI reference is with respect to an LDEF centered LVLH frame. Some sampled readings are shown in figure 10-1. When the ADI reads 90, 0, 180 (pitch, yaw and roll respectively), the pilot knows he is directly below LDEF or on the LDEF radius vector to the center of the earth.

As a side note, suppose for some reason the rendezvous with LDEF should be delayed or aborted after the braking sequence. There is only one place where the Orbiter may efficiently station keep with the LDEF and

$156°$

$134°$

$112°$

$\overline{V}$

LDEF

$-Z_B$ LOS
R = 1000 ft.

$66°$

$44°$

$22°$

= 156
= 0
= 180

t_m

$-Z_B$ LOS
R = 1000 ft.

$-Z_B$ LOS
R = 1000 ft

P = 134
Y = 0
R = 180

t_m + 338 sec.

$-Z_B$ LOS
R = 1000 ft.

t_m + 677 sec.

P = 112
Y = 0
R = 180

t_m + 1015 sec
P = 90
Y = 0
R = 180

P
Y
R
} Aft ADI Readings
(−Z Sense Switch)

$\overline{R}$

t_m − Time at which Orbiter is Commanded
to Rotate at $-2\Omega_{LDEF}$ about $+Y_B$ axis
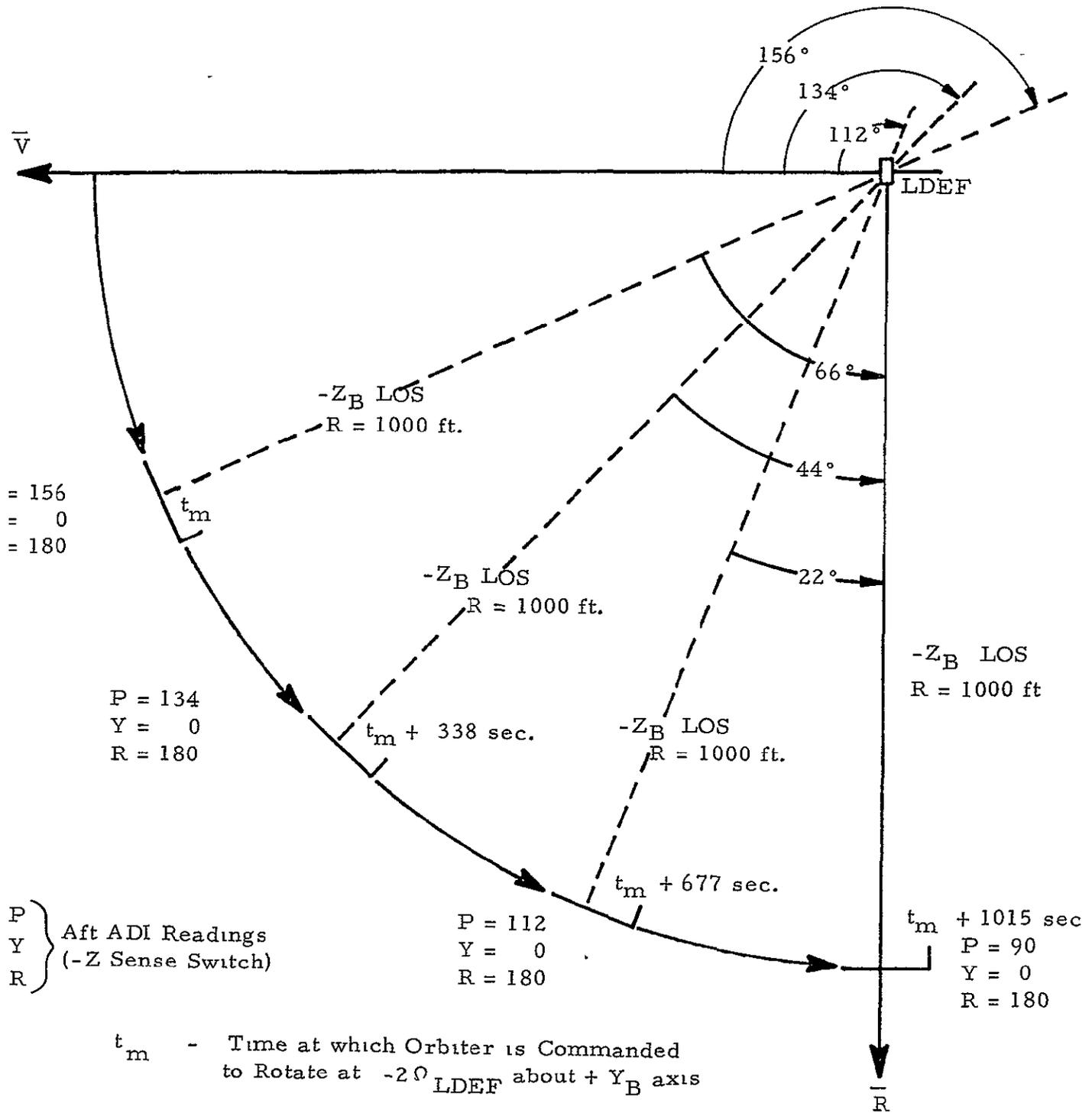
Figure 10-1.− Orbiter Translating to LDEF $\overline{R}$

38

that is on the LDEF orbital path or $\bar{V}$. Here there are no relative accelerations. The range rate may be nulled and a stand-off range maintained without thrusting (assuming no differential aerodynamic drag). To move to $\bar{V}$ the pilot need only retain attitude hold (DAP in Manual Mode) at the end of braking, maintain his range at 1000 feet, and translate to maintain LDEF centered in the COAS. Under these circumstances the Orbiter will move to $\bar{V}$ in the LDEF LVLH frame at an LOS angular rate of Ω_L. Inertially speaking the LOS is not rotating. Indeed, the radar LOS Needle Display reads 0 and 0. Instead, the LDEF $\bar{V}$ is rotating down to the Orbiter at $+\Omega_L$. Once again the pilot knows he has arrived on $\bar{V}$ when the aft ADI (sense switch to $-Z_B$) reads 180, 0, 180. From a fuel economy standpoint, moving $\bar{V}$ is a very cheap maneuver. The initialization of the Orbiter on $\bar{V}$ is similar to an initialization on $\bar{R}$, which will be discussed. Once a decision is made to rendezvous, moving the Orbiter to $\bar{R}$ is accomplished as explained.

11.0 Initializing on $\bar{R}$

When the Orbiter arrives at the LDEF $\bar{R}$, the UPS load is changed to place the Orbiter in an earth track mode. The new UPS load is:

1. Point $+Z_B$ at the earth.

2. Omicron = 0 degrees.

The Omicron specifies an orientation about $+Z_B$ such that $+Y_B$ is pointed along the negative LDEF momentum vector, $-\bar{H}_L$.[1]

---

[1]There are situations (see section 20.0) where an Omicron of 180 degrees would be specified. This would cause $+X_B$ to point along $-\bar{V}_L$ instead of $+\bar{V}_L$.

39

The new UPS load does not cause an Orbiter attitude change.
Instead, it removes the Orbiter from the "open loop," constant rate,
barbecue mode about $+Y_B$ to a "closed loop," controlled orientation about
$+Y_B$. If LDEF is in a circular orbit, the angular rate about $+Y_B$ will
be constant (at Ω_L) as $+Z_B$ tracks the earth's center. If LDEF is in an
elliptical orbit, the angular rate will vary because the sweep rate
of $\bar{R}$ varies with the LDEF position in the orbit.

Next, the pilot must concentrate on maintaining his position on
$\bar{R}_{LDEF}$. It will be recalled that the radar LOS is rotating at $2\ \Omega_L$ as
$\bar{R}$ is approached. But now the radar LOS must be slowed to the $\bar{R}_L$ sweep
rate. Using the THC the pilot fires the Orbiter's tail jets until the
radar LOS Needle Display indicates $+1.13$ milliradians per second, the
LDEF orb rate. At the same time the pilot observes the LDEF position
in the COAS. His objective is to have the LDEF centered in the COAS
when the LOS Needles indicate the LDEF orb rate. When this occurs, the
radar LOS (representing relative position) is once again synchronized
with the UPS controlled COAS LOS. If the LDEF is centered in the COAS
and the LOS Needles read less than orb rate, the Orbiter is moving
ahead of LDEF in the LVLH frame. If the LDEF is centered in the
COAS and the LOS Needles read more than orb rate, the Orbiter is
falling behind LDEF. Throughout these adjustments, the pilot uses
only the THC. Touching the RHC would immediately drop the DAP from
the Auto Mode to the Manual Mode; the Orbiter would revert to inertial
attitude hold and UPS commands would be ignored.

12.0 The $\bar{R}$ Approach

During initialization on $\bar{R}_L$, the Orbiter is constantly accelerating away from LDEF. The pilot must thrust upward just to maintain his range at 1000 feet. An explanation of this lies in orbital mechanics. But even in the world of engineers, orbital mechanics is a relatively mysterious and esoteric subject. Fortunately the $\bar{R}$ approach possesses characteristics which make it amenable to straightforward explanations.

Station keeping on $\bar{R}_L$ at 1000 feet below LDEF is not a natural situation. This can be explained with the aid of figures 12-1 and 12-2. Assume that the Orbiter and LDEF are in two concentric circular orbits but LDEF is in the higher orbit. The Orbiter's orbit will have a shorter period, or its orbital rate, Ω_o, will be faster than LDEF's orbital rate, Ω_L. If at some time, t_o, the two orbits share a common radius vector, they will subsequently separate with a phase angle of $(\Omega_o - \Omega_L)$ times $(t - t_o)$ as shown in figure 12-1. When initializing on $\bar{R}_L$, the differential orbital rate is reduced to zero, but the differential altitude is maintained at 1000 feet. In this situation the tangential velocity of the Orbiter is insufficient for a circular orbit. Indeed, if the Orbiter were released from the $\bar{R}_L$ through lack of THC commands from the pilot, the Orbiter would fall away from LDEF and along an elliptical orbit. An exaggerated depiction of this is shown in figure 12-2. Figure 12-3 shows this same effect in the LVLH frame. Note that the first motion after release is downward. This reduces the radius vector, or moment arm, and through conservation of angular momentum the Orbiter's orbital sweep rate, Ω_o, increases and the Orbiter moves ahead of LDEF.

41
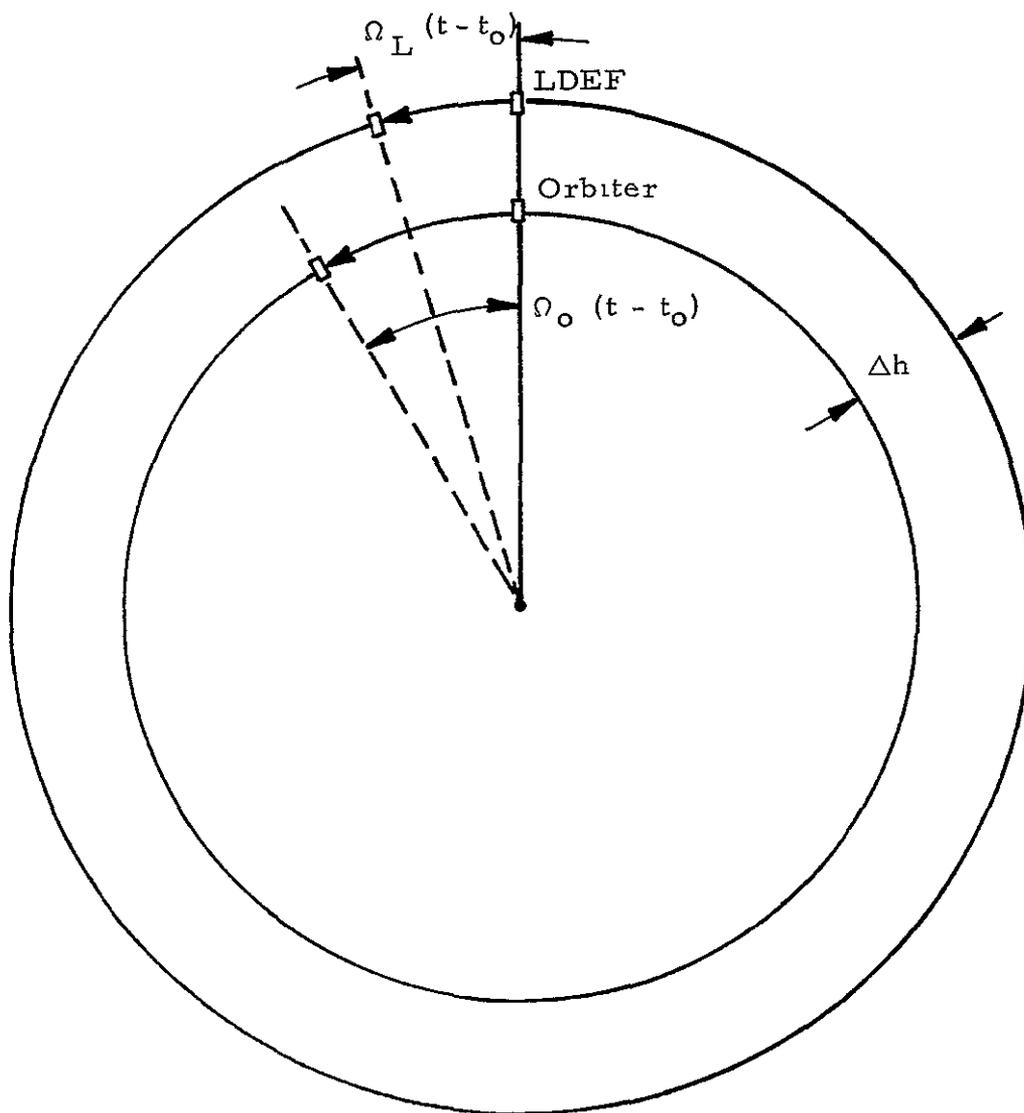
Figure 12-1.- Phasing of Two Circular Geocentric Orbits
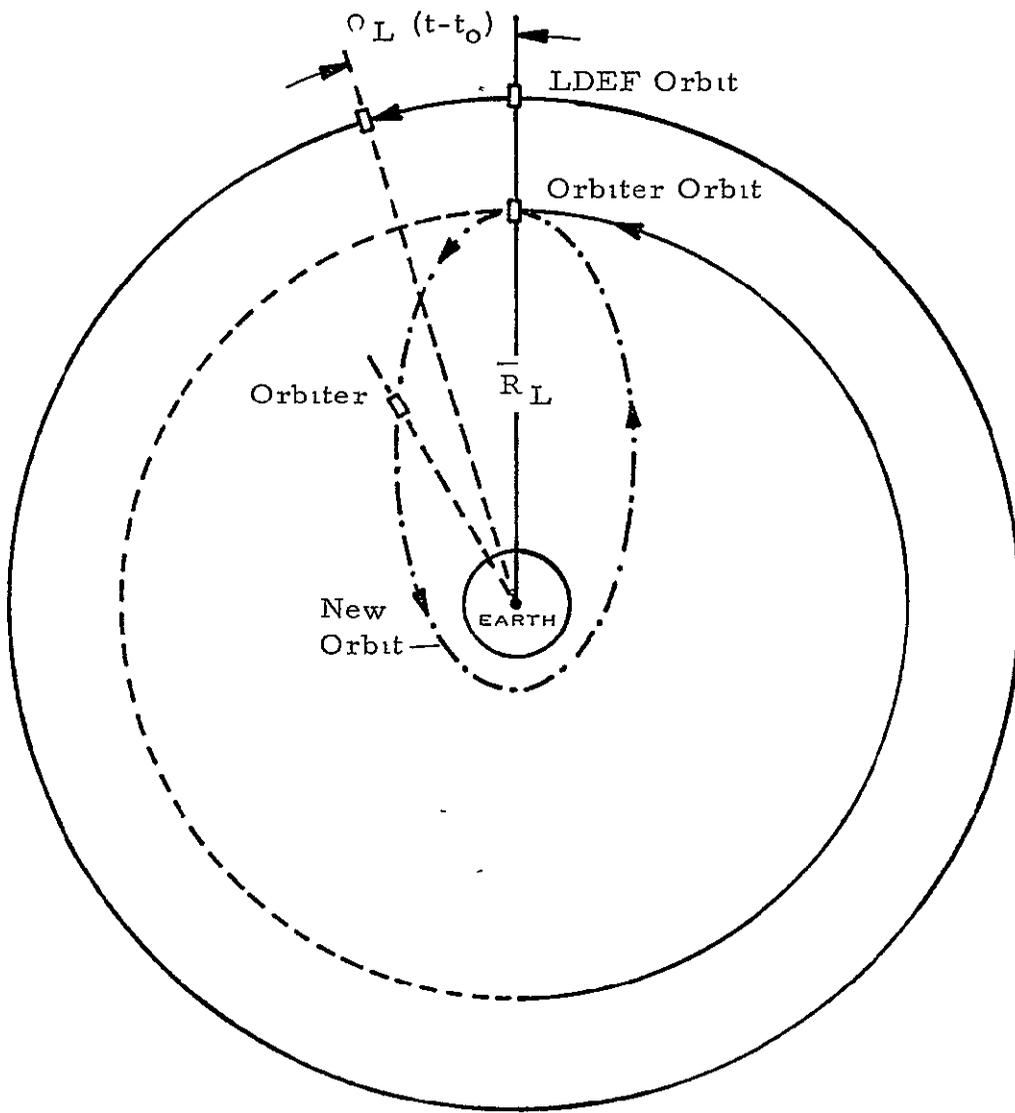
Figure 12-2.- Releasing the Orbiter from $\bar{R}_L$

43

$\bar{V} \leftarrow$

$\bar{V} \leftarrow$

$\bar{V} \leftarrow$

$\bar{V} \leftarrow$

1000 ft

INITIALIZE
WITH ZERO
RELATIVE RATES

ⓐ

ⓑ

ORBITER MOVEMENT
WITHOUT PILOT
ACTION

ⓒ

ORBITER TRANSLATING
TO REMAIN ON $\bar{R}$ WILL
MOVE DOWNWARD

PILOT HOLDS $\bar{R}$ POSITION
AND TRANSLATES UPWARD ⓓ
- ORBITAL MECHANICS
  PROVIDES BRAKING
  FORCES

$\bar{R}$

$\bar{R}$

$\bar{R}$

$\bar{R}$
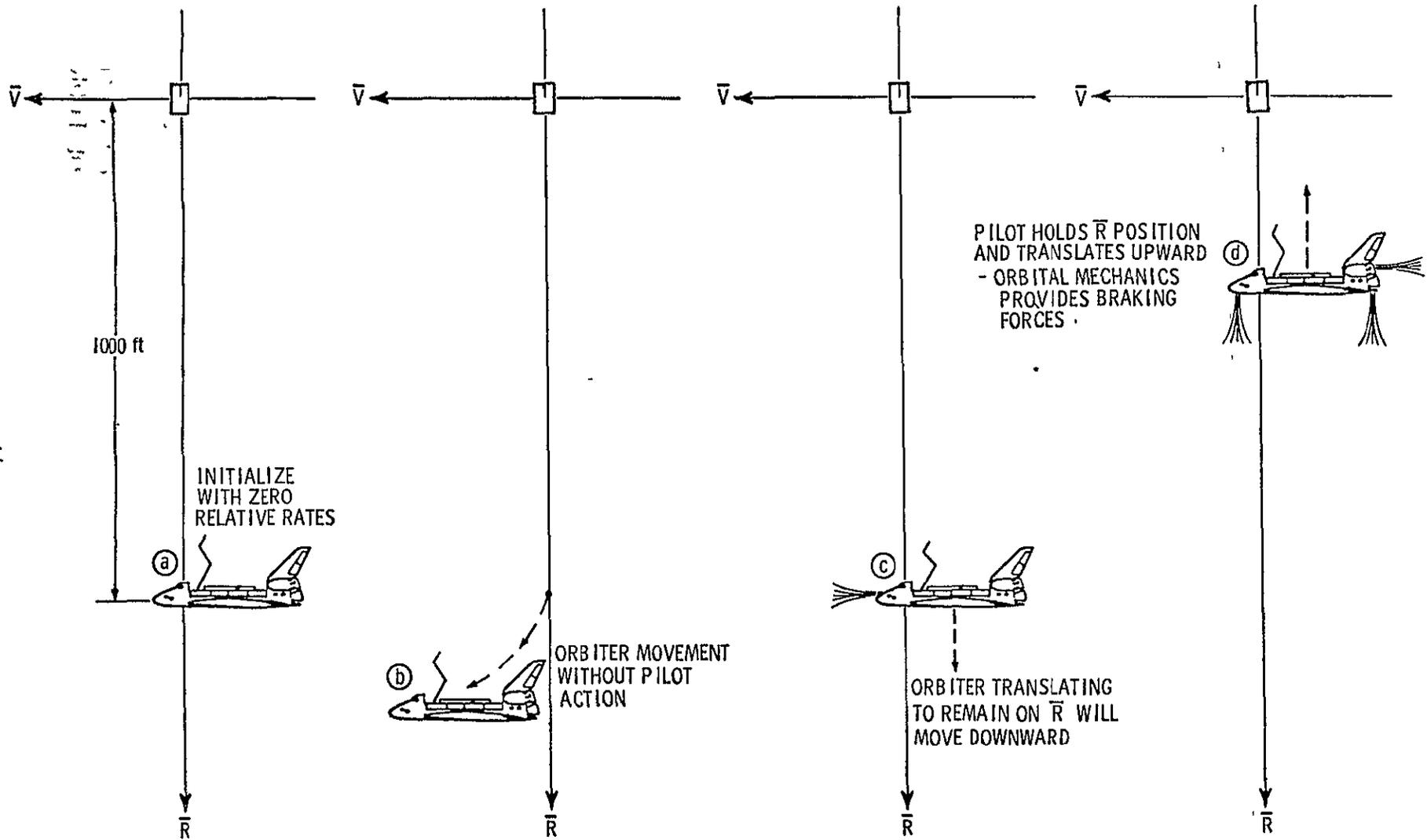
Figure 12-3.- The $\bar{R}$ Approach in the LVLH Frame

Now consider the thrusting requirements to maintain the Orbiter's position on $\bar{R}_L$ at 1000 feet. This may be accomplished by writing an equation which relates all of the forces acting on the Orbiter and directed along $\bar{R}_L$, or

$$F_T + F_c = F_g$$

where
F_T = upward thrusting force along $\bar{R}_L$

F_c = centrifugal force (upward)

F_g = gravitational force (downward)

Rearranging,

$$F_T = F_g - F_c$$

Most engineers will recall that

$$F_g = G \frac{m_1 m_2}{r^2}$$

where
F_g = gravitational attraction force between two bodies

G = universal gravitational constant

m_1 = mass of the first body

m_2 = mass of the second body

r = distance between the centers of the two bodies

In orbital mechanics terminology,

$$F_g = \frac{\mu_e m_o}{r_o^2}$$

where
μ_e = Earth's gravitational constant = Gm_e

m_o = mass of the Orbiter

45

r_o = Orbiter's radial distance from the center of the Earth

It should also be recalled that the common expression for centrifugal acceleration, $\ddot{r}_c$, is

$$\dot{r}_c = \omega^2 r$$

where
ω = angular velocity in radians per second

r = moment arm

Returning to orbital mechanics terminology

$$F_c = m_o \ddot{r}_c = m_o \Omega_o^2 \, r_o$$

where
Ω_o = Orbiter's orbital sweep rate in radians per second

Thus,

$$F_T = \frac{\mu \, m_o}{r_o^2} - m_o \Omega_o^2 \, r_o$$

If the orbiter were in its own natural circular orbit, F_T would be equal to zero because

$$m_o \Omega_o^2 r_o = \frac{\mu m_o}{r_o^2}$$

or

$$\Omega_o = \frac{1}{r_o} \left(\frac{\mu}{r_o}\right)^{1/2}$$

But during the $\bar{R}$ approach Ω_o is initialized to be equal to the LDEF orbital rate, Ω_L, or

$$\Omega_o = \Omega_L = \frac{1}{r_L} \left(\frac{\mu}{r_L}\right)^{1/2}$$

Substituting Ω_L for Ω_o gives

$$F_T = \frac{\mu m_o}{r_o^2} - \frac{\mu m_o r_o}{r_L^3}$$

but

$$r_o = r_L - R$$

where R is the Orbiter's range from LDEF along $\bar{R}_L$. Finally,

$$F_T = \frac{\mu m_o}{(r_L - R)^2} - \frac{\mu m_o (r_L - R)}{r_L^3}$$

where

$$m_o = \frac{W_o}{g_e} = \frac{\text{Orbiter's weight}}{\text{one earth g}}$$

$$r_L = h_L + r_e$$

$$= \text{LDEF orbital altitude} + \text{Earth's equatorial radius}$$

Let

$$\mu = 1.4077 \times 10^{16} \text{ ft}^3/\text{sec}^2$$

$$W_o = 180,000 \text{ lbs.}$$

$$h_L = 190 \text{ n. miles} = 1.154462 \times 10^6 \text{ ft.}$$

$$r_e = 6378.163 \text{ km} = 2.0925732 \times 10^7 \text{ ft.}$$

Some representative values of the F_g, F_c, and their differences, F_T, are listed in Table 12-1 as a function of range, R.

Two facts are readily apparent from table 12-1. First, over the ranges presented, F_T grows linearly with R. This suggests that the equation for F_T may be reduced to a simpler form. Second, with opening range the gravitational force, F_g, _increases_ twice as fast as the centrifugal force, F_c, _decreases._ This is confirmed by taking the partial of F_T with respect to R, that is,

$$\frac{\partial F_T}{\partial R} = \frac{\partial F_g}{\partial R} - \frac{\partial F_c}{\partial R}$$

47

Table 12-1. – Orbital Mechanics Forces During an $\bar{R}$ Approach

R (ft.)	F_g (lbs)	F_c (lbs)	F_T (lbs)
0	161406.48	161406.48	0.00
20	161406.78	161406.34	0.44
100	161407.95	161405.75	2.19
200	161409.41	161405.02	4.39
300	161410.87	161404.29	6.58
400	161412.33	161403.56	8.77
500	161413.79	161402.83	10.97
600	161415.26	161402.10	13.16
700	161416.72	161401.37	15.35
800	161418.18	161400.63	17.54
900	161419.64	161399.90	19.74
1000	161421.10	161399.17	21.93
1100	161422.57	161398.44	24.12
1200	161424.03	161397.71	26.32
1500	161428.42	161395.52	32.90
2000	161435.73	161391.86	43.86

$$\frac{\partial F_c}{\partial R} = \frac{\partial}{\partial R} \left\{ \frac{\mu m_o \ (r_L - R)}{r_L^3} \right\} = \frac{-\mu m_o}{r_L^3}$$

$$\frac{\partial F_g}{\partial R} = \frac{\partial}{\partial R} \left\{ \frac{\mu m_o}{(r_L - R)^2} \right\}$$

$$= 2 \ \mu m_o \ (r_L - R)^{-3}$$

$$= \frac{2 \ \mu m_o}{r_L^3} \left(1 - \frac{R}{r_L} \right)^{-3}$$

Using the binomial expansion,

$$\left(1 - \frac{R}{r_L} \right)^{-3} = 1 + \frac{3R}{r_L} + \frac{3(4)}{2!} \left(\frac{R}{r_L} \right)^2 + \cdots$$

Since

$$\frac{R}{r_L} = \frac{10^3}{22 \ X \ 10^6} = 4.5 \ X \ 10^{-5}$$

$$\left(1 - \frac{R}{r_L} \right)^{-3} = 1 \ \text{within} \ 136 \ \text{ppm}$$

and

$$\frac{\partial F_g}{\partial R} = \frac{2\mu m_o}{r_L^3}$$

Finally,

$$\frac{\partial F_T}{\partial R} = \frac{2\mu m_o}{r_L^3} + \frac{\mu m_o}{r_L^3}$$

and

$$F_T = R \ \frac{\partial F_T}{\partial R} = \frac{3\mu m_o R}{r_L^3}$$

This is the reduced but very accurate form of F_T for proximity operations.

It is important at this point that the real significance of F_T be appreciated. That is, an "artificial" circular orbit with an orbital rate of Ω_L can be maintained at some reasonable range below LDEF if the appropriate thrust, F_T, is precisely and continuously applied. The initialized range remains constant which dictates that the orbiter's angular momentum is invariant. Thus no thrusting either along or against the orbiter's velocity vector is required to maintain the orbiter on $\bar{R}_L$ as the two bodies circle the Earth. If less than F_T is applied, the Orbiter starts to fall and move forward. If more than F_T is applied, the Orbiter climbs toward LDEF and moves behind. In each case conservation of angular momentum applies if no forward or aft jets are fired.

Since the Orbiter is always accelerating away from LDEF, it is possible to insert a closing range rate which would decay to zero as a desired range is achieved. The history of $\dot{R}$ versus R is not obvious because the acceleration decays as the range collapses. The solution is simplified if it is assumed that the pilot maintains the Orbiter on $\bar{R}_L$ during the ascent. Then,

$$\ddot{R} = \frac{F_T}{m_o} = \frac{3\mu R}{r_L^3}$$

Letting $\qquad C = \frac{3\mu}{r_L^3}$

$$\ddot{R} - CR = 0$$

but
$$\dot{R} = \frac{dR}{dt} = \frac{d\dot{R}}{dR}\frac{dR}{dt} = \frac{d\dot{R}}{dR}\dot{R}$$

Therefore

$$\dot{R}\frac{d\dot{R}}{dR} = CR$$

$$\int_{\dot{R}_o}^{\dot{R}} \dot{R}\,d\dot{R} = C\int_{R_o}^{R} R\,dR$$

$$\frac{\dot{R}^2}{2}\left|\begin{matrix}\dot{R} = \dot{R}\\[2mm]\dot{R} = \dot{R}_o\end{matrix}\right. = \frac{CR^2}{2}\left|\begin{matrix}R = R\\[2mm]R = R_o\end{matrix}\right.$$

Finally,

$$\dot{R}^2 - \dot{R}_o^2 = C\,(R^2 - R_o^2)$$

where

$\dot{R}$ = <u>opening</u> range rate

$\dot{R}_o$ = initial <u>opening</u> range rate

R = range

R_o = initial range below LDEF

The first integral solution is a hyperbolic function. If $\dot{R}_o$ is set equal to zero,

$$\dot{R} = m\,(R^2 - R_o^2)^{1/2}$$

where $m = (C)^{1/2} = \left(\dfrac{3\mu}{r_L^3}\right)^{1/2} = 1.98 \times 10^{-3}\ \text{sec}^{-1}$

51

Plots* of this equation for a variety of R_o's are shown in figure 12-4. They are a family of hyperbolas with a straight line asymptote of mR. Each plot shows the range rate versus range if the Orbiter is allowed to separate along the LDEF radius vector. For example, if the range is 300 feet at release, the Orbiter will accelerate from a zero range rate to approximately 1.8 fps at 1000 feet. Conversely, if a _closing_ range rate of 1.8 fps is inserted at 1000 feet, the Orbiter will stop and begin to fall back at a range of 300 feet. In the latter case, the parameters may be redefined such that the equation reads

$$\dot{R} = m \ (R^2 - R_S^2)^{1/2}$$

where

$\dot{R}$ = _closing_ range rate, at R, which is required to stop

at R_S

R_S = desired station keeping range for retrieval operations

Obviously upward thrust would still be required to maintain a fixed station keeping range. But the magnitude of the thrust would become quite small for close proximity operations.

As previously mentioned, conservation of angular momentum dictates that the Orbiter's tangential velocity will decrease during the ascent to LDEF. Therefore, some thrusting along $\bar{V}$ is required to remain on

*The curves in figure 12-4 were plotted by a JSC computer which used the Clohessy Wiltshire equations of relative orbital motion and assumed the Orbiter was maintained within one degree of $\bar{R}_L$ after release. Although an m of 1.98×10^{-3} sec.$^{-1}$ was computed by the writer, the curves indicate an m of 1.96×10^{-3} sec.$^{-1}$. This can be explained by small differences in the input parameters.
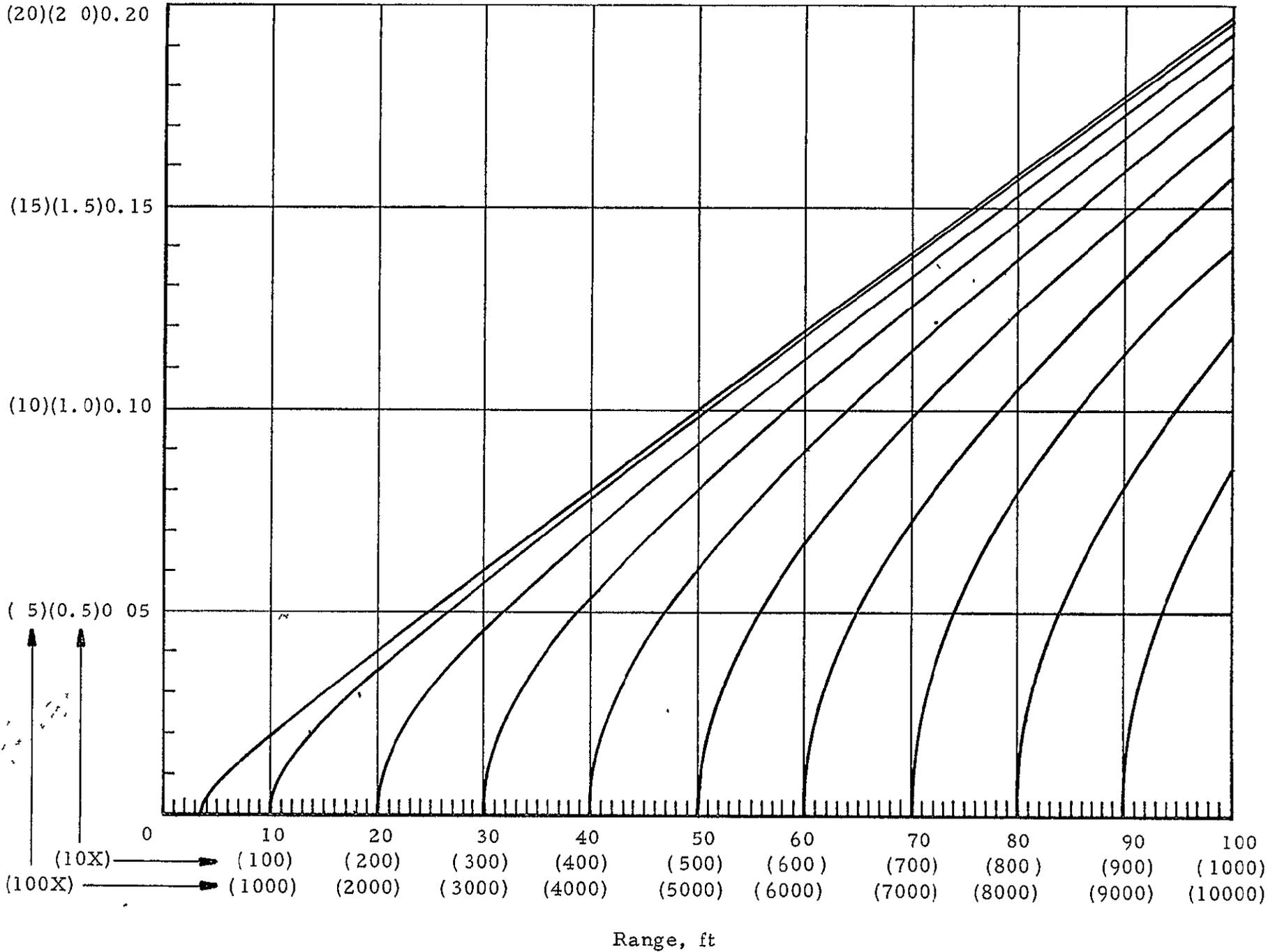
Figure 12-4.— The $\bar{R}$ Approach in the State Domain of Range and Range Rate

53

$\bar{R}_L$ _during_ the ascent. This may be expressed by

$$\frac{dV_o}{dt} = -\Omega_L \frac{dR}{dt} = -\Omega_L \dot{R}$$

where V_o is the Orbiter's tangential velocity. Since $\dot{R}$ is maximum when the ascent is initiated, the tangential thrusting requirements are also maximum at that point. The total ΔV_o required during the ascent is

$$\Delta V_o = -\Omega_L \Delta R = -\frac{1}{r_L} (\frac{\mu}{r_L})^{1/2} \Delta R$$

If R_S equals 20 feet and the initial R equals 1000 feet,

$$\Delta R = - (R - R_S) = - 980 \text{ feet}$$

and

$$\Delta V_o = (1.14 \times 10^{-3}) \Delta R = 1.12 \text{ fps}$$

Heretofore, the Orbiter's motion along $\bar{R}_L$ has been described in the state domain of $\dot{R}$ versus R. The motion may be described in the time domain by completely solving the original differential equation of

$$\dot{R} - RC = 0$$

Using Laplace transforms, let the initial conditions be defined as

$$\dot{R}(0^+) = \dot{R}_o$$

$$R(0^+) = R_o$$

54

then,

$$s^2 R(s) - s R_o - \dot{R}_o - CR(s) = 0$$

and,

$$R(s) = \frac{R_o s + \dot{R}_o}{(s - \sqrt{C})(s + \sqrt{C})}$$

$$= \frac{K_1}{s - \sqrt{C}} + \frac{K_2}{s + \sqrt{C}}$$

$$K_1 = \left[\frac{R_o s + \dot{R}_o}{s + \sqrt{C}} \right]_{s=\sqrt{C}} = \frac{R_o \sqrt{C} + \dot{R}_o}{2\sqrt{C}}$$

$$K_2 = \left[\frac{R_o s + \dot{R}_o}{s - \sqrt{C}} \right]_{s=-\sqrt{C}} = \frac{R_o \sqrt{C} - \dot{R}_o}{2\sqrt{C}}$$

Substituting and taking the inverse of R(s) yields the general solution,
or

$$R = \left(\frac{R_o}{2} + \frac{\dot{R}_o}{2\sqrt{C}} \right) e^{\sqrt{C}\, t} + \left(\frac{R_o}{2} - \frac{\dot{R}_o}{2\sqrt{C}} \right) e^{-\sqrt{C}\, t}$$

Let

$$\tau = \frac{1}{\sqrt{C}} = \text{time constant}$$

Then

$$R = \frac{1}{2}(R_o + \tau\dot{R}_o)\, e^{t/\tau} + \frac{1}{2}(R_o - \tau\dot{R}_o)e^{-t/\tau}$$

and

$$\dot{R} = \frac{dR}{dt} = \frac{1}{2}\left(\frac{R_o}{\tau} + \dot{R}_o\right)e^{-t/\tau} - \frac{1}{2}\left(\frac{R_o}{\tau} - \dot{R}_o\right)e^{-t/\tau}$$

The time constant, τ, can be expressed in terms of a variety of parameters. For example,

$$\tau = \frac{1}{m} = \frac{1}{1.96 \times 10^{-3}} = 510.20 \text{ sec.}$$

55

where m is the slope of the straight line asymptote of $\dot{R}$ versus R. Also,

$$\tau = \frac{1}{\sqrt{3} \ \Omega_L} = \frac{T_L}{2\pi \ \sqrt{3}} = \frac{T_L}{10.88}$$

where T_L is the LDEF orbital period.

A physical understanding of the general solutions for R and $\dot{R}$ may be obtained from some special cases. The first example is perhaps the most poignant. Assume that a closing $\dot{R}_o$ equivalent to $\frac{R_o}{\tau}$ (or mR_o, the asymptote value) is introduced at a range of R_o. The general solution for R reduces to

$$R = R_o e^{-t/\tau}$$

In other words, an infinite amount of time is required to reach LDEF. (Sometimes this is more easily understood in terms of separating from LDEF, i.e., if the initial range is extremely small, the acceleration at release will also be extremely small). If m equals 1.96×10^{-3} a closing rate of 1.96 fps at 1000 feet will create this situation, or

$$R = 1000 e^{-t/\tau}$$

A plot of this equation is shown in figure 12-5. In reality the desired final range is 20 feet. The time to travel from 1000 feet to 20 feet is expressed by

$$t = -\tau \ \ln \left(\frac{R_S}{1000}\right) \quad \text{where } R_S = 20 \text{ ft.}$$

Thus,
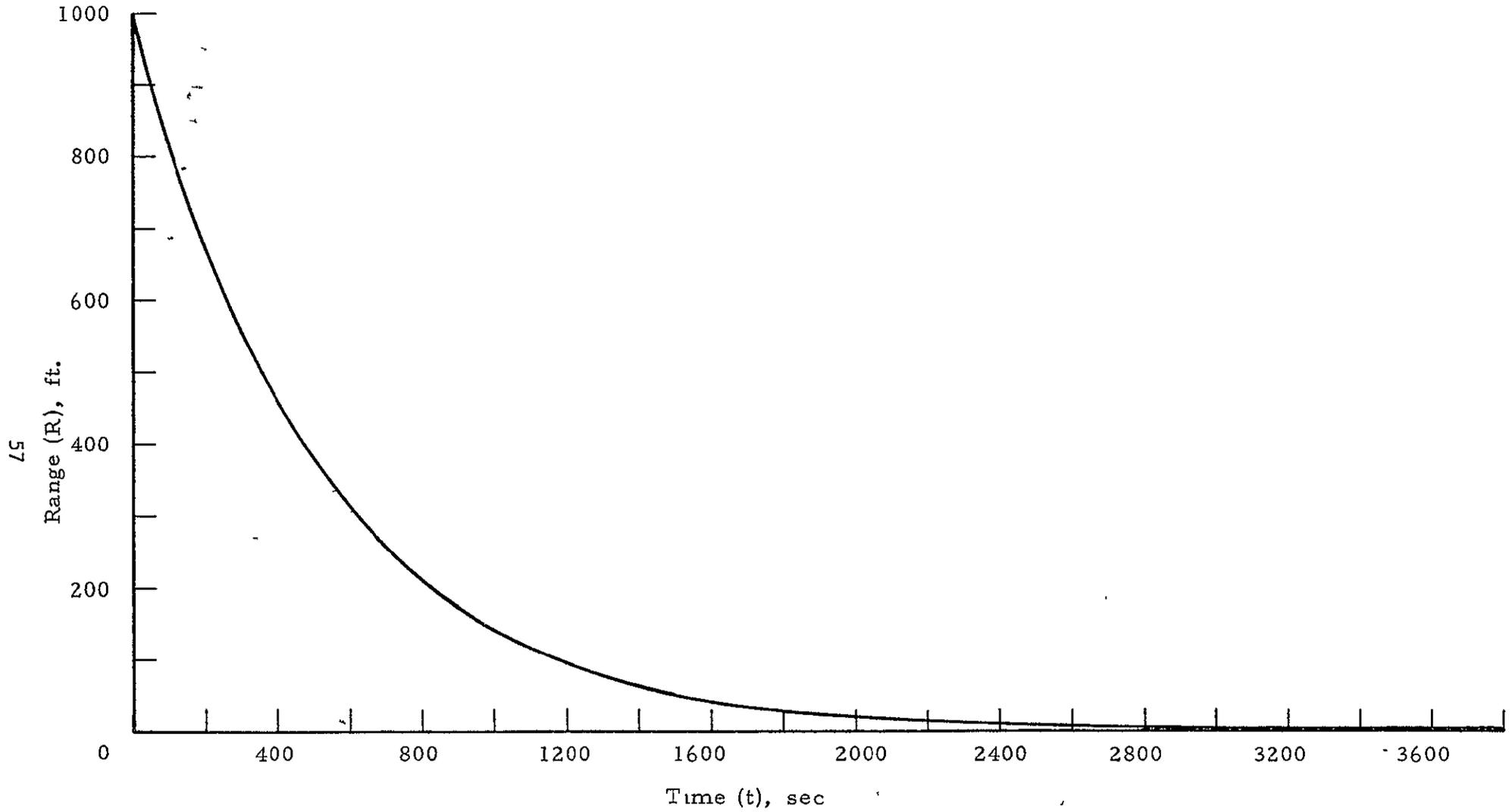
Figure 12-5.- Range Versus Time when following the Hyperbolic Asymptote in the Ṙ versus R Domain

$$t = 1996 \text{ seconds or } 33.3 \text{ minutes}$$

It is interesting to note that the range collapses to 50 feet in 3 time constants or 1531 seconds. But, 465 seconds is required to travel the remaining 30 feet. The closing rate at 20 feet, where some braking is required, is obviously quite small. For this special case,

$$\dot{R} = \frac{dR}{dt} = \frac{-R_o}{\tau} e^{-t/\tau}$$

Thus, $\dot{R}$ equals -0.039 fps at 20 feet.

Another special case may be created by setting $\dot{R}_o$ equal to zero in the general solution. This makes

$$\frac{R}{R_o} = \frac{e^{t/\tau} + e^{-t/\tau}}{2} = \cosh\left(\frac{t}{\tau}\right)$$

Thus, if the Orbiter is released along $\bar{R}_L$ with zero initial range rate, the same amount of time is required to fall from 10 feet to 100 feet as is required to fall from 100 feet (with zero initial rate) to 1000 feet. Conversely, if the required closing $\dot{R}_o$'s to stop at 100 and 10 feet are precisely inserted at 1000 feet and 100 feet, respectively, both the 900 feet and 90 feet of travel require the same amount of time.

A very useful form of the last equation is obtained by solving for the inverse hyperbolic cosine; that is,

$$\frac{t}{\tau} = \cosh^{-1}\left(\frac{R}{R_o}\right)$$

or

Table 12-2. – Optimum $\bar{R}$ Approach Times

$\frac{R}{R_o}$	$\frac{t}{\tau}$	t (sec)	t (min)
1.5	0.962	491	8.18
2.0	1.317	672	11.20
3.0	1.763	899	14.99
4.0	2.063	1053	17.55
5.0	2.292	1170	19.49
10.0	2.993	1527	25.45
20.0	3.688	1882	31.36
30.0	4.094	2089	34.81
40.0	4.382	2236	37.26
50.0	4.605	2350	39.16
100.0	5.298	2703	45.05
1000.0	7.601	3878	64.63

$$\frac{t}{\tau} = \ln \{\frac{R}{R_0} + [(\frac{R}{R_0})^2 - 1]^{1/2}\} \quad (\text{for } \frac{R}{R_0} \geq 1)$$

Some values of t/τ and t (for a τ of 510.2 sec) corresponding to a variety of representative $\frac{R}{R_0}$'s are provided in Table 12-2. Note that if the desired station keeping range is 20 feet, it should take, theoretically, only 6 minutes longer to start from 2000 feet rather than 1000 feet.

Some readers may find the following expansion[1] to be useful.

$$\frac{t}{\tau} = \cosh^{-1} (\frac{R}{R_0})$$

$$= \ln (\frac{2R}{R_0}) - \frac{1}{4} (\frac{R_0}{R})^2 - \frac{3}{32} (\frac{R_0}{R})^4 - \cdots$$

$$(\text{for } |\frac{R}{R_0}| > 1)$$

If one minute is the required accuracy, it may be shown that

$$\frac{t}{\tau} \cong \ln (\frac{2R}{R_0}) \quad (\text{for } \frac{R}{R_0} \geq 1.566)$$

13.0 $\bar{R}$ Approach Sensitivity

Referring to the family of curves given in figure 12-4, the top curve (in the 10X scale) represents the range rate, at a given range,

---

[1] Milton Abramowitz and Irene A. Stegun (ed.), <u>Handbook of Mathematical Functions</u> (New York: Dover Publications, Inc., 1965), p. 88.

which will cause the Orbiter to stop at 35 feet. This curve is a plot
of the hyperbolic function,

$$\dot{R}_{max} = m(R_T^2 - R_S^2)^{1/2}$$

where

$\dot{R}_{max}$ = maximum allowable closing range rate to avoid

braking at R_S

m = slope of the hyperbola's straight line asymptote

R_T = true range

R_S = station keeping range (in this case 35 feet)

Because the pilot has imperfect knowledge of range and range rate, any
attempt to follow the optimum curve can result in either a "hot" or
"cold" approach. Cold trajectories are those which stop short of R_S.
Hot trajectories are those which have a residual velocity when R_S is
reached. When using the 1X scale of figure 12-4, four hot trajectories
are presented. They stop at 30, 20, 10 and 3.5 feet. Each hot
trajectory is the result of exceeding $\dot{R}_{max}$, in increasing amounts, at
any range out to the start point or 1000 feet. The hyperbolic asymptote
defines a special $\dot{R}_{max}$ which if exceeded, causes a residual $\dot{R}$ to exist
at zero range. The trajectories in this category are defined by a
family of hyperbolas which have their foci on the $\dot{R}$ axis. A complete
set of representative hot and cold trajectories for ascending and
descending $\bar{R}$ approaches is shown in figure 13-1.

The sensitivity of the $\bar{R}$ approach to range rate errors, $\delta\dot{R}$, can
be shown by differencing the equations for two hyperbolas.

61

Range
Rate
$(\dot{R})$

ASCENDING

Hot Ascending
Approach

This Area
Presented
in Fig. 12-4

R_S

ABOVE

Cold Ascending Approach

R_S

Range (R)

BELOW

Cold Descending
Approach

Hot
Descending
Approach

DESCENDING
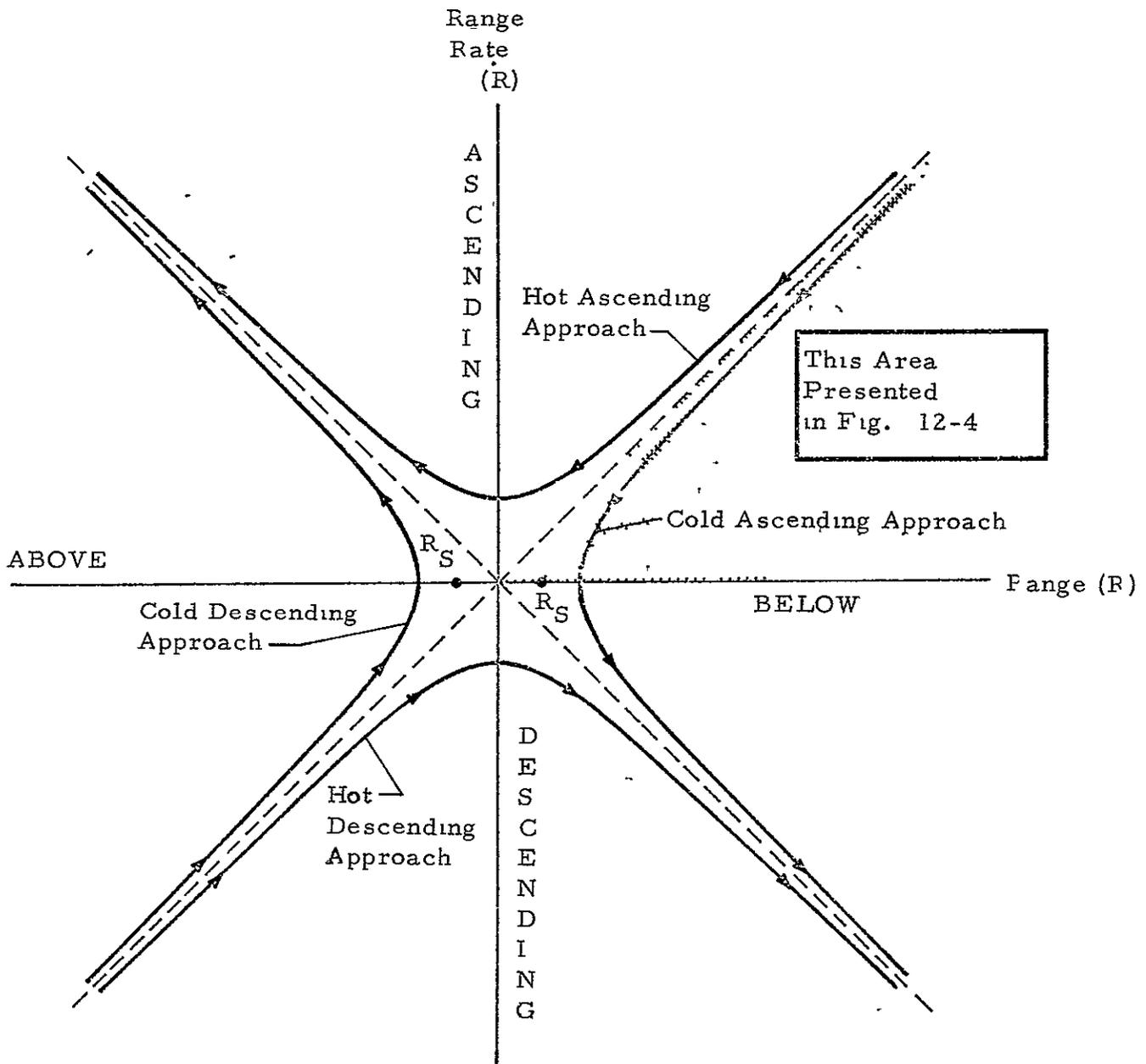
R_S - Desired Station Keeping Range

Figure 13-1.- Hot and Cold $\dot{R}$ Approaches

62

$$\dot{\delta R} = \dot{R}_{max_2} - \dot{R}_{max_1}$$

where $\dot{R}_{max_2}$ = maximum allowable closing range rate to stop at R_{S_2}

$\dot{R}_{max_1}$ = maximum allowable closing range rate to stop at R_{S_1}

$\dot{\delta R}$ = the difference in range rate at some given range

which will cause the Orbiter to stop at R_{S_2} instead

of R_{S_1}.

This may be simplified by letting R_{S_2} equal zero and R_{S_1} equal the

desired station keeping range, R_S. Then,

$$\dot{\delta R} = mR_T - m(R_T^2 - R_S^2)^{1/2} \qquad \text{(for } R_T \geq R_S\text{)}$$

$$= \text{asymptote limit} - \dot{R}_{max}$$

When R_T equals R_S, $\dot{\delta R}$ equals mR_S. As R_T becomes larger and larger,

$\dot{R}_{max}$ approaches mR_T, the asymptote, and $\dot{\delta R}$ approaches zero.

Now suppose that the $\dot{R}$ limit defined by the asymptote is exceeded

at some time during the approach. In this case, orbital mechanics

braking is still decelerating the Orbiter with respect to the target,

but insufficient range exists to entirely "bleed off" the closing

range rate. In such situations the trajectories are defined by

$$\dot{R}'_{max} = [\dot{R}_o^2 + (mR_T)^2]^{1/2}$$

where $\dot{R}_o$ = residual closing range rate at zero range

m = slope of the asymptote common to both hot and cold

approaches

$\dot{R}'_{max}$ = maximum allowable closing rate to avoid exceeding

$\dot{R}_o$ at zero range.

(As mentioned earlier, this equation defines a family of hyperbolas which have their foci on the $\dot{R}$ axis). If R equals R_S, $\dot{R}'_{max}$ is the braking ΔV, $\dot{R}_b$, required to stop at R_S. Or,

$$\dot{R}_b = (\dot{R}'_{max})_{R=R_S} = [\dot{R}_o^2 + (m\ R_S)^2]^{1/2}$$

The objective is to get $\dot{R}'_{max}$ in a form where it is expressed as a function of $\dot{R}_b$ and R. Rearranging the preceding equation gives

$$\dot{R}_o^2 = \dot{R}_b^2 - (mR_S)^2$$

Substituting this into $\dot{R}'_{max}$ gives

$$\dot{R}'_{max} = [\dot{R}_b^2 - (mR_S)^2 + (mR_T)^2]^{1/2}$$

Now the difference between $\dot{R}'_{max}$ and $\dot{R}_{max}$ is the allowable range rate error, $\delta\dot{R}$, as a function of range which will create a braking requirement of $\dot{R}_b$ at R_S. That is,

$$\delta\dot{R} = \dot{R}'_{max} - \dot{R}_{max}$$

$$= [\dot{R}_b^2 - (mR_S)^2 + (mR_T)^2]^{1/2} - m[R_T^2 - R_S^2]^{1/2}$$

$$(\text{for } R_T \geq R_S)$$

Figure 13-2 presents representative plots of $\delta\dot{R}$. Both curves assume that R_S equals 20 feet and m equals 1.96×10^{-3} sec^{-1}. The top curve assumes that 0.5 fps may be removed near the target. The bottom curve
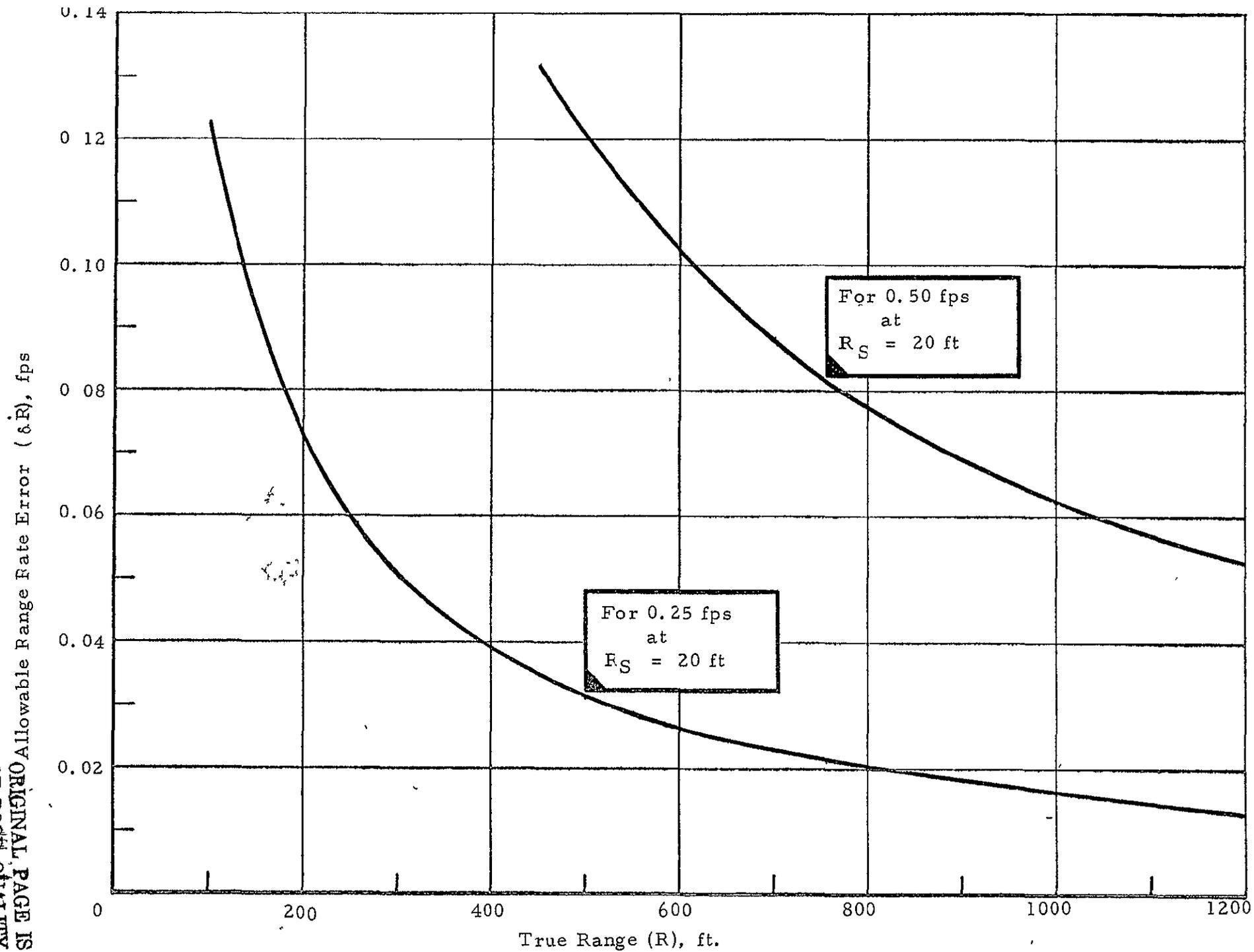
Figure 13-2.- Allowable Range Rate Errors Versus True Range

65
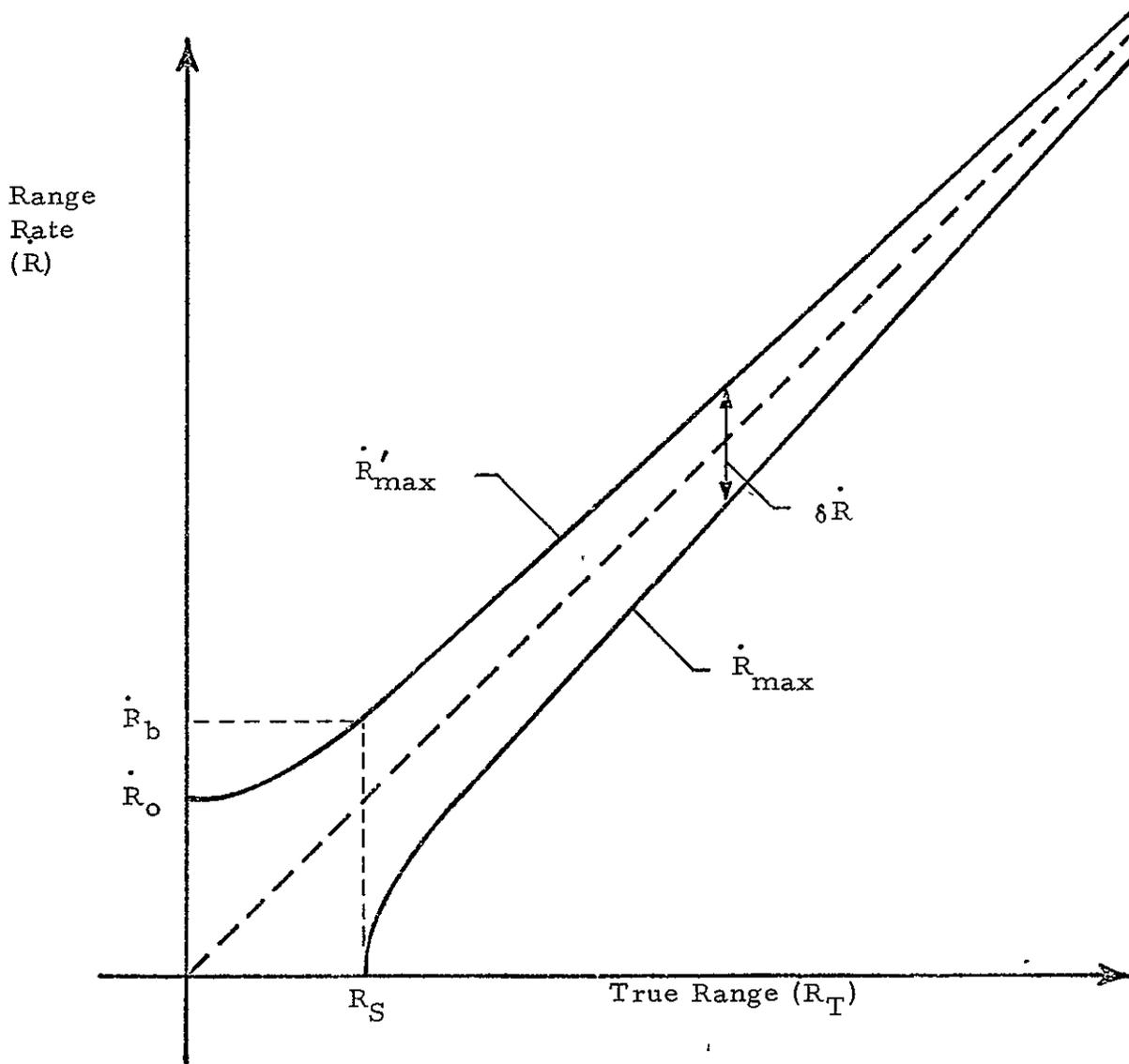
Figure 13-3.- $\delta \dot{R}$ in the $\dot{R}$ versus R_T Domain

assumes only 0.25 fps of braking is allowable. Figure 13-3 shows $\delta \dot{R}$ in the $\dot{R}$ versus R_T domain. There are several ways of interpreting these figures. For example, when R_T is large, only very small excursions above $\dot{R}_{max}$ precipitate large requirements for braking near the target. Or, for a given $\dot{R}_b$ the allowable error increases as the range collapses. Perhaps the most important conclusions become evident if the pilot wishes to follow the optimum trajectory to the target. They are:

    1. Very accurate range and range rate knowledge is required.

    2. Very tight control of the Orbiter is required.

These areas, state knowledge and Orbiter control, are the subjects in the remainder of this paper. They are the areas which separate the theoretical from the practical.

14.0 The Digital Auto Pilot

The DAP (Digital Auto Pilot) is not a piece of hardware but a module of software in an Orbiter computer. Its function is to control the Orbiter's attitude and translation by using the Reaction Control System (RCS). The DAP performs this function by first differencing a desired Orbiter state with the current Orbiter state and second, commanding the appropriate RCS jets to drive this difference close to zero. (The term "close to zero" is used because the minimum available jet "ON" time is 40 milliseconds). During the $\dot{R}$ approach, the desired Orbiter attitude is provided to the DAP by the UPS (Universal Pointing System). Translational inputs are provided to the DAP by the THC (Translational Hand Controller).

67

The DAP may be placed into either of two software configurations or modes. These are called DAP A and DAP B. The character of these modes is dependent on the mission phase. During the $\bar{R}$ approach they assume the following significance:

DAP A –

1. All upward firing jets are inhibited for attitude control.

2. All jets are active for translational control.

3. Each "hit" of THC will provide a ΔV of 0.25 fps in the commanded direction.

DAP B –

1. All upward firing jets are inhibited for attitude control.

2. The upward firing +Z jets are inhibited for translational control.

3. Simultaneous firing of the +X and –X jets occurs in lieu of all +Z jet commands for translation. (The X jets have ten percent of their thrust directed downward along $+Z_B$.)

4. Each "hit" of the THC will provide a ΔV of 0.03 fps in the commanded direction.

Regardless of which configuration is selected, the DAP is placed in the Automatic Mode to respond to the UPS. In addition, the Translational Pulse Mode is called; this mode computes the proper number of 40 millisecond jet commands required to achieve the specified ΔV for each THC deflection from detent. Figure 14-1 shows the DAP Control Panel in its $\bar{R}$ approach configuration.

Although the Rotational Discrete Mode is also called during an $\bar{R}$

ORBITAL DAP

SELECT

| A | B |

CONTROL

| AUTO | MAN |

RCS JETS

| NORM | VERN |

MANUAL MODE

TRANSLATION

| | X | Y | Z |

ROTATION

| | ROLL | PITCH | YAW |

HIGH	HIGH	HIGH	DISC RATE	DISC RATE	DISC RATE
NORM	NORM	NORM	ACCEL	ACCEL	ACCEL
PULSE	PULSE	PULSE	PULSE	PULSE	PULSE

☐ - ON

☐ - OFF
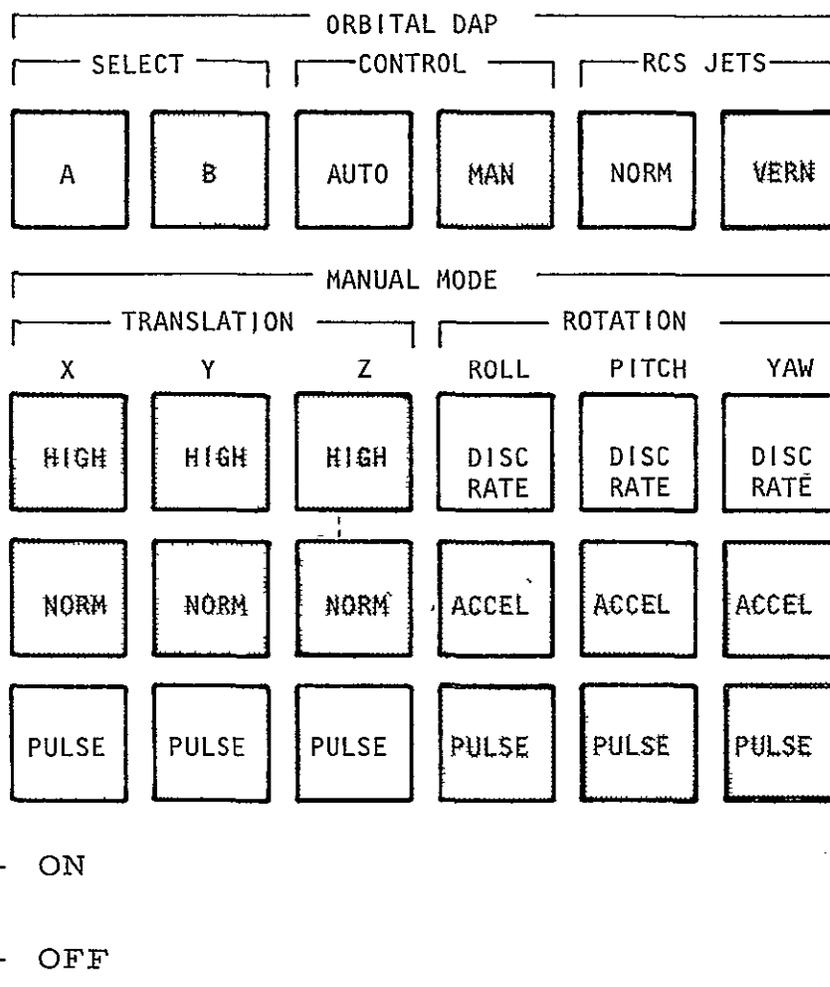
Figure 14-1.- Digital Auto Pilot (DAP) Control Panel Configured for an $\bar{R}$ Approach

69

approach, it has no meaning unless the DAP, for some reason, is placed in the Manual Mode. Then, holding the RHC (Rotational Hand Controller) out of detent causes the Orbiter to assume and maintain a preprogrammed rotation rate until the RHC is released; at release the Orbiter reverts to inertial attitude hold at the current attitude. Though the Manual Mode may be called from the DAP Control Panel, any momentary deflection of the RHC will also change the DAP from the Automatic Mode to the Manual Mode.

The DAP A and DAP B designs serve two purposes. First, they minimize plume impingement on LDEF. In particular, using the $\pm$X jets for any close in braking has been shown[1] to be significantly less disturbing to LDEF than using the more direct Z jets (See figure 14-2a and 14-2b). Second, the designs provide the fine ΔV control resolution demanded by an $\bar{R}$ approach.

The designs also cause an undesirable side effect. Since only downward firing jets are used for pitch and roll attitude control, each correction introduces an increment of closing ΔV. Translations along X or Y also affect range rate. In the case of X translations, ten percent of the thrust is along $+Z_B$. This is partially offset by the creation of a pitching moment which requires an upward thrust to correct. In the case of Y translations the problem is more serious. Thrusting the Y jets creates a significant roll torque. Roll jets

[1] Reference the JSC PDRS III Post-Simulation Report, CG5-77-222, November 7, 1977.
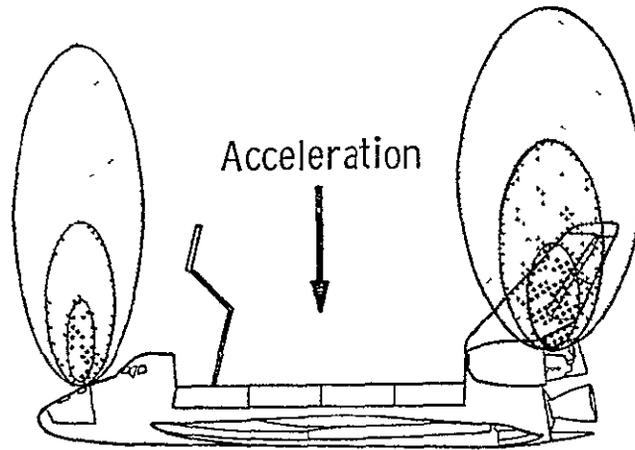
Figure 14-2a.- Normal Z Jet Braking (0.45 ft/sec^2 at 30 lb/ft/sec)
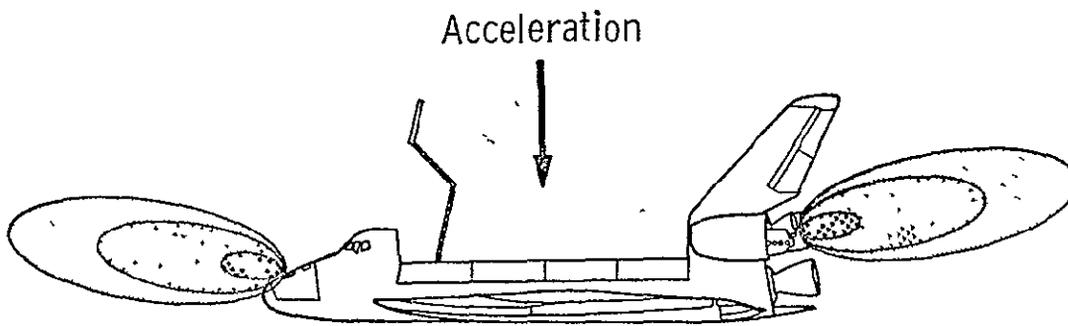
Figure 14-2b.- $\pm$ X Jet Braking (0.05 ft/sec^2 at 280 lb/ft/sec)

exist only in the tail of the Orbiter and have relatively short moment
arms. When the upward firing jets are inhibited, half of the roll
torque capability is lost. Indeed, if either the +Y or -Y jets are
held ON, the Orbiter's roll attitude diverges even though the downward
firing roll jet is ON. This single 875 lb. roll jet is also thrusting
the Orbiter along $-Z_B$ (or toward the LDEF). The resultant pitching
moment is counteracted by an upward thrusting nose jet, which
aggravates the situation.

The most important conclusion of the preceding paragraph is obvious:
minimize Y translation requirements. This imposes an attitude con-
straint during the $\bar{R}$ approach. As the Orbiter ascends along $\bar{R}_L$, the
tangential velocity must be increased. This is best accomplished by
thrusting either the +X or -X jets. Thus during an $\bar{R}$ approach the
Orbiter's X axis must always reside in the orbit plane.

Another important conclusion is that the Orbiter will probably not
follow the $\dot{R}$ versus R curves of figure 12-4. The curves are ideal in
that they assume accelerations along $\bar{R}$ are derived solely from orbital
mechanics effects. As was mentioned, several increments of ΔV are
randomly imparted along Z_B during the $\bar{R}$ approach. The net effect may
manifest itself as an apparent increase or decrease in the natural
braking along $\bar{R}$.

As a final note, $\pm X$ jet braking does have two potential drawbacks
which, if ignored, can cause problems. First, $\pm X$ jet braking is very
inefficient with respect to fuel usage. +Z jet braking expends 30
pounds of fuel per foot per second of ΔV. $\pm X$ jet braking uses 280

pounds of fuel per foot per second. Second, ±X jet braking acceleration is only 0.05 ft/sec^2 compared to 0.45 ft/sec^2 for +Z jet braking. In summary, therefore, precautions must still be taken during an $\bar{R}$ approach to assure that the need for braking is minimized.

15.0 <u>Using the COAS During an $\bar{R}$ Approach.</u> Prior to the $\bar{R}$ final approach the use of the COAS is limited to that of aiding the pilot in laterally positioning and/or pointing the Orbiter's $-Z_B$ axis. During the $\bar{R}$ approach the COAS continues to be used as a lateral positioning aid while the UPS controls the pointing of the $-Z_B$ axis. But in addition, there is a point in the approach where the third function of the COAS comes into play, namely, that of providing range and range rate data.

The transition point, where COAS data is used in lieu of radar data, is dependent on the errors in the two measurement schemes. Therefore, the development of any $\bar{R}$ approach strategy must be preceded by some quantification of the errors in both systems. The radar errors have already been presented. The purpose of this section is to address the errors and limitations associated with the use of the COAS.

15.1 <u>Determining Range with the COAS</u>

Range to the target is determined with the COAS by the following equation:

$$R = \frac{W}{2} \left(\frac{1}{\tan \left(\frac{\theta}{2} \right)} \right)$$

where
          R = range to the target in feet

          W = target width in feet

          θ = degrees of COAS field of view subtended by the target

For small subtended angles as experienced in the COAS,

$$R = \frac{W}{\theta} \left(\frac{180}{\pi}\right)$$

15.2 LDEF Ranging Targets

LDEF provides at least three targets for approach and station keeping. They are shown in figure 15.2-1. A duplicate set of targets are provided on the forward end to accommodate an LDEF end-for-end tumble after release by the Orbiter.[1] The first target is the total LDEF end face, which has an average diameter or target width, W, of 14.0 feet. The second target is a painted pair of dashed lines whose centers are at Y_o = -19.93 and Y_o = -60.23. This provides a target width of 40.3 inches or 3.36 feet. The third target is formed by the dashed lines with centers at Y_o = -60.23 and Y_o = -70.23, which provide a target width of 10 inches or 0.83 feet. (A duplicate 10-inch target is oriented 90 degrees to the first. The purpose of this duplication is discussed later). Figures 15.2-2, 15.2-3, and 15.2-4 present the COAS angle versus range curves for the three targets. A copy of these curves or a tabular representation will be used by the pilot during the $\bar{R}$ approach.

15.3 COAS Ranging Sensitivity

Sensitivity, S, is defined as the change in target image size for a given change in range, or,

---

[1] A descending $\bar{R}$ approach is just as viable as an ascending $\bar{R}$ approach. But, operationally speaking, there is a distinct preference for the ascending approach because there is no visual background noise (cloud patterns, etc.) in the COAS field of view.
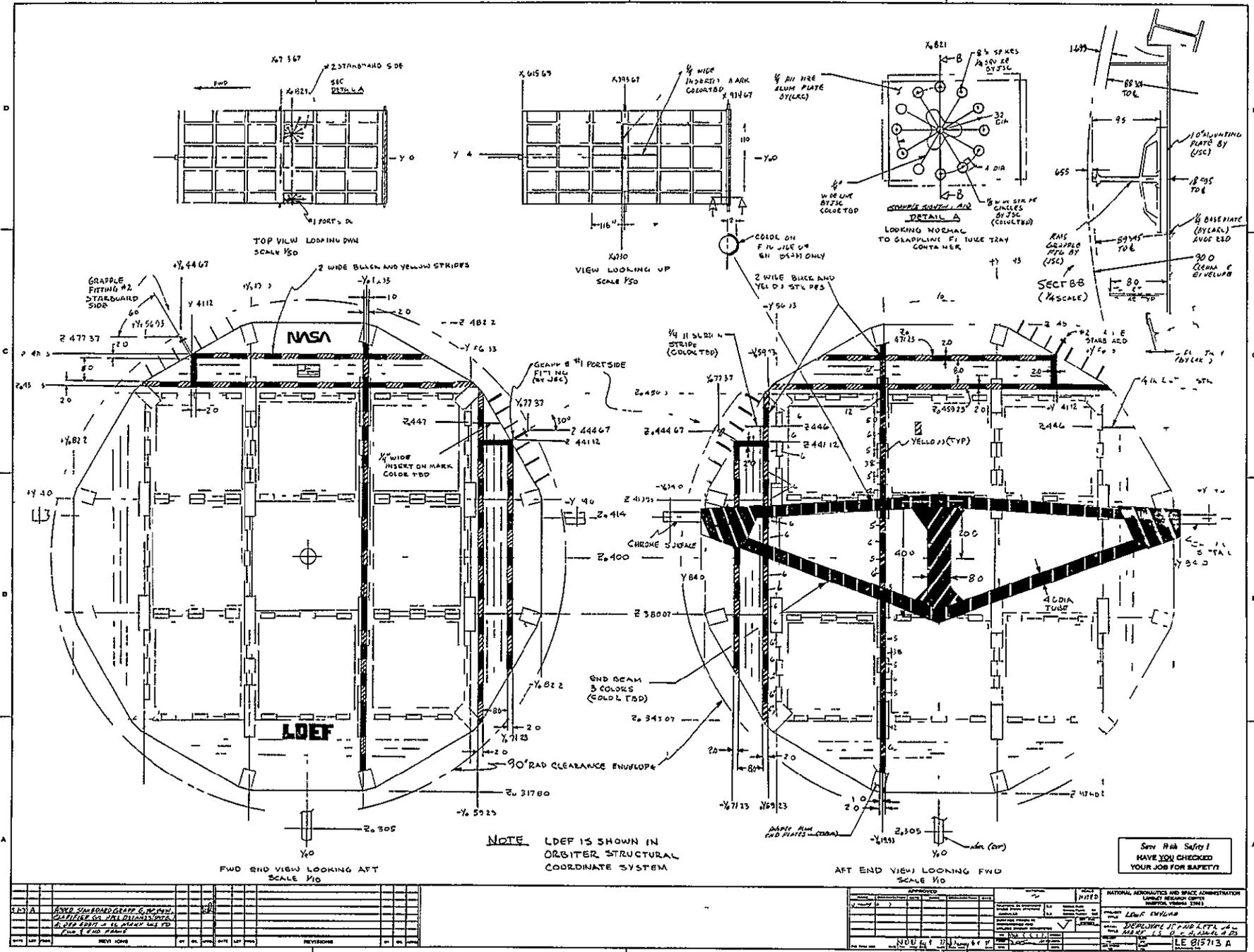
Figure 15.2-1.- Deployment and Retrieval Markings - Operational Aids (LaRC Dwg. LE-815713A)
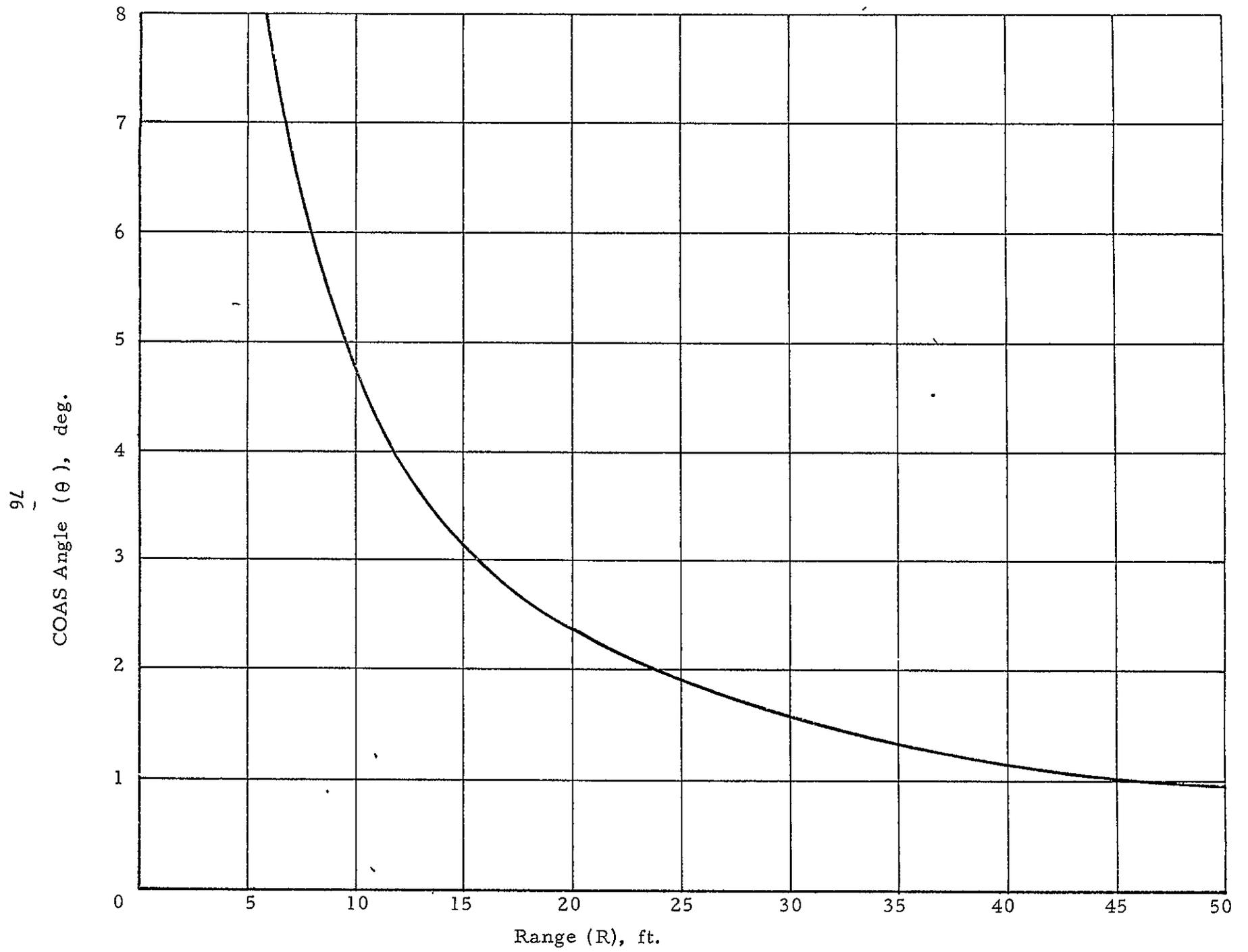
Figure 15.2-2.- Ranging with the 0.83 ft. LDEF Target
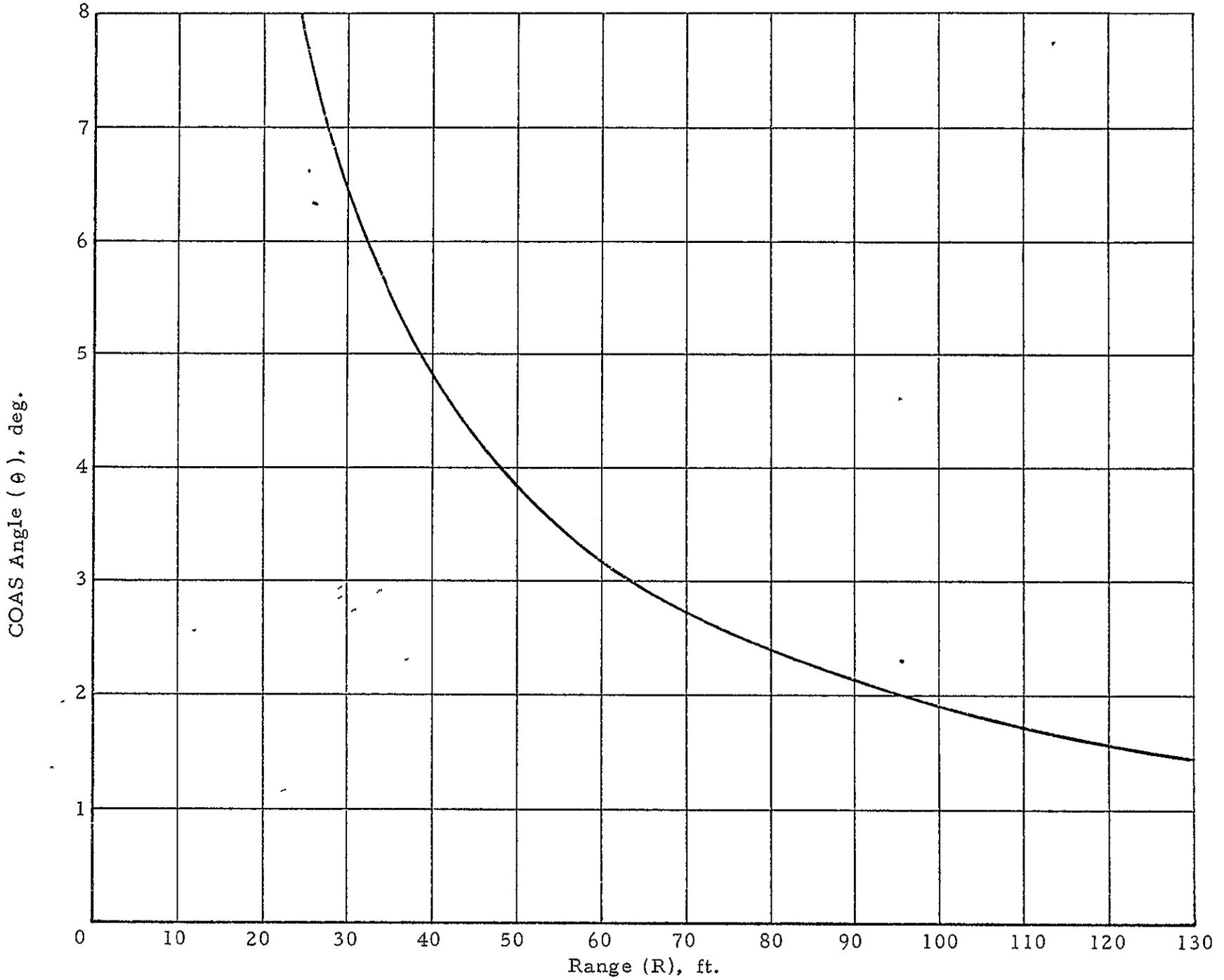
Figure 15.2-3.- Ranging with the 3.36 ft. LDEF Target
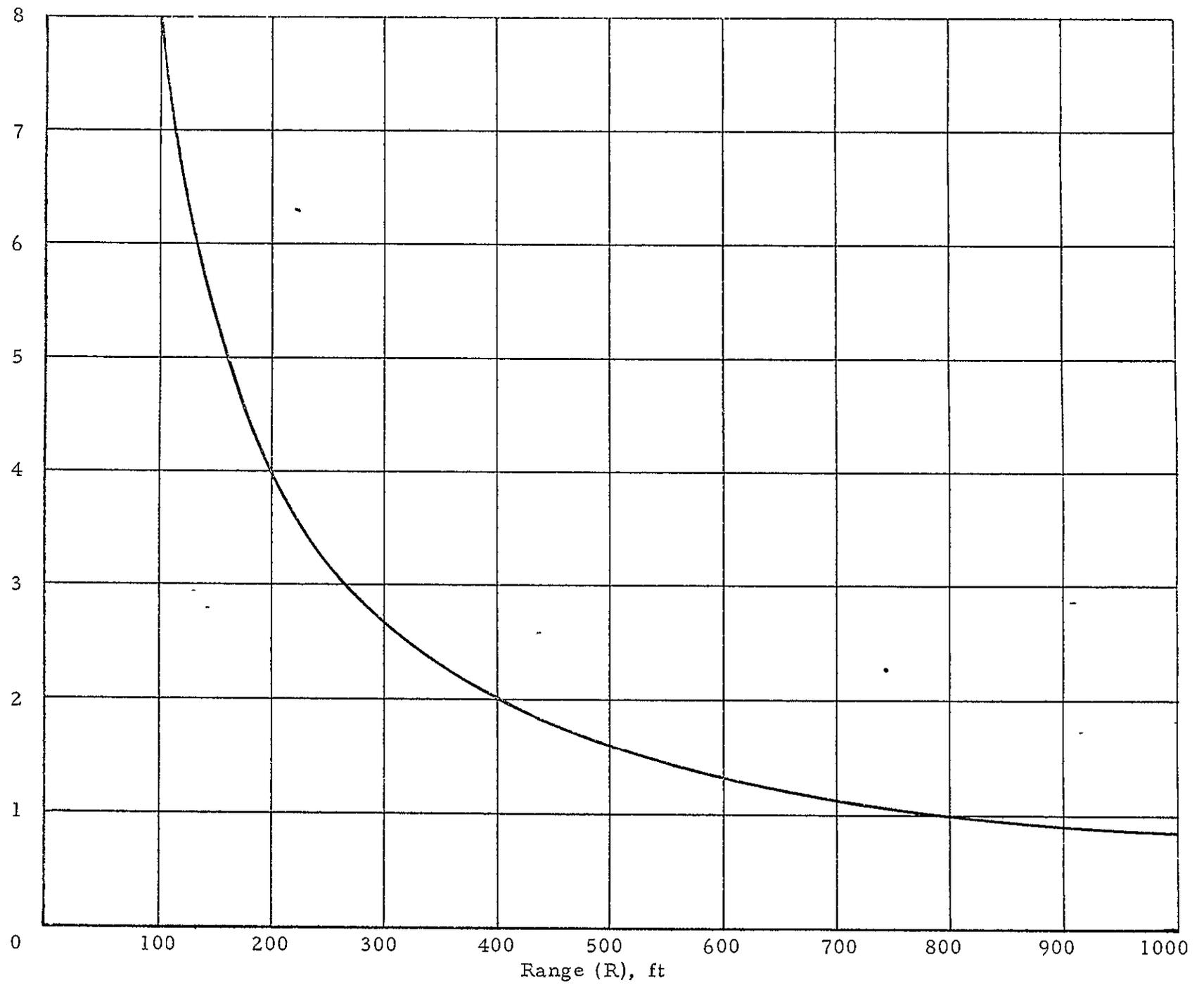
Figure 15.2-4.- Ranging with the 14 ft. LDEF End Face Target

$$S = \frac{d\theta}{dR} = -\frac{W}{R^2} \left(\frac{180}{\pi}\right) \text{ deg/ft}$$

If a target must be useful over a range of R and 3R, the sensitivity will vary 9 fold. The highest sensitivity occurs at R and the lowest occurs at 3R.

15.4 Determining Range Rate with the COAS

One of the most striking implications of this variable sensitivity is that the pilot's direct perception of range rate in the COAS is acutely dependent on range. Suppose that the pilot attempts to perceive $\dot{R}$ as a time rate of change of the subtended target angle, $\dot{\theta}$. If R_2 equals $3R_1$ and $\dot{\theta}_1 = \dot{\theta}_2$, how does $\dot{R}_1$ compare to $\dot{R}_2$?

$$\frac{S_1 \dot{R}_1}{S_2 \dot{R}_2} = \frac{\dot{\theta}_1}{\dot{\theta}_2} = 1$$

and

$$\dot{R}_2 = \left(\frac{S_1}{S_2}\right) \dot{R}_1 = 9 \ \dot{R}_1$$

In other words, a constant image growth rate over a range spread of 3 times yields a 9 fold change in the actual range rate. The conclusion is that developing an intuitive feeling for the magnitude of range rate based on image growth rate is extremely difficult if not impossible.

Even differencing COAS readings over an interval, t, can provide an erroneous indication of range rate. This method only provides an

indication of the mean range rate over the interval. If the orbiter

is experiencing any acceleration relative to the target, the computed $\dot{R}$

will always be in error. This can be shown as follows:

$$\delta\dot{R} = \dot{R} - \dot{R}_T$$

$$= \frac{R - R_o}{\Delta t} - \dot{R}_T$$

where

$$\delta\dot{R} = \text{uncertainty in the computed } \dot{R}$$

$$\dot{R} = \text{computed } \dot{R}$$

$$\dot{R}_T = \text{true } \dot{R}$$

$$R = \text{range at time } t$$

$$R_o = \text{range at time } t_o$$

$$\Delta t = t - t_o$$

Assuming, for simplicity, that $\ddot{R}$ equals a constant,

$$R = R_o + \dot{R}_o \, \Delta t + \frac{\ddot{R}(\Delta t)^2}{2}$$

$$\dot{R}_T = \dot{R}_o + \ddot{R}\Delta t$$

Substituting,

$$\delta\dot{R} = \frac{-\ddot{R}\Delta t}{2}$$

In other words, the computed $\dot{R}$ is always behind the current $\dot{R}$.

Though the error equation implies that the error may be minimized by

reducing the interval between COAS readings, the situation is not that

straightforward. Each reading of the COAS is corrupted by a minimum

resolution error. Thus, sufficient time must exist to allow the target image to grow some $\Delta\theta$ which is large compared to the resolution error.

Only one conclusion can be drawn from the foregoing discussion: determining the magnitude of range rate with the COAS leaves a lot to be desired.

15.5 Target Width

COAS readout errors, $\delta\theta$, map into range estimation errors through sensitivity, S. That is,

$$\delta R \approx \frac{1}{S} \delta\theta = \frac{-R^2}{W} \delta\theta$$

Clearly, δR may be minimized by making W, the target width, as large as possible.

The available field of view in the COAS constrains target size as the range collapses. If the target must be useful down to a minimum range, R_{min}, the target width is constrained by

$$W_{max} < \theta_a \left(\frac{\pi}{180}\right) R_{min}$$

where θ_a is the available field of view in degrees.

Not all of the ten degree COAS field of view is considered to be available. Some margin must exist to accommodate (1) in- and out-of-plane position errors while ascending along $\bar{R}$, and (2) the limit cycle motion of the Orbiter. For example, assume that the target is centered in the COAS. The remaining available field of view, θ_r, on each side of the target image is

Table 15.5-1 <u>Allowable Positioning Error about $\bar{R}$</u>

A. LDEF Station Keeping Target, W = 0.83 ft.

<u>Range (ft)</u>	<u>x (ft)</u>
50	3.95
40	3.08
30	2.20
20	1.33
15	0.89

B. LDEF Approach Target, W = 3.36 ft.

<u>Range (ft)</u>	<u>x (ft)</u>
200	15.77
150	11.41
100	7.05
50	2.68
25	0.50

C. LDEF End Face, W = 14.0 ft.

<u>Range (ft)</u>	<u>x (ft)</u>
1000	80.27
600	45.36
400	27.91
200	10.45

$$\theta_r = 5 \left(\frac{\pi}{180}\right) - \frac{W}{2R} \quad \text{(in radians)}$$

θ_r subtends an arc length, x, at the target, of

$$x = R\theta_r = R(5)\left(\frac{\pi}{180}\right) - \frac{W}{2}$$

This x is also the allowable positioning error, in the Orbiter's $\bar{V} - \bar{H}$ plane, which will assure maintenance of the target image in the COAS field of view. Table 15.5-1 gives the values of x for the LDEF targets as a function of range.

15.6 COAS Range Error Vs. Resolution

When ranging with the COAS, the pilot must mentally record and difference two COAS readings (one reading for each edge of the target). The uncertainty in the difference is a function of the uncertainty in each of the two readings. That is,

$$3 \sigma_\theta = 3 \left(\sigma_{\theta_L}^2 + \sigma_{\theta_R}^2\right)^{1/2}$$

where

σ_θ = variance in the target's total subtended angle, θ

σ_{θ_L} = variance in the COAS angle for left edge of the target

σ_{θ_R} = variance in the COAS angle for the right edge of the target

No specific study exists to quantify $3\sigma_\theta$. However, personnel who have

participated in simulations at JSC generally believe that each edge of a target may be read to within 0.25 degrees 3σ (even though the COAS cross hairs are indexed in one degree increments). This makes $3\sigma_\theta$ equal to 0.35 degrees.

The ranging errors resulting from the COAS angle uncertainty may be computed by referring to figure 15.6-1. Let

R = computed range

R_T = true range

δR = range error

θ = estimated subtended target angle

θ_T = true subtended target angle

$\delta\theta$ = angle measurement error

Then,

$$\frac{\delta R}{R_T} = \frac{R - R_T}{R_T}$$

$$= \frac{\frac{W}{\theta} - R_T}{R_T} = \frac{\frac{W}{\theta_T + \delta\theta} - R_T}{R_T}$$

$$= \frac{\frac{W}{\frac{W}{R_T} + \delta\theta} - R_T}{R_T}$$

$$= \frac{-1}{1 + \frac{W}{R_T \, \delta\theta}}$$

Let $\qquad \frac{W}{\delta\theta} = k$

$$\theta = \theta_T + \delta_\theta$$

θ_T

δR

R R_T

R	-	Computed Range
R_T	-	True Range
δ_R	-	Range Error
θ	-	Estimated Subtended Target Angle
θ_T	-	True Subtended Target Angle
δ_θ	-	Angle Measurement Error

Figure 15.6-1.- COAS Resolution Error

TABLE 15.6-1 Range Error Vs. COAS Resolution Error for LDEF
Station Keeping Target, W = 0.83 Ft.

R (ft)	θ (deg)	S $\frac{deg}{ft}$	δθ = +0.35 deg.		δθ = -0.35 deg.	
			δR (ft)	$\frac{\delta R}{R_T}$ %	δR (ft)	$\frac{\delta R}{R_T}$ %
5	9.55	-1.910	- 0.2	- 3.5	0.2	3.8
10	4.77	- .477	- 0.7	- 6.8	0.8	7.9
15	3.18	- .212	- 1.5	- 9.9	1.9	12.4
20	2.39	- .119	- 2.6	-12.8	3.4	17.2
25	1.91	- .076	- 3.9	-15.5	5.6	22.4
30	1.59	- .053	- 5.4	-18.0	8.5	28.2
35	1.36	- .039	- 7.1	-20.4	12.1	34.5
40	1.19	- .030	- 9.1	-22.7	16.5	41.5
45	1.06	- .024	-11.2	-24.8	22.2	49.2
50	0.95	- .019	-13.4	-26.8	28.9	57.9
55	0.87	- .016	-15.8	-28.7	37.2	67.6
60	0.80	- .013	-18.3	-30.5	47.1	78.5

TABLE 15.6-2 Range Error Vs. COAS Resolution Error for LDEF
Approach Target, W = 3.36 Ft.

R (ft)	θ (deg)	S $\frac{deg}{ft}$	$\delta\theta = +0.35$ deg.		$\delta\theta = -0.35$ deg.	
			δR (ft)	$\frac{\delta R}{R_T}$ %	δR (ft)	$\frac{\delta R}{R_T}$ %
20	9.63	−.481	− 0.7	− 3.5	0.8	3.8
25	7.70	−.308	− 1.1	− 4.3	1.2	4.8
30	6.42	−.214	− 1.6	− 5.2	1.7	5.8
35	5.50	−.157	− 2.1	− 6.0	2.4	6.8
40	4.81	−.120	− 2.7	− 6.8	3.1	7.8
45	4.28	−.095	− 3.4	− 7.6	4.0	8.9
50	3.85	−.077	− 4.2	− 8.3	5.0	10.0
55	3.50	−.064	− 5.0	− 9.1	6.1	11.1
60	3.21	−.053	− 5.9	− 9.8	7.3	12.2
65	2.96	−.046	− 6.9	−10.6	8.7	13.4
70	2.75	−.039	− 7.9	−11.3	10.2	14.6
75	2.57	−.034	− 9.0	−12.0	11.8	15.8
80	2.41	−.030	−10.2	−12.7	13.6	17.0
85	2.26	−.027	−11.4	−13.4	15.5	18.3
90	2.14	−.024	−12.7	−14.1	17.6	19.6
95	2.03	−.021	−14.0	−14.7	19.8	20.9
100	1.93	−.019	−15.4	−15.4	22.2	22.2
110	1.75	−.016	−18.3	−16.7	27.5	25.0
120	1.60	−.013	−21.5	−17.9	33.5	27.9
130	1.48	−.011	−24.9	−19.1	40.2	30.9

TABLE 15.6-3   Range Error Vs. COAS Resolution Error for LDEF End
Face Target, W = 14.0 Ft.

R (ft)	θ (deg)	S $\frac{deg}{ft}$	δθ = +0.35 deg.		δθ = -0.35 deg.	
			δR (ft)	$\frac{\delta R}{R_T}$ %	δR (ft)	$\frac{\delta R}{R_T}$ %
85	9.44	-.110	- 3.0	- 3.6	3.3	3.9
90	8.91	-.099	- 3.4	- 3.8	3.7	4.1
95	8.44	-.089	- 3.8	- 4.0	4.1	4.3
100	8.02	-.080	- 4.2	- 4.2	4.6	4.6
110	7.29	-.066	- 5.0	- 4.6	5.5	5.0
120	6.68	-.056	- 6.0	- 5.0	6.6	5.5
130	6.17	-.047	- 7.0	- 5.4	7.8	6.0
140	5.73	-.041	- 8.1	- 5.8	9.1	6.5
150	5.35	-.036	- 9.2	- 6.1	10.5	7.0
160	5.01	-.031	-10.4	- 6.5	12.0	7.5
170	4.72	-.028	-11.7	- 6.9	13.6	8.0
180	4.46	-.025	-13.1	- 7.3	15.3	8.5
190	4.22	-.022	-14.5	- 7.7	17.2	9.0
200	4.01	-.020	-16.1	- 8.0	19.1	9.6
220	3.65	-.017	-19.3	- 8.8	23.4	10.6
240	3.34	-.014	-22.3	- 9.5	28.1	11.7
260	3.09	-.012	-26.5	-10.2	33.3	12.8
280	2.86	-.010	-30.5	-10.9	39.0	13.9
300	2.67	-.009	-34.7	-11.6	45.2	15.1
350	2.29	-.007	-46.4	-13.2	63.1	18.0
400	2.01	-.005	-59.4	-14.9	84.6	21.1
450	1.78	-.004	-73.9	-16.4	109.9	24.4
500	1.60	-.003	-89.5	-17.9	139.5	27.9

Then

$$\frac{\delta R}{R_T} \% = \frac{-100}{1 + \frac{k}{R_T}}$$

If $\delta\theta$ is expressed in degrees,

$$k = \frac{W}{\delta\theta} \left(\frac{180}{\pi}\right)$$

For positive $\delta\theta$'s the range error approaches -100% as R_T approaches infinity. For negative $\delta\theta$'s, the error is less straight forward. For example, as R_T approaches $\left|\frac{k}{2}\right|$, the range error approaches $+100\%$, the physical significance is that when θ_T equals $+2$ $\delta\theta$, θ equals $+\delta\theta$.

Tables 15.6-1, 15.6-2, and 15.6-3 provide, as a function of range, the values of the important parameters for each target.

15.7 Optimizing Target Size

Any target becomes less accurate as range increases. Therefore, if accuracy is the most important parameter, the minimum target width, W_{min}, is constrained by the accuracy requirement at the maximum range, R'_{max}. Referring to the preceding paragraphs, note that

$$W = -\delta\theta \left(\frac{\pi}{180}\right) \left[\frac{1}{\frac{\delta R}{R_T}} + 1 \right] R_T$$

If $R_T = R'_{max}$, then $W = W_{min}$ for a specified $\delta\theta$ and $\frac{\delta R}{R'_{max}}$, or

$$W_{min} = -\delta\theta \left(\frac{\pi}{180}\right) \left[\frac{1}{\epsilon_R} + 1\right] R'_{max}$$

89

where
$$\varepsilon_R = \frac{\delta R}{R'_{max}}$$

Since W_{min} is maximized when $\varepsilon_R > 0$ (corresponding to a $\delta\theta < 0$), the preceding equation may be rewritten as

$$W_{min} = |\delta\theta| \, (\frac{\pi}{180}) \left[\frac{1}{|\varepsilon_R|} + 1\right] R'_{max}$$

Correspondingly, the minimum usable range, R'_{min}, for a target width, W_{min}, is constrained by the COAS's available field of view, θ_a. Or,

$$R'_{min} = \frac{W_{min}}{\theta_a} \, (\frac{180}{\pi})$$

The R'_{min} and R'_{max} are annotated with "primes" because they may not bound the total R_{min} to R_{max} spread for which targets are required. That is, usually more than one target is necessary. The number of targets may be determined as follows.

A range spread factor, J, may be defined for each target, where

$$J = \frac{R'_{max}}{R'_{min}} = \frac{\theta_a}{|\delta\theta|\left[\frac{1}{|\varepsilon_R|} + 1\right]}$$

Assuming each target is fully utilized over its optimum range (i.e., R'_{min} to R'_{max}),

$$R_{min}(J)^n = R_{max}$$

$$n = \frac{\log\left(\frac{R_{max}}{R_{min}}\right)}{\log (J)}$$

where n is the number of targets, with equal J factors, required to cover a total range of R_{min} to R_{max}. For two consecutive targets, R'_{min_1} equals R'_{max_2}. Therefore,

$$\frac{W_{min_1}}{W_{min_2}} = J$$

The following example may be used to show the application of the preceding equations.

The LDEF end face is the first available target during the $\bar{R}$ approach. Assuming $\delta\theta = -0.35$ degrees, there is a range where ε_R will be the same for radar ranging and COAS ranging. This range is 390 feet where ε_R equals 0.2051.[1] Assuming 20.51% is the maximum allowable error from 390 feet to 10 feet, and that θ_a equals 8 degrees, what are the target requirements?

$$J = \frac{8}{0.35 \left[\frac{1}{.2051} + 1\right]} = 3.89$$

$$n = \frac{\log\left(\frac{390}{10}\right)}{\log (3.89)} = 2.70$$

---

[1] Assuming a 3σ radar range error of 80 feet.

In other words, at least three LDEF targets are required. The target

width requirements[2] and their respective ranges are as follows:

<u>Target #1</u>

$$R_{max_1} = 390 \text{ feet}$$

$$W_{min_1} = 14 \text{ feet}$$

$$R_{min_1} = \frac{R_{max_1}}{J} = \frac{390}{3.89} = 100.26 \text{ feet}$$

<u>Target #2</u>

$$R_{max_2} = 100.26 \text{ feet}$$

$$W_{min_2} = \frac{W_{min_1}}{J} = 3.60 \text{ feet}$$

$$R_{min_2} = \frac{R_{max_2}}{J} = 25.77 \text{ feet}$$

<u>Target #3</u>

$$R_{max_3} = 25.77 \text{ feet}$$

$$W_{min_3} = \frac{W_{min_2}}{J} = 0.93 \text{ feet}$$

$$R_{min_3} = \frac{R_{max_3}}{J} = 6.62 \text{ feet}$$

---

[2] Note that the optimum targets are essentially the same as those on LDEF. The minor exceptions are:

<u>Actual</u>	<u>Optimum</u>	<u>Δ</u>	
14.00 ft.	14.00 ft.	0	
3.36 ft.	3.60 ft.	-2.88	inches
0.83 ft.	0.93 ft.	-1.20	inches

The two inch width of each line representing the edges of each target essentially nullifies these differences.

Each target is utilized until it subtends an eight degree angle in the COAS. In each case the error at that point is identical. Note that:

$$\frac{W_{min}}{R'_{min}} = |\delta\theta| \ (\frac{\pi}{180}) \left[\frac{1}{|\epsilon_R|} + 1 \right]$$

but

$$\theta_a \ (\frac{\pi}{180}) = \frac{W_{min}}{R'_{min}}$$

Substituting and rearranging gives

$$|\epsilon_R| = \frac{1}{\frac{\theta_a}{|\delta\theta|} - 1}$$

For θ_a equal to 8 degrees and $|\delta\theta|$ equal to 0.35 degrees,

$$|\epsilon_R| = 4.58\%$$

This is the minimum ranging error for each target.

A plot of $|\epsilon_R|$ versus $\frac{R}{R'_{min}}$ is shown in figure 15.7-1. The curve is obtained from the following equation.[1]

$$|\epsilon_R| = \frac{1}{\left(\frac{\frac{B}{R}}{R'_{min}}\right)}$$

_____

[1] This equation is just another form a previously developed equation, i.e.,

$$\frac{\delta R}{R_T} = \frac{-1}{1 + \frac{W}{R_T \delta\theta}}$$
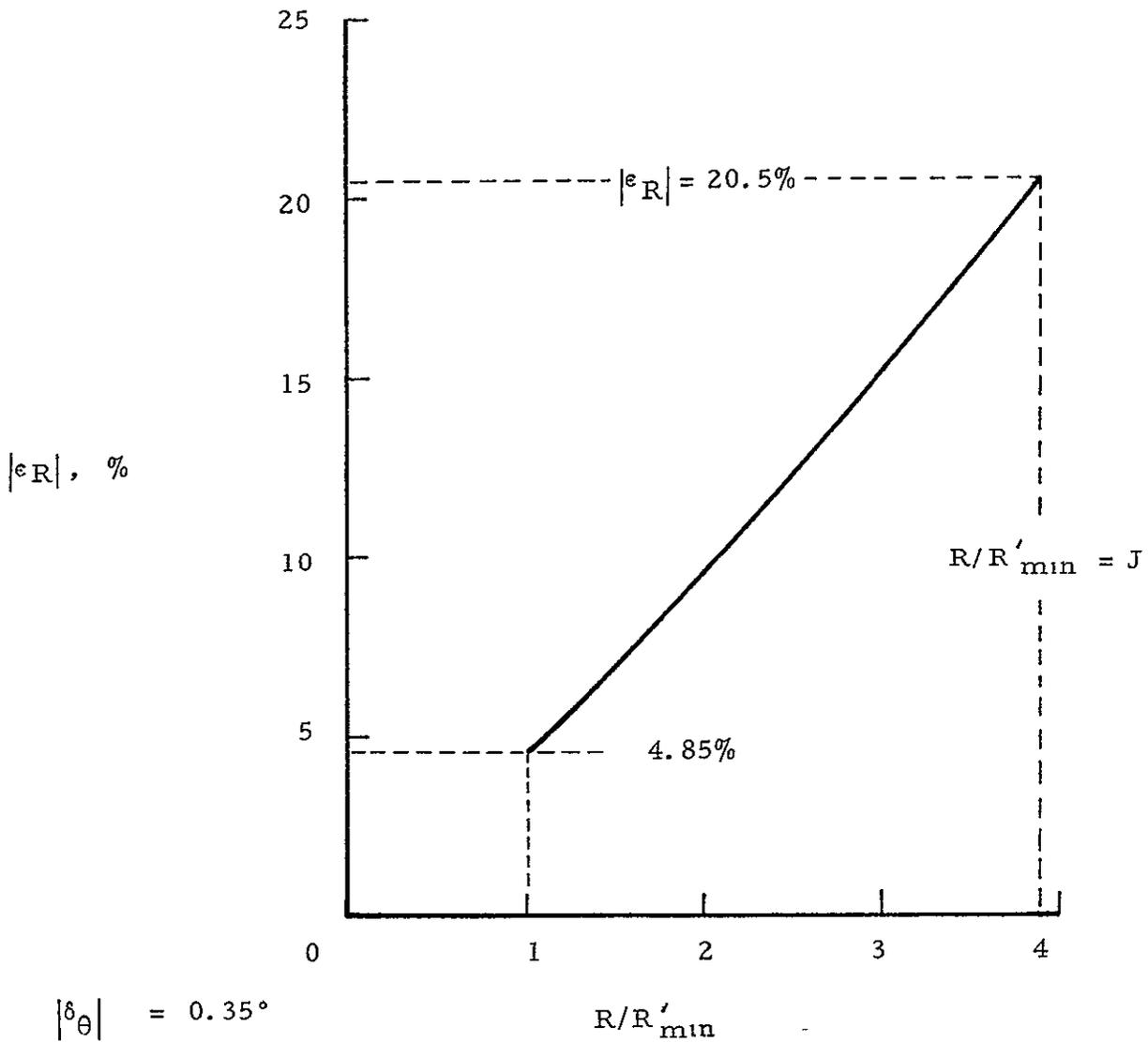
Figure 15.7-1.- COAS Ranging Error $|\varepsilon_R|$ Versus R/R'_{min}
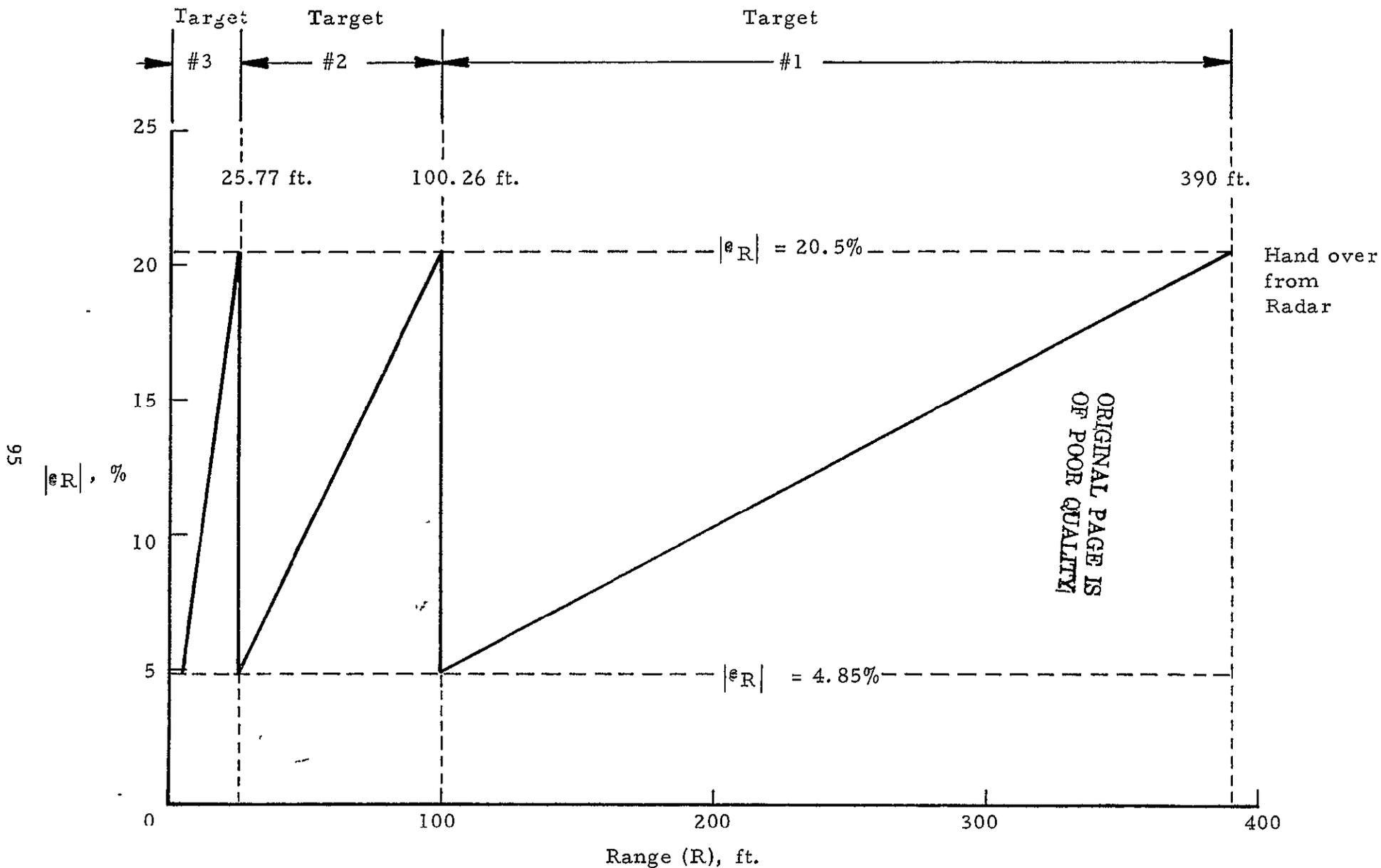
Figure 15.7-2.- $|\varepsilon_R|$ Versus Range

95
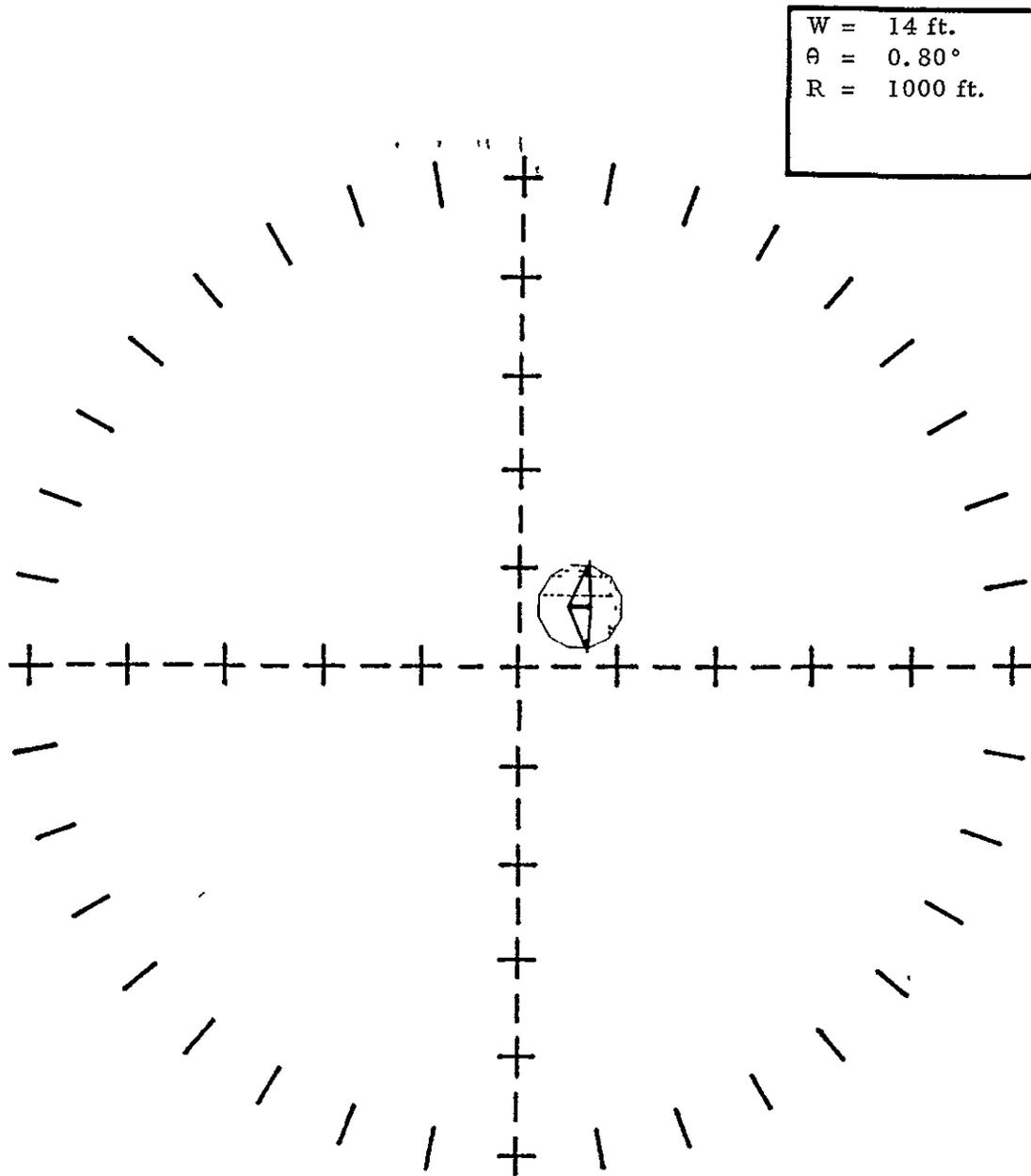
Figure 15.7-3a.- Utilizing the LDEF Targets
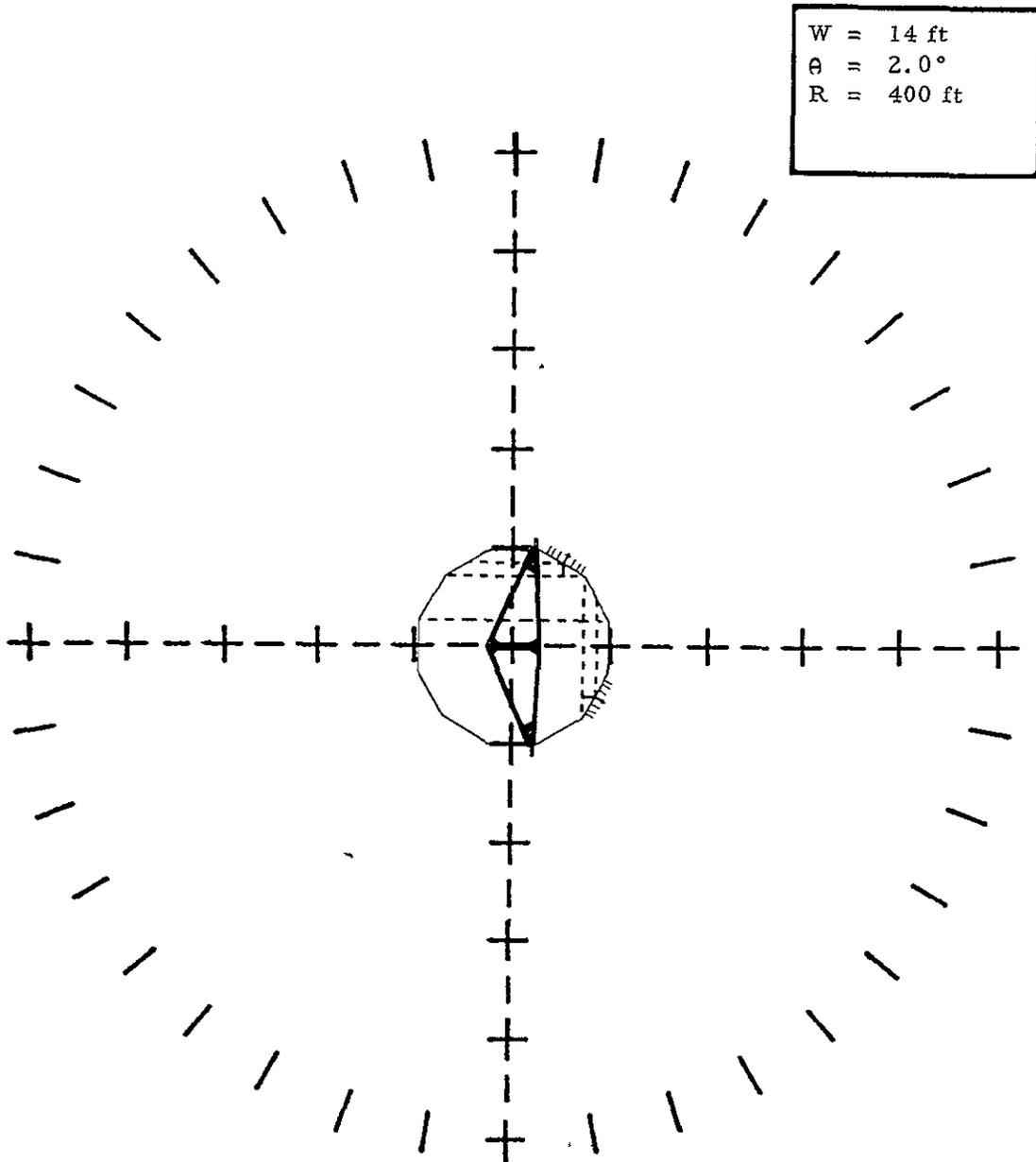
W = 14 ft
θ = 2.0°
R = 400 ft

Figure 15.7-3b.- Utilizing the LDEF Targets

97
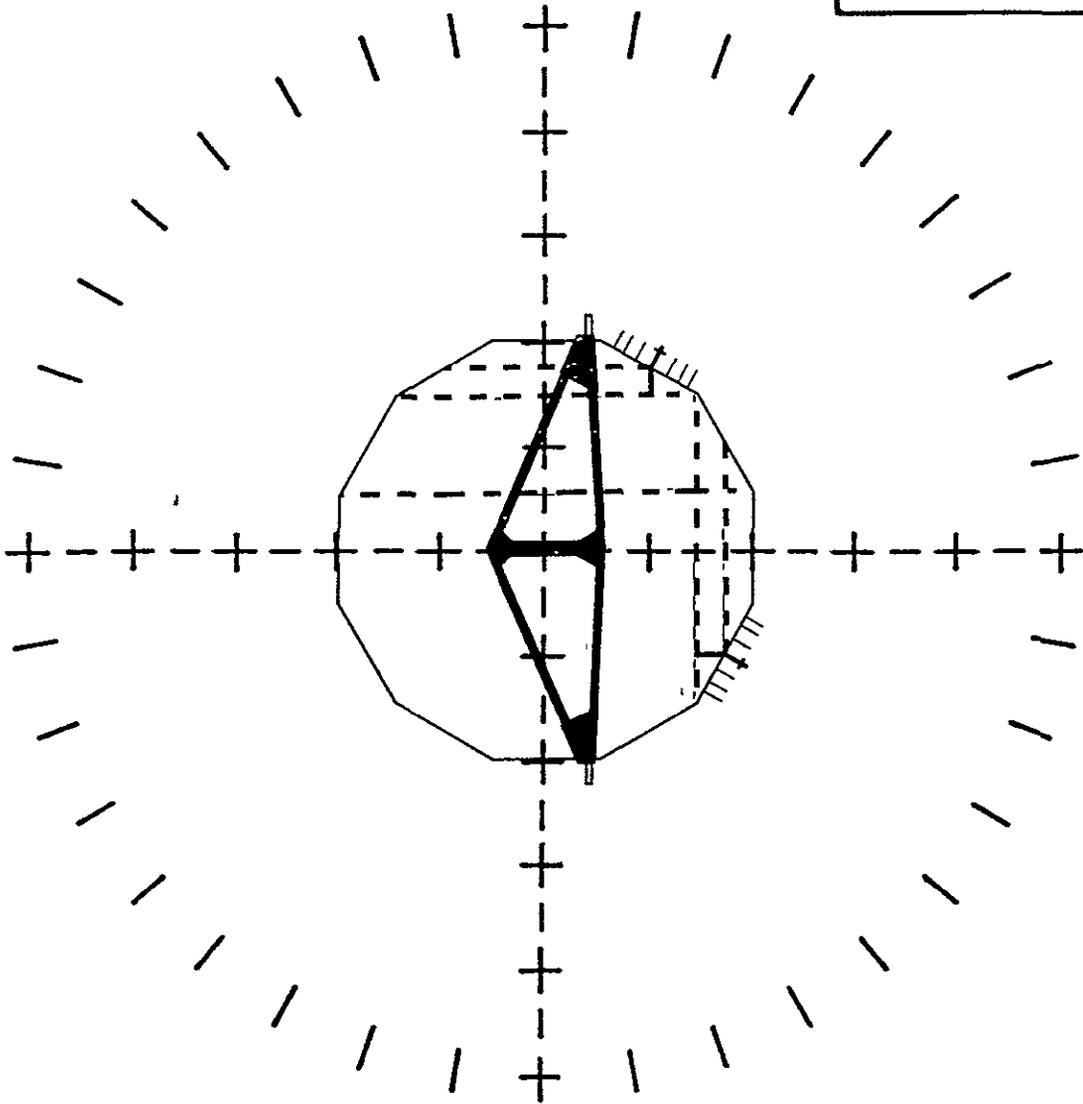
Figure 15.7-3c.- Utilizing the LDEF Targets
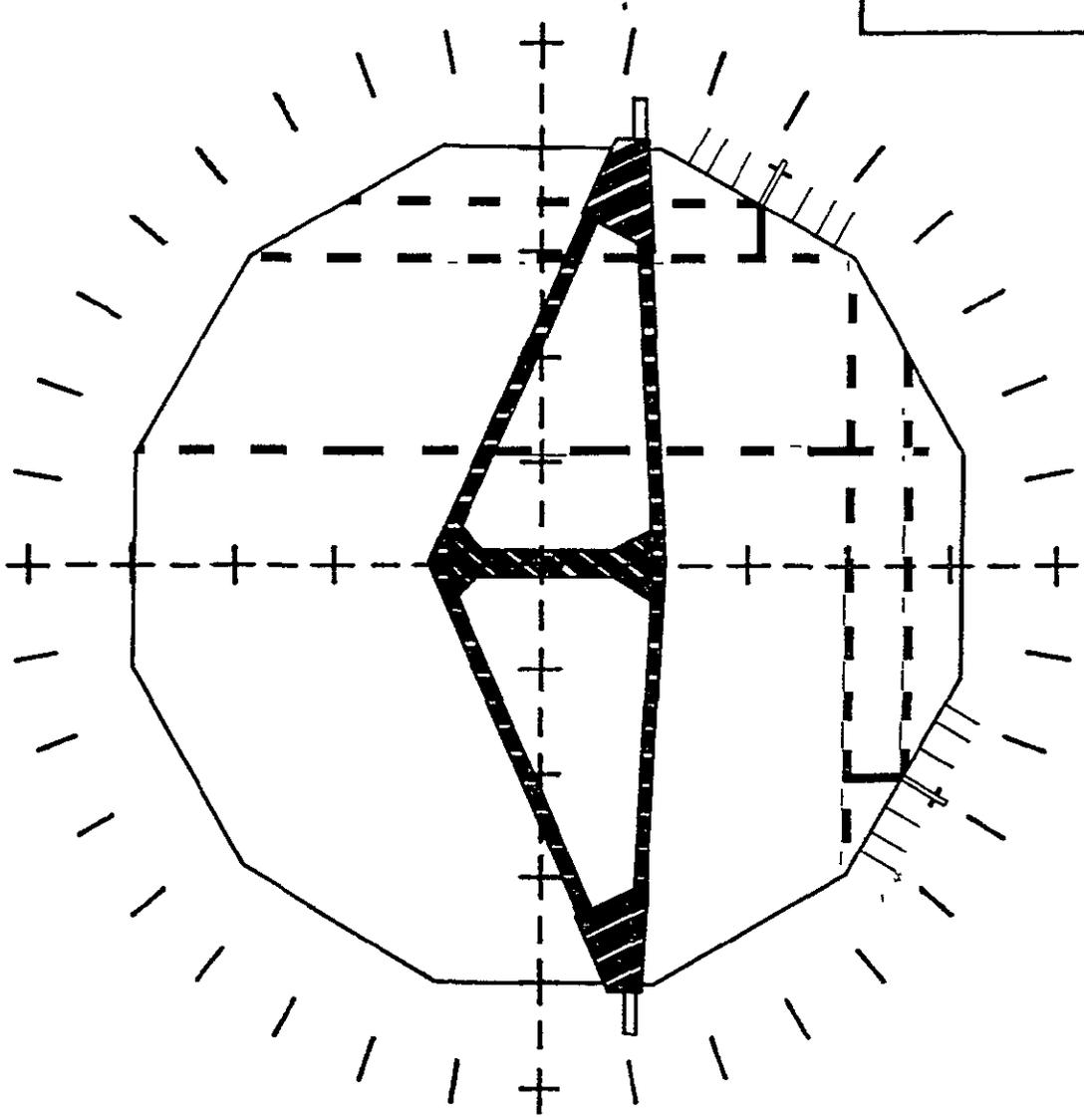
Figure 15.7-3d.- Utilizing the LDEF Targets
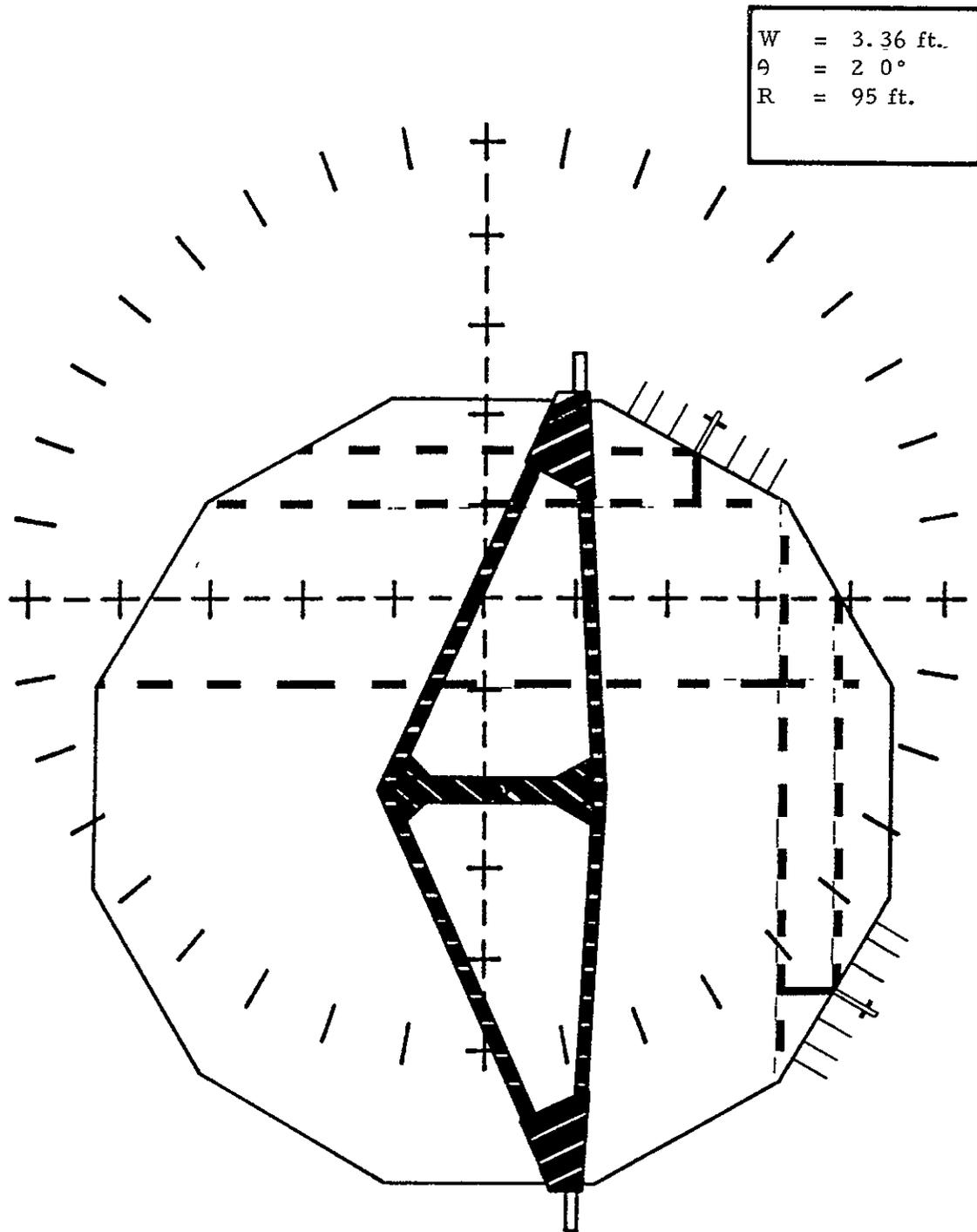
Figure 15.7-3e.- Utilizing the LDEF Targets

100
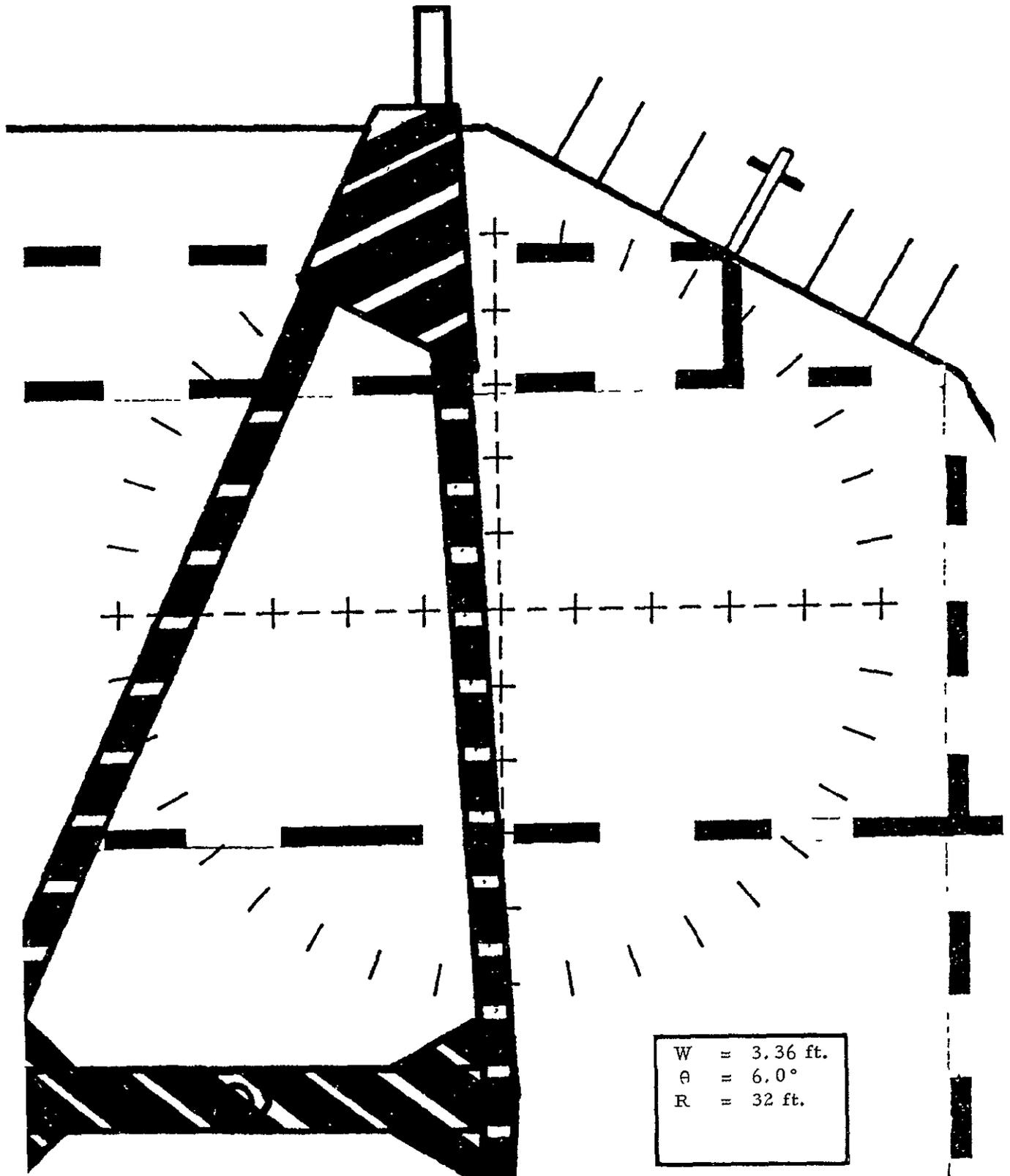
Figure 15.7-3f.- Utilizing the LDEF Targets

W = 3.36 ft.
θ = 6.0°
R = 32 ft.

101

W = 3 36 ft.
θ = 8.0°
R = 24 ft.
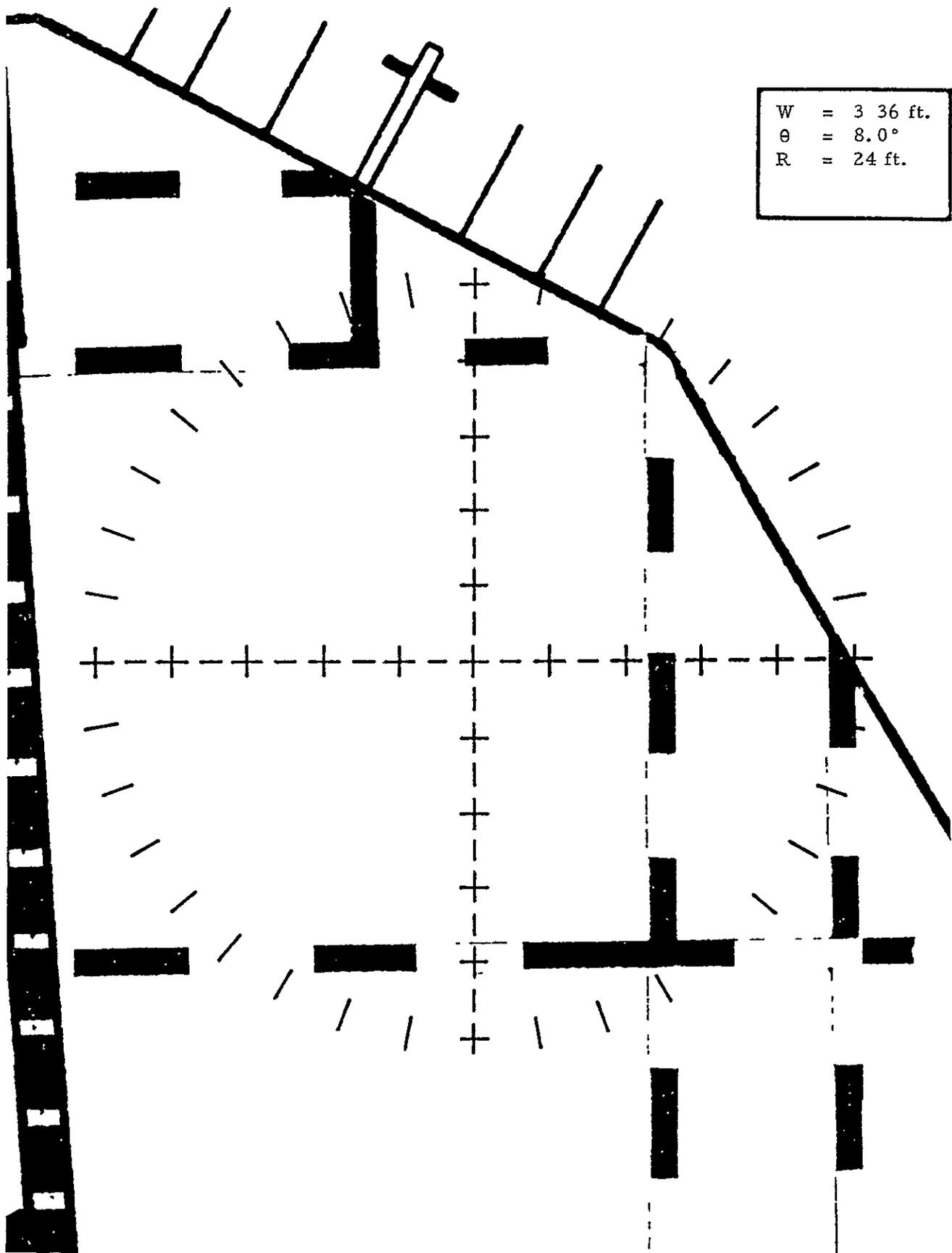
Figure 15.7-3g – Utilizing the LDEF Targets

102

Figure 15.7-3h.- Utilizing the LDEF Targets

103

where $$B = \frac{\theta_a}{|\delta\theta|} = \frac{8}{.35} = 22.86$$

$|\varepsilon_R|$ traces out three of these essentially sawtooth patterns as the range collapses from 390 feet to 6.62 feet. This is shown in figure 15.7-2 (straight line approximations are used).

Figures 15.7-3a through 15.7-3h show how the targets may be utilized during an approach.

15.8 <u>COAS Ranging Error due to LDEF/Orbiter Yaw Attitude Skew</u>

During an $\bar{R}$ approach the Orbiter's yaw axis (Z_B) and the LDEF's yaw axis (X_L) are essentially alined to $\bar{R}_L$, the LDEF orbital radius vector. The yaw attitude of each body determines the orientation the targets with respect to the COAS reticles. (See Figure 15.8-1.) Any misalignment introduces a ranging error. Referring to figure 15.8-2,

$$\delta R = R - R_T$$

$$= \frac{W}{\theta} - R_T$$

but $$\theta = \frac{W}{R_T \cos \psi}$$

After substituting and simplifying,

$$\frac{\delta R}{R_T} \% = 100 \ (\cos \psi - 1)$$

Note that the percent error is independent of range. Some representative values are:
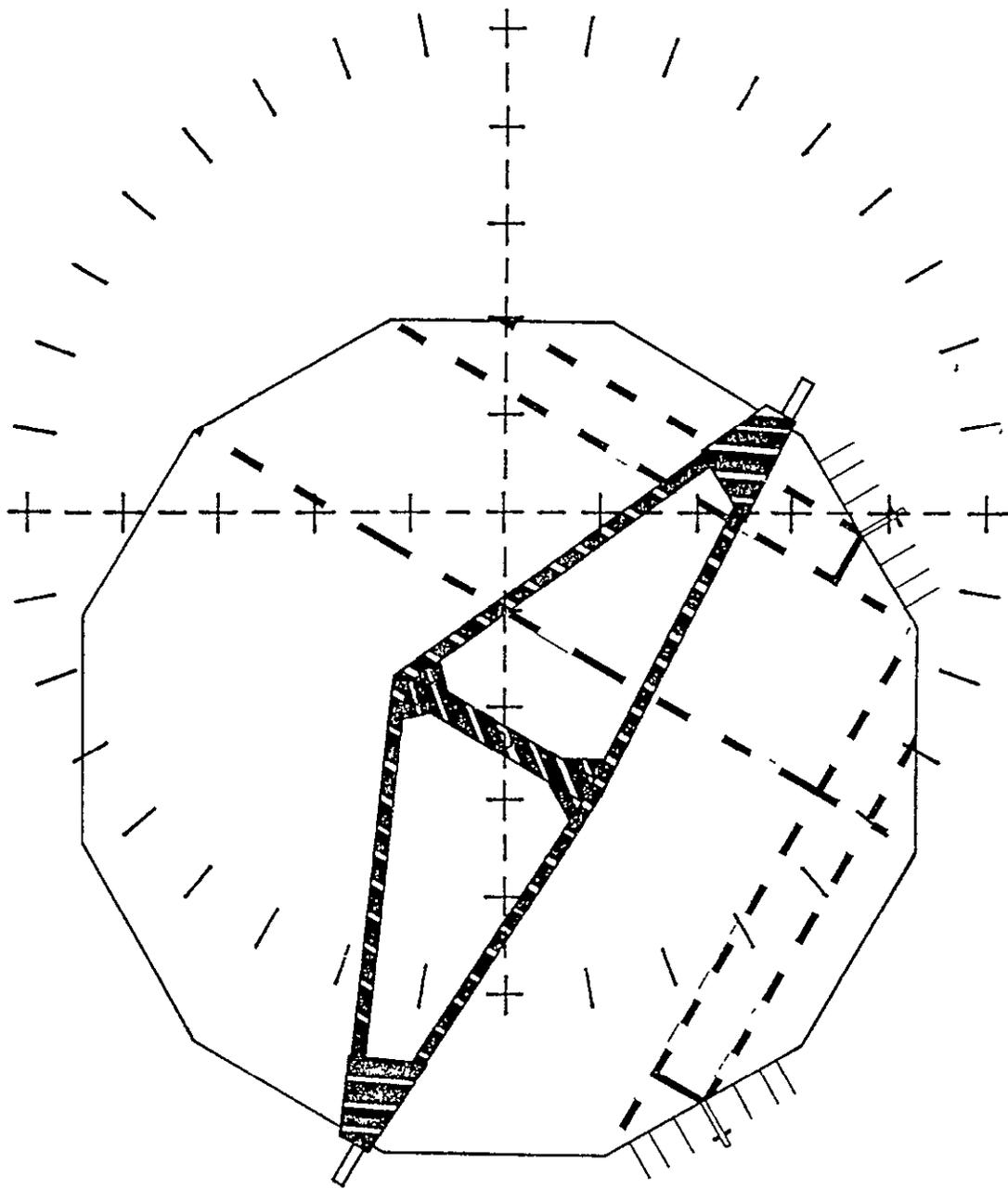
Figure 15.8-1.- Skewed Orbiter/LDEF Yaw Attitudes during Approach
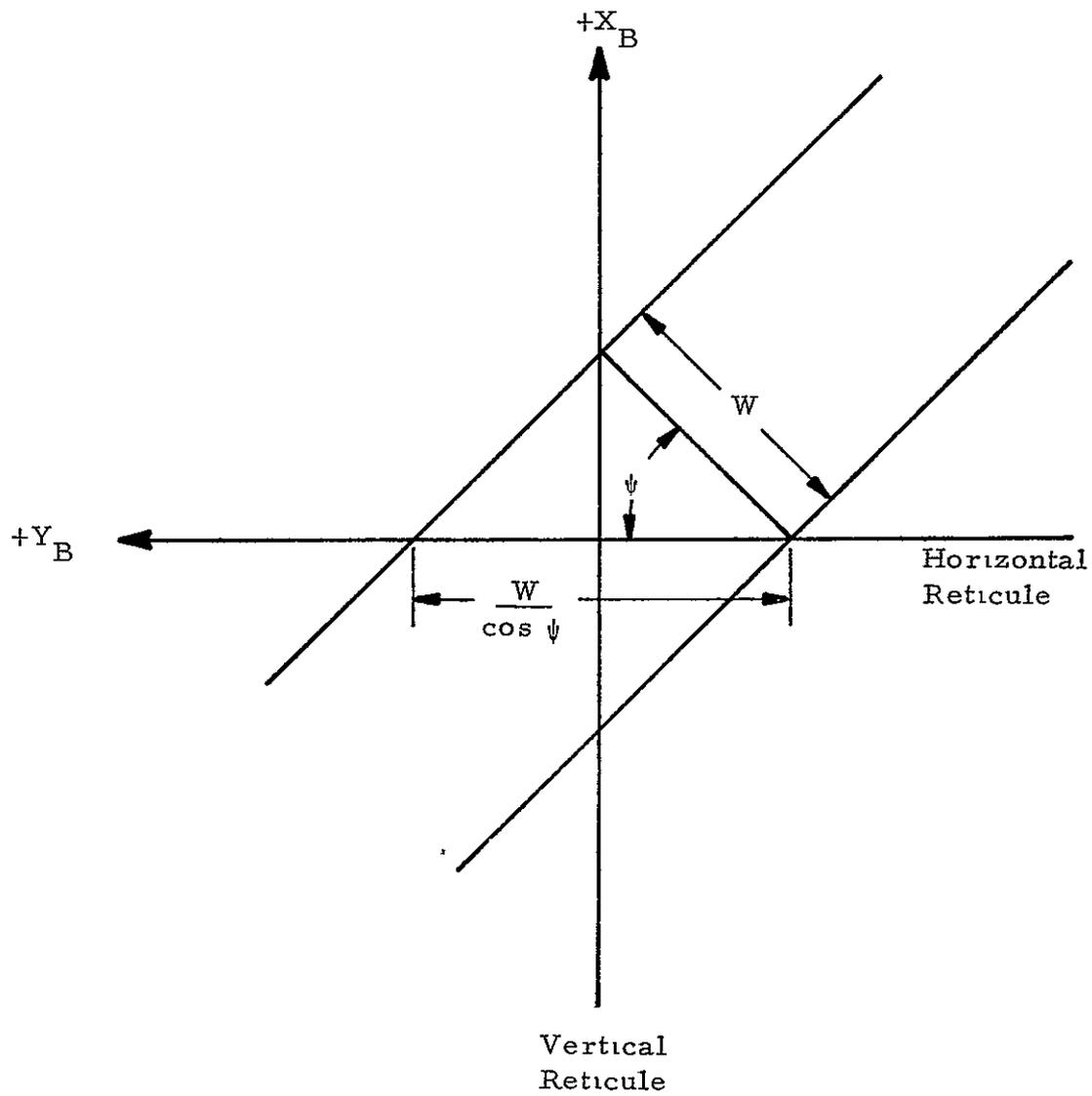
Figure 15.8-2.- Target/Reticle Skew

ψ degrees	$\frac{\delta R}{R}$ %
5	− 0.4
10	− 1.5
15	− 3.4
20	− 6.0
25	− 9.4
30	−13.4
35	−18.1
40	−23.4
45	−29.4
50	−35.7
55	−42.6

The equation for $\frac{\delta R}{R_T}$ indicates that the error may grow to a maximum of

−100% as ψ approaches 90 degrees. The physical significance is that

the apparent target width grows to infinity, which collapses the

computed range to zero. In reality, there are constraints which cause

the maximum error to be considerably less.

First, the pilot will always measure the subtended angle with the

optimum reticle. That is, as ψ passes through 45 degrees, he would

switch from one reticle to the other. This limits the maximum error

to −29.4%.

Second, the available field of view, θ_a, will at some ranges limit

the maximum ψ to less than 45 degrees. This may be expressed by

$$\frac{W}{R_T \cos \psi} \leq \theta_a \left(\frac{\pi}{180}\right)$$

which gives

$$\psi_{max} = \cos^{-1} \left(\frac{180 \; W}{\pi \; R_T \; \theta_a}\right)$$

Assuming θ_a equals 8 degrees, the ψ_{max} (and corresponding $\frac{\delta R}{R_T}$) for each target is.

1. LDEF Approach Target, W = 3.36 ft.

$$\psi_{max} = \cos^{-1} \left(\frac{24.06}{R_T}\right) \text{ for } R_T \geq 24.06 \text{ ft.}$$

R	ψ_{max}	$\frac{\delta R}{R_T}$ %
24.06	0	0
25	15.8	-3.8
30	36.7	-19.8
34	45.0	-29.3

2. LDEF Station Keeping Target, W = 0.83 ft.

$$\psi_{max} = \cos^{-1} \left(\frac{5.94}{R_T}\right) \text{ for } R_T \geq 5.94 \text{ ft.}$$

R	ψ_{max}	$\frac{\delta R}{R_T}$ %
5.94	0	0
7	31.9	-15.1
8	42.1	-25.8
8.4	45.0	-29.3

Operationally speaking, any yaw skew forces the pilot to switch from the approach target to the station keeping target prematurely (i.e., before the optimum range is achieved). For example, if ψ equals 45 degrees, the pilot must switch to the station keeping target at 34 feet instead of 24.06 feet. This causes the $\frac{\delta R}{R_T}$ due to yaw skew to remain the same, but the $\frac{\delta R}{R_T}$ due to resolution error steps from +6.59% to +33.37% (assuming the effects of the two error sources are uncorrelated).

For an obvious reason the LDEF end face target is omitted from this discussion. A circular target does not suffer from a yaw skew error.

Instead, circular targets are sensitive to lateral positioning errors about the LOS. If the center of a circular target does not fall on either the vertical or horizontal reticle, the reticles will measure a chord of the circle, not the diameter. In this case, the apparent range is always greater than the true range. For any circular target (see figure 15.8-3),

$$\ell = 2(r^2 - d^2)^{1/2}$$

where

ℓ = chord length

r = circle's radius = $\frac{W}{2}$

d = the chord's distance from the circle's center
measured along the radius normal to the chord (i.e., position error about $\bar{R}_L$).

W = target width

Therefore,

$$\theta = \frac{2[(\frac{W}{2})^2 - d^2]^{1/2}}{R_T}$$

where θ is the apparent subtended angle.

Recalling that

$$\frac{\delta R}{R_T} = \frac{\frac{W}{\theta} - R_T}{R_T}$$

and substituting the preceding equation for θ gives

109
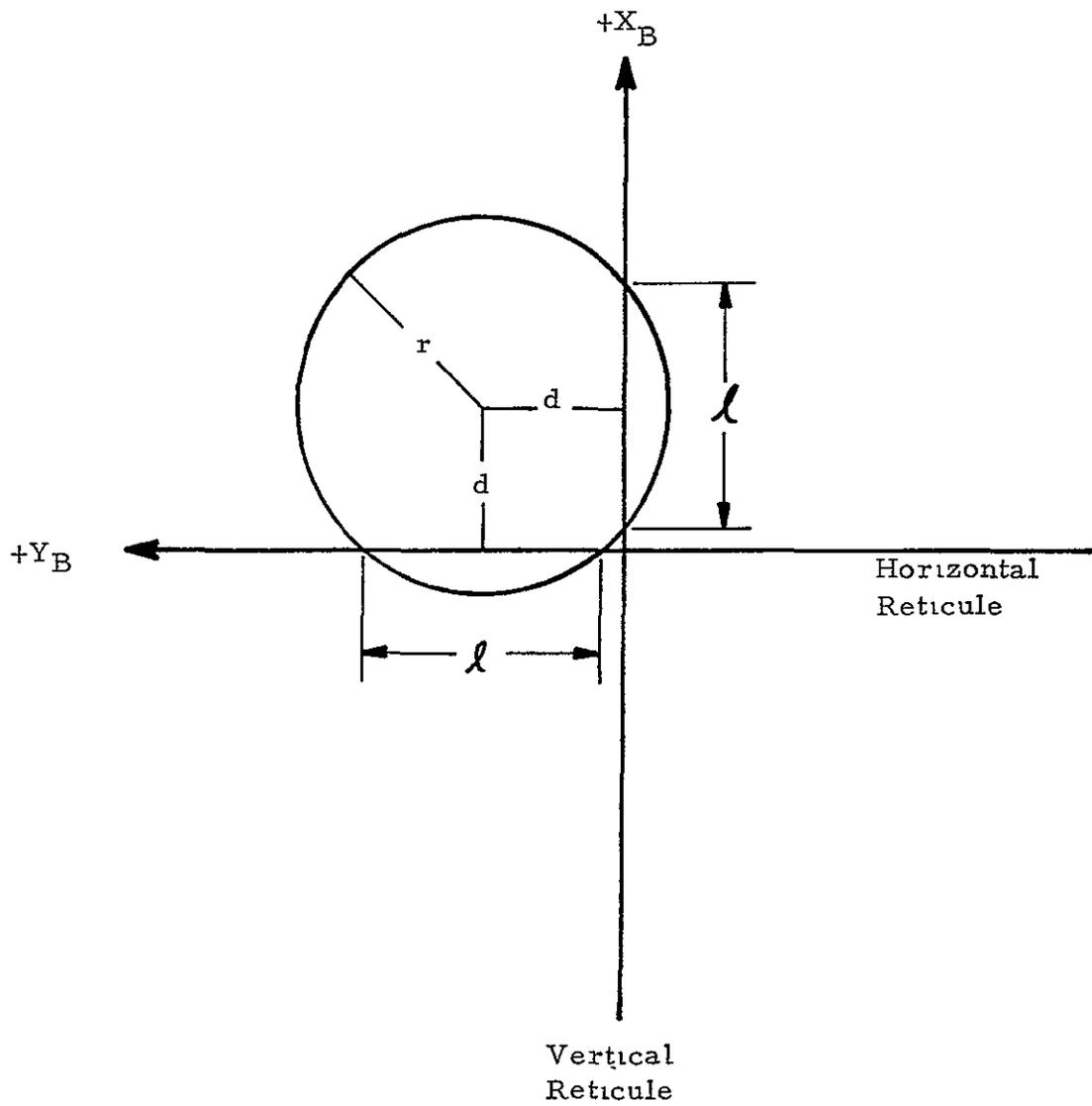
Figure 15.8-3.- Circular Target Positioning Errors in COAS

$$\frac{\delta R}{R_T}\% = 100\left\{\frac{1}{\left[1 - 4(\frac{d}{W})^2\right]^{1/2}} - 1\right\}$$

Once again, the percent error is independent of range. Also, large

target widths (or diameters) minimize the error. Some representative

values of the percentage error (for W equal to 14 feet) are:

d feet	$\frac{\delta R}{R_T}\%$
1	1.0
2	4.3
3	10.7
4	21.9
5	42.9
6	94.1

At first the growth in error is shocking; in fact it approaches infinity

as the positioning error about $\overline{R}_L$ approaches 7 feet. But two opera-

tional considerations help to keep the error in check. First, the

pilot can measure a mental projection of the total target width on the

nearest reticle. Second, the pilot can control to a large extent the

position of the target in the COAS. Although the target may never by

stationary, the pilot can defer a reading until the cyclic, transla-

tional motion causes the target center to pass near or across a reticle.

15.9 Combining the Resolution and Skew Errors

Heretofore, the two ranging errors were treated as being independent

of one another. In reality, they operate collectively and their

combined effect is different than a simple sum of the two. Once again,

$$\frac{\delta R}{R_T} = \frac{\frac{W}{\theta} - R_T}{R_T}$$

But now

$$\theta = \frac{W}{R_T \cos \psi} + \delta\theta$$

Again let

$$k = \frac{W}{\delta\theta} \left(\frac{180}{\pi}\right)$$

where $\delta\theta$ is specified in degrees.

Substituting and rearranging gives

$$\frac{\delta R}{R_T} \% = \left\{ \frac{-1 + \left(1 - \frac{R_T}{k}\right) \cos \psi}{1 + \frac{R_T}{k} \cos \psi} \right\}^{*} 100$$

Establishing a finite value for ψ is difficult. Assume that the Orbiter's X_B axis (because of the previously discussed coupling problems) is maintained in the orbit plane. In addition, the reference image of the baseline COAS cannot be rotated with respect to the Orbiter's body axis. Therefore, the reference image is fixed with respect to the LVLH frame. This reduces the problem of defining ψ to one of describing the LDEF yaw attitude with respect to the LVLH frame.

*Note when ψ equals zero degrees, cos ψ equals one and this equation
 reduces to the resolution error equation,

$$\frac{\delta R}{R_T} \% = \frac{-100}{1 + \frac{k}{R_T}}$$

The LDEF attitude state at retrieval is specified in the LDEF

Mission Requirements Document (MRD). The September 15, 1977 issue of

the MRD essentially describes the LDEF yaw attitude, ψ_L, as follows:

$$\psi_L = \psi_b + \psi_o$$

where $\quad\quad \psi_b$ = bias or time invariant component of ψ_L in degrees

ψ_o = oscillatory component of ψ_L in degrees

When ψ_L equals zero, the LDEF approach target (W = 3.36 ft.) and

station keeping target (W = 0.83 ft.) are normal to a COAS reticle

(assuming the Orbiter's X_B resides in the orbit plane). The MRD

values for ψ_b, ψ_{omax}, and $\dot{\psi}_{max}$ (which are reproduced below) bound the

non-zero values for ψ_L.

Parameter	Maximum Value	
	215 n. miles (nominal retrieval)	175 n. miles (contingency retrieval)
ψ_b	± 21.0 deg. or 180 ± 21.0 deg.	± 33.0 deg. or 180 ± 33.0 deg.
$\psi_{o\ max}$	± 10.8 deg.	± 10.2 deg.
$\dot{\psi}_{max}$	± 0.007 deg/sec	± 0.007 deg/sec.

For a nominal retrieval, $|\psi_L|$ can assume a value anywhere from

zero to 31.8 degrees. For a contingency retrieval, the corresponding

spread is zero to 43.2 degrees. (In each case 180 degrees may be added

to the spread because the LDEF is bistable about yaw; however, assessing

either of the two stable states suffices for both). For the two

affected targets, tables 15.9-1 and 15.9-2 give representative, combined

TABLE 15.9-1 – Combined Resolution and Skew Errors

for LDEF Station Keeping Target, W = 0.83 ft.

A. $\psi = 10^{\circ}$

R_T (ft)	$\frac{\delta R}{R_T}$ %	
	$\delta\theta = +0.35$ deg.	$\delta\theta = -0.35$ deg.
5	− 5.0	2.2
10	− 8.1	6.1
15	−11.1	10.4
20	−13.9	15.1
25	−16.6	20.2
30	−19.1	25.7
35	−21.4	31.8

B. $\psi = 30^{\circ}$

5	−16.1	−10.6
10	−18.6	− 7.5
15	−20.9	− 4.3
20	−23.2	− 0.8
25	−25.3	+ 2.9
30	−27.3	7.0
35	−29.1	11.3

C. $\psi = 45^{\circ}$

5	−31.1	−27.4
10	−32.8	−25.4
15	−34.4	−23.3
20	−35.9	−21.1
25	−37.4	−18.8
30	−38.8	−16.3
35	−40.1	−13.6

TABLE 15.9-2 – Combined Resolution and Skew Errors

for LDEF Approach Target, W = 3.36 ft.

A. ψ = 10 degrees

R_T (ft)	$\frac{\delta R}{R_T}$ %	
	$\delta\theta$ = +0.35 deg.	$\delta\theta$ = −0.35 deg.
20	− 4.9	2.1
30	− 6.5	4.1
40	− 8.1	6.1
50	− 9.6	8.2
60	−11.1	10.3
70	−12.5	12.6
80	−13.9	14.9
90	−15.2	17.4
100	−16.5	20.0
110	−17.7	22.6

B. ψ = 30 degrees

20	−16.0	−10.6
30	−17.3	− 9.1
40	−18.3	− 7.6
50	−19.7	− 6.0
60	−20.9	− 4.4
70	−22.0	− 2.7
80	−23.1	− 0.9
90	−24.1	+ 0.9
100	−25.2	2.8
110	−26.2	4.7

C. ψ = 45 degrees

20	−31.1	−27.4
30	−31.9	−26.5
40	−32.7	−25.5
50	−33.6	−24.4
60	−34.4	−23.4
70	−35.1	−22.3
80	−35.9	−21.2
90	−36.6	−20.0
100	−37.3	−18.9
110	−38.0	−17.6

error values for ψ equal to 10, 30, and 45 degrees.

When tables 15.9-1 and 15.9-2 are compared to tables 15.6-1 and 15.6-2, the effect of combining errors is apparent. For example the errors in the approach target (W = 3.36 ft.) versus ψ at 80 feet are:

	$\dfrac{\delta R}{R_T}$ %	
ψ (deg)	$\delta\theta = +0.35$ deg.	$\delta\theta = -0.35$ deg.
0	-12.7	+17.0
10	-13.9	+14.9
30	-23.1	- 0.9
45	-35.9	-21.2

At ψ equal to zero, the percent error is unbalanced about zero. When ψ equals ten degrees, the percent error tends to balance itself about zero. For larger values of ψ, the skew error predominates. In fact, at ψ equal to 45 degrees, the percent error becomes relatively insensitive to range as shown below.

	$\dfrac{\delta R}{R_T}$ %		
R_T (ft)	$\delta\theta = +0.35$ deg.	mean	$\delta\theta = -0.35$ deg.
30	-31.9	-29.2	-26.5
50	-33.6	-29.0	-24.4
80	-35.9	-28.6	-21.2
100	-37.3	-27.8	-18.2

Note that the mean error closely approximates -29.4% which is the percent error for a skew of 45 degrees and no resolution error. All of this implies that the pilot should have a set of ranging tables which would minimize errors by accommodating a range of ψ's. Unfortunately

116

this adds complexity to the approach operation.

Even if additional ranging tables were available, a change from an initial selection (based on ψ_L at 1000 ft.) may be indicated as the approach progresses ψ_0 is the time varying component of ψ_L. It is a periodic function which consists of several components at different frequencies. However, the maximum change in ψ_L over the approach interval, Δt_a, is bounded by

$$\Delta\psi_L = \dot{\psi}_{max} \Delta t_a \leq 2 \psi_{o\ max}$$

where

$$\dot{\psi}_{max} = 0.007 \text{ deg/sec}$$
$$\psi_o = \pm 10.8 \text{ deg.}$$

As previously stated, a typical $\bar{R}$ approach (from SES runs) takes approximately 45 minutes. This allows $\Delta\psi_L$ to be as great as 18.9 degrees. Thus, as the approach proceeds, ψ_L may (for example) change from 0 to 18.9 degrees or 43.2 to 24.3 degrees. The operational need and technique to accommodate ψ and its changes will be studied by JSC in the near future.

16.0 Man-in-the-Loop Simulation Findings

On the surface, the Orbiter state uncertainties with respect to LDEF appear unreconcilable with the $\bar{R}$ approach sensitivity. A + 1.0 fps $\dot{R}$ error (due to radar uncertainty) at 1000 feet requires 2.2 fps of braking near the target. To a lesser degree the radar range error also appears to be a problem. The radar δR of 80 feet 3σ maps into an equivalent range rate error of mδR or 0.052 fps, which still results in

117

0.45 fps of braking at LDEF. When the LDEF ranging targets come into play, range rate _magnitude_ information is exceptionally poor.

But one fact remains: During July, August, and September of 1977, successful $\bar{R}$ approaches were being performed on a regular basis in the Shuttle Engineering Simulator at JSC. Many important operational techniques became apparent during this period* Some of the most relevant findings are presented below.

1. When the pilot was utilizing the radar for range and range rate information, he was found to mentally average consecutive radar updates. This effectively filtered the scatter to the point that the residual uncertainty in the average was reduced to almost one third of the specified radar uncertainties.

2. Establishing the magnitude of the range rate with the COAS was confirmed to be very difficult and subject to large errors. But the COAS was found to be of some use in differentiating between opening, closing, and zero range rates.

3. Knowledge of either a zero or opening range rate was found to be particularly useful. Under such situations the pilot knew that he could introduce a closing ΔV at least equivalent to the $\dot{R}_{max}$ allowed for his current range. The ΔV could be inserted very accurately by utilizing the DAP's translational pulse mode.

---

*The results are presented and discussed by JSC in the PDRS III Post-Simulation Report.

4. The aft payload bay CCTV (closed circuit television camera) was found to be even more effective than the COAS in differentiating between opening, closing, or zero range rates. This was due to the fact that motion is more easily detected if the LOS is at some angle to the path of motion*. A description and analysis of this measurement technique is provided in the following section.

5. Some degree of $\pm$ X jet braking was found to be acceptable. That is, the LDEF could tolerate some plume impingement (disregarding contamination) without violating the LDEF to Orbiter relative state constraints for RMS grappling operations.

At least three pilots performed $\bar{R}$ approaches in the SES. Each pilot's technique had its nuances but the principles behind each case were the same. These were:

1. In order to accommodate range and range rate errors, margins were always maintained between the allowable $\dot{R}_{max}$ and the closing velocity inserted at any range.

2. When radar range rate became useless, no further range rate adjustments were made until the range rate was determined to be either zero or opening.

In other words, state knowledge uncertainties always demanded that the

---

*Future simulations will study the feasibility of obtaining non-zero range rate magnitudes with the aft CCTV. In addition, a camera elevation angle display will be added to the SES cockpit. The display will be used to study the technique and utility of CCTV ranging in lieu of COAS/target ranging.

pilot fly the approach in a conservative manner. Instead of the optimal

single burn approach, multiple small burns were utilized to reach LDEF.

In contrast to the 37.9 minute optimal approach, the elapsed time was

approximately 45 minutes.

17.0 <u>Establishing Zero Range Rate with the Aft P/L Bay CCTV</u>

The <u>basic</u> technique of establishing zero range rate with the aft

P/L bay CCTV is straightforward. Referring to figure 17-1, the camera

elevation, θ_c, is adjusted to aim the CCTV LOS at the facing lower edge

of LDEF. With elevation fixed, the LDEF is observed on a cockpit

monitor to either drift up or down or remain stationary. Sensitivity

is maximized by zooming the camera lens to approximately a 9 degree

(diagonal) field of view. When the LDEF image is stationary, range

rate is assumed to be zero.

The <u>specific</u> technique of utilizing the aft CCTV is more involved.

Even though range rate occasionally goes to zero, the LDEF image on the

CCTV may not be stationary. This is because the movement on the screen

is subject to Orbiter motions other than range rate along the COAS LOS.

For example, if range rate is zero but the Orbiter is pitching up, the

LDEF image will fall on the screen. Or, if range rate is zero but the

Orbiter is moving forward, the LDEF image will climb on the screen.

Such image motion (i.e., from sources other than range rate) is "noise"

or an error in the measurement system. Since by definition pitching

motion and translation normal to the COAS LOS must be cyclic, the

pilot under some circumstances may filter the noise by observing the

120
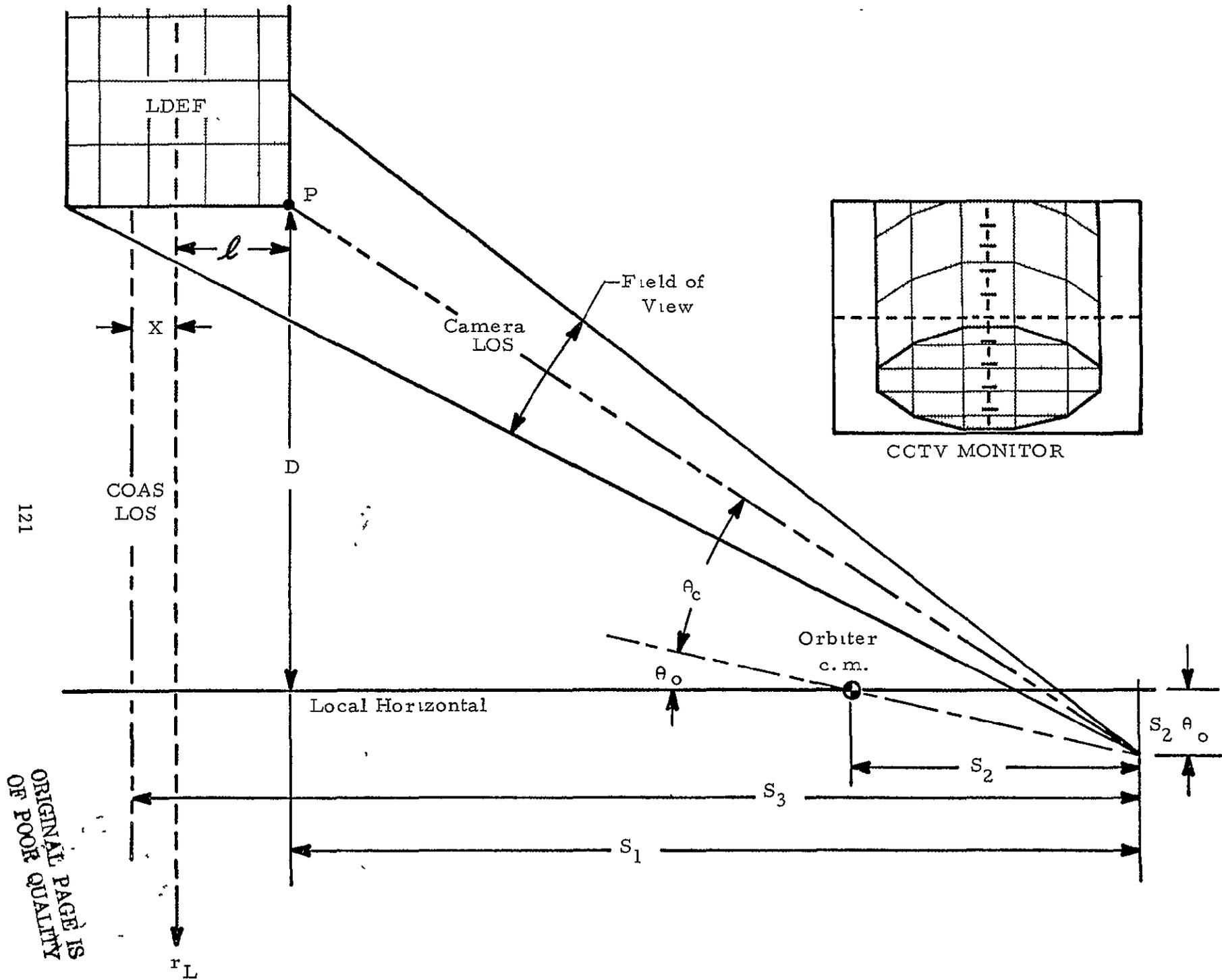
Figure 17-1.- Establishing Zero Range Rate with the Aft P/L Bay CCTV

average motion on the screen. But if the cycles are long, there may be times when the noise must be accepted as an error. It is necessary, therefore, to assess both situations.

Assume that range rate is zero. Referring again to figure 17-1 point P represents the intersection of the camera LOS and a line which is collinear with the facing vertical edge of LDEF. When point P rises or falls, the LDEF image falls or rises, respectively, on the monitor. P is positioned at a vertical distance, D, from a local horizontal reference line which passes through the Orbiter c.m. The distance, D, may be expressed as

$$D = S_1 \tan \theta_s - S_2 \theta_o$$

where $S_1 = S_3 - X - \ell$

S_3 = distance between the COAS LOS and the CCTV or 63 ft.

X = in-plane positioning error of the COAS LOS WRT the LDEF radius vector (positive along $\bar{V}$)

ℓ = LDEF radius or 7 feet

S_2 = camera distance from the Orbiter c.m.

$\theta_s = \theta_o + \theta_c$

θ_o = Orbiter pitch WRT the local horizontal reference

θ_c = camera LOS elevation WRT Orbiter X axis

Image motion is related to the time derivative of D which is

$$\dot{D} = \frac{d}{dt} \left(S_1 \tan \theta_s - S_2 \theta_o \right)$$

$$= \dot{S}_1 \tan \theta_s + \frac{S_1 \dot{\theta}_s}{\cos^2 \theta_s} - S_2 \dot{\theta}_o$$

$$= \dot{X} \tan(\theta_o + \theta_c) + \frac{(S_3 - X - \ell)\dot{\theta}_o}{\cos^2 (\theta_o + \theta_c)} - S_2 \dot{\theta}_o$$

The physical significance of the last equation is more apparent if the equation is assessed in 2 parts, some simplifying assumptions are made, and the parts are expressed in terms of range, R. That is, let

$$\dot{D} = \dot{D}_1 + \dot{D}_2$$

First,

$$\dot{D}_1 = \dot{X} \tan (\theta_o + \theta_c)$$

If it is assumed that θ_o and X equal zero, a condition exists where $\tan \theta_c$ is equal to $\frac{R}{S_3 - \ell}$. Then,

$$\dot{D}_1 = \frac{\dot{X}R}{S_3 - \ell} - n\dot{X}$$

where $\qquad S_3 - \ell = A = 56$ feet

and, $\qquad n = \frac{R}{A}$

This equation represents the sensitivity of the camera system to in-plane horizontal velocities relative to the LDEF LVLH frame. The "mapping ratio", n, grows linearly with R, and at a range of 56 feet (where $\theta_c =$

123

45°) the horizontal velocities map one for one into the indicated range rate.

Proceeding to the second part of $\dot{D}$,

$$\dot{D}_2 = \frac{(S_3 - X - \ell)\dot{\theta}_o}{\cos^2 (\theta_o + \theta_c)} - S_2 \dot{\theta}_o$$

Again let X and θ_o equal zero. Then

$$\dot{D}_2 = \frac{A\dot{\theta}_o}{\cos^2 \theta_c} - S_2 \dot{\theta}_o$$

$$= A\dot{\theta}_o (1 + \tan^2 \theta_c) - S_2 \dot{\theta}_o$$

$$= A\dot{\theta}_o + \frac{\dot{\theta}_o R^2}{A} - S_2 \dot{\theta}_o$$

$$= A\dot{\theta}_o \left\{ \left(1 - \frac{S_2}{A} \right) + n^2 \right\}$$

where, once again, n equals $\frac{R}{A}$. Since S_2 equals 18 feet,

$$1 - \frac{S_2}{A} = 0.68$$

And, if $\dot{\theta}$ is expressed in degrees

$$\dot{D}_2 = A\dot{\theta}_o \left(\frac{\pi}{180}\right) (0.68 + n^2)$$

But $\quad \frac{A\pi}{180} = 0.977$ ft/deg.

124

Finally,

$$\dot{D}_2 \cong \dot{\theta}_o \ (0.68 + n^2) \ \text{(within 2.3\%)}$$

where $\dot{\theta}_o$ is in degrees per second and $\dot{D}_2$ is in feet per second. The equation shows that the camera system's sensitivity to Orbiter pitch rates is never less than 0.68 and grows rapidly with increasing range. For example, for n equal to 3 (corresponding to a range of 168 feet) the mapping ratio, $0.68 + n^2$, is 9.68.

$\dot{X}$ and $\dot{\theta}_o$ are directly related to Orbiter control system performance. For example, in a minimum impulse attitude limit cycle, each jet pulse causes a $\Delta\dot{\theta}_o$ of $\pm$ 0.1 deg/sec. Similarly, minimum ΔV's of $\pm$ 0.25 fps and $\pm$ 0.03 fps are available from single THC hits in DAP A and DAP B respectively. Therefore, $\dot{X}$ and $\dot{\theta}_o$ may assume the following range of values.

$$-0.1 \ \text{deg/sec} \leq \dot{\theta}_o \leq + 0.1 \ \text{deg/sec}$$
$$-0.25 \ \text{fps} \leq \dot{X} \leq + 0.25 \ \text{fps (DAP A)}$$
$$-0.03 \ \text{fps} \leq \dot{X} \leq + 0.03 \ \text{fps (DAP B)}$$

The DAP controls the pitch attitude error, θ_o, to within $\pm$ 0.2 degrees of the UPS reference (the local horizontal). The pilot controls the position error, X, to assure proper use of the COAS (see the section on target width). Therefore, $\dot{X}$ and $\dot{\theta}_o$ are cyclic and have zero means.

As mentioned earlier, the periods of the $\dot{X}$ and $\dot{\theta}_o$ cycles will influence the pilot's course of action. If the periods are relatively short the pilot will attempt to "filter" the corrupting image motion to establish zero range rate. But if the periods are long, the motion

125

is characterized by small angular rates and normal velocities which are interrupted by short bursts of relatively high rates and velocities. In such situations the pilot does not average the motion but accepts the error during the "quiet" phases of the cycles. The errors in this case are expressed by the equations for $\dot{D}_1$ and $\dot{D}_2$. For example, assume the following conditions.

$\dot{\theta}_o = 0.002$ deg/sec

$\dot{X} = 0.030$ fps

$n = 4$ (R = 224 ft)

$X = \pm 3$ ft.

$\theta_{o_{max}} = \pm 0.2$ deg

The period of $\dot{\theta}_o$ is 204 seconds in which 200 seconds is spent rotating at 0.002 deg/sec and 4 seconds is spent returning at close to 0.1 deg/sec. The period of $\dot{X}$ is 227 seconds in which 200 seconds is spent translating at 0.03 fps and 27 seconds is spent returning at 0.22 fps. If the pilot elects to establish zero range rate during the quiet phases, the errors will be

$\dot{D}_1 = 4 \ (.030) = 0.12$ fps

$\dot{D}_2 = 0.002 \ (0.68 + 16) = 0.033$ fps

The total error is, depending on the phasing of the two motions, 0.15 fps or 0.09 fps.

As the cyclic motions approach symmetry about zero in the attitude rate and translational velocity domains, the periods become shorter and shorter. When symmetry exists (a reasonable probability in this random process),

$$\dot{\theta}_o = \pm\ 0.05\ \text{deg/sec}$$

$$\dot{X} = \pm\ 0.125\ \text{fps for DAP A}$$

$$\dot{X} = \pm\ 0.015\ \text{fps for DAP B}$$

Inserting these values into the previous example gives,

$$\dot{D}_1 = 4\ (0.125) = 0.5\ \text{fps}$$

$$\dot{D}_2 = 0.05\ (0.68 + 16) = 0.83\ \text{fps}$$

But in such situations, $\dot{D}_1$ and $\dot{D}_2$ are not the errors in establishing

zero rate. Instead, $\dot{D}_1$ and $\dot{D}_2$ represent the "noise" which exists in the

system. The errors in this case are due to the inability of the pilot to

precisely establish zero range rate in the presence of the noise.

The pilot's task of mentally filtering image motion corrupted by

noise is better understood in the ΔD_1 and ΔD_2 versus time domain, where

ΔD_1 and ΔD_2 are treated as independent components of D due to X and θ_o

respectively. If X is initially zero and θ_o is always zero, the initial

value of D is

$$D_o = (S_3 - \ell)\tan\ \theta_c$$

where

$$\tan\ \theta_c = \frac{R}{S_3 - \ell} = n$$

If at some time later X is non-zero and θ_c remains unchanged.

$$D_t = (S_3 - \ell - X)\ n$$

and

$$\Delta D_1 = D_t - D_o = -Xn$$

Similarly, if θ_o is initially zero and X is always zero,

127

$$D_o = (S_3 - \ell) \tan \theta_c$$

If at some time later θ_o is non-zero,

$$D_t = (S_3 - \ell) \tan (\theta_c + \theta_o) - S_2 \theta_o$$

and

$$\Delta D_2 = D_t - D_o$$

$$= (S_3 - \ell) [\tan(\theta_o + \theta_o) = \tan \theta_c] - S_2 \theta_o$$

But, $\qquad \tan(\theta_c + \theta_o) = \dfrac{\tan \theta_c + \tan \theta_o}{1 - \tan \theta_c \tan \theta_o}$

Substituting,

$$\Delta D_2 = (S_3 - \ell) \left\{ \frac{\tan \theta_o (1 + \tan^2 \theta_c)}{1 - \tan \theta_o \tan \theta_c} \right\} - S_2 \theta_o$$

Since $\qquad \theta_o \leq 0.2 \text{ deg}$

$\qquad\qquad \tan \theta_o = \theta_o \text{ radians}$

Also $\qquad \tan \theta_c = \text{constant} = \dfrac{R}{S_3 - \ell} = n$

Substituting

$$\Delta D_2 = (S_3 - \ell) \left\{ \frac{\theta_o (1 + n^2)}{1 - \theta_o n} \right\} - S_2 \theta_o$$

Since $\qquad (1 - \theta_o n)^{-1} = 1 + \theta_o n + (\theta_o n)^2 + (\theta_o n)^3 + \ldots$

and $\qquad n \leq 5 \text{ (for } R \leq 280 \text{ ft)}$

$$(1 - \theta_o n)^{-1} = 1 \text{ (within 1.7\%)}$$

Simplifying and rearranging,

$$\Delta D_2 = \theta_o \ (S_3 - \ell) \left\{ \left(1 - \frac{S_2}{S_3 - \ell} \right) + n^2 \right\}$$

(Note the relationship of ΔD_2 to the exact time derivative, $\dot{D}_2$). If θ_o is expressed in degrees,

$$\Delta D_2 = \theta_o \ (0.68 + n^2) \ \text{(within 2.3\%)}$$

where ΔD_2 is in feet.

Returning to the example where

$$\dot{\theta}_o = \pm \ 0.05 \ \text{deg/sec}$$

$$\dot{X} = \pm \ 0.125 \ \text{fps}$$

$$\theta_{o_{max}} = \pm \ 0.2 \ \text{deg}$$

$$X = \pm \ 3 \ \text{ft}$$

$$n = 4$$

the noise on D is characterized by a pair of triangular wave forms with peak values of

$$\Delta D_1 = nx = \pm \ 12 \ \text{feet}$$

and

$$\Delta D_2 = \theta_o \ (0.68 + n^2) = \pm \ 3.34 \ \text{feet}$$

The periods are

$$T_1 = \frac{4 \ \theta_o}{\dot{\theta}_o} = 16 \ \text{seconds}$$

$$T_2 = \frac{4 \ X}{\dot{X}} = 96 \ \text{seconds}$$

129

Plots of ΔD_1, ΔD_2, and their algebraic sum, $\Delta D_1 + \Delta D_2$, versus time are shown in figure 17-2. When the pilot is observing image motion, two thoughts are passing through his mind. First, no -Z THC hits are to be executed until $\dot{R}$ is observed to be essentially zero. Second, any image noise is cyclic. His task, therefore, is one of testing the image motion for a zero mean. Procedures for accomplishing this can be explained with the aid of figure 17-3.

In figure 17-3 a closing range rate of 0.05 fps (represented by a ramp) has been added to $\Delta D_1 + \Delta D_2$. In essence a constant 0.05 fps is "buried" in a ΔD wave form which has a peak velocity of 0.83 + 0.5 + 0.05 or 1.18 fps. The composite wave form is superimposed on an orthographic projection of LDEF. The projection closely resembles the true perspective from the aft bay camera at a COAS LOS range of 224 feet and a camera elevation of 76 degrees. If the linear dimension of the ΔD time scale is collapsed to zero while centered on LDEF, the wave form represents the locus of point P on LDEF. Initially the center of the monitor recticles (which always represents point P) lies on the facing lower edge of LDEF. As time elapses point P "walks" up and down the facing side of LDEF.

There are several ways in which the mean value of the motion may be tested, but all of them are based on observing and remembering the relative positions of the image and the reticles during major positive or negative peaks in the motion. For example, at time t_1, the horizontal reticle falls on the LDEF center ring or point P_1. Subsequently at time t_2, the horizontal reticle momentarily stops at a higher position on

130
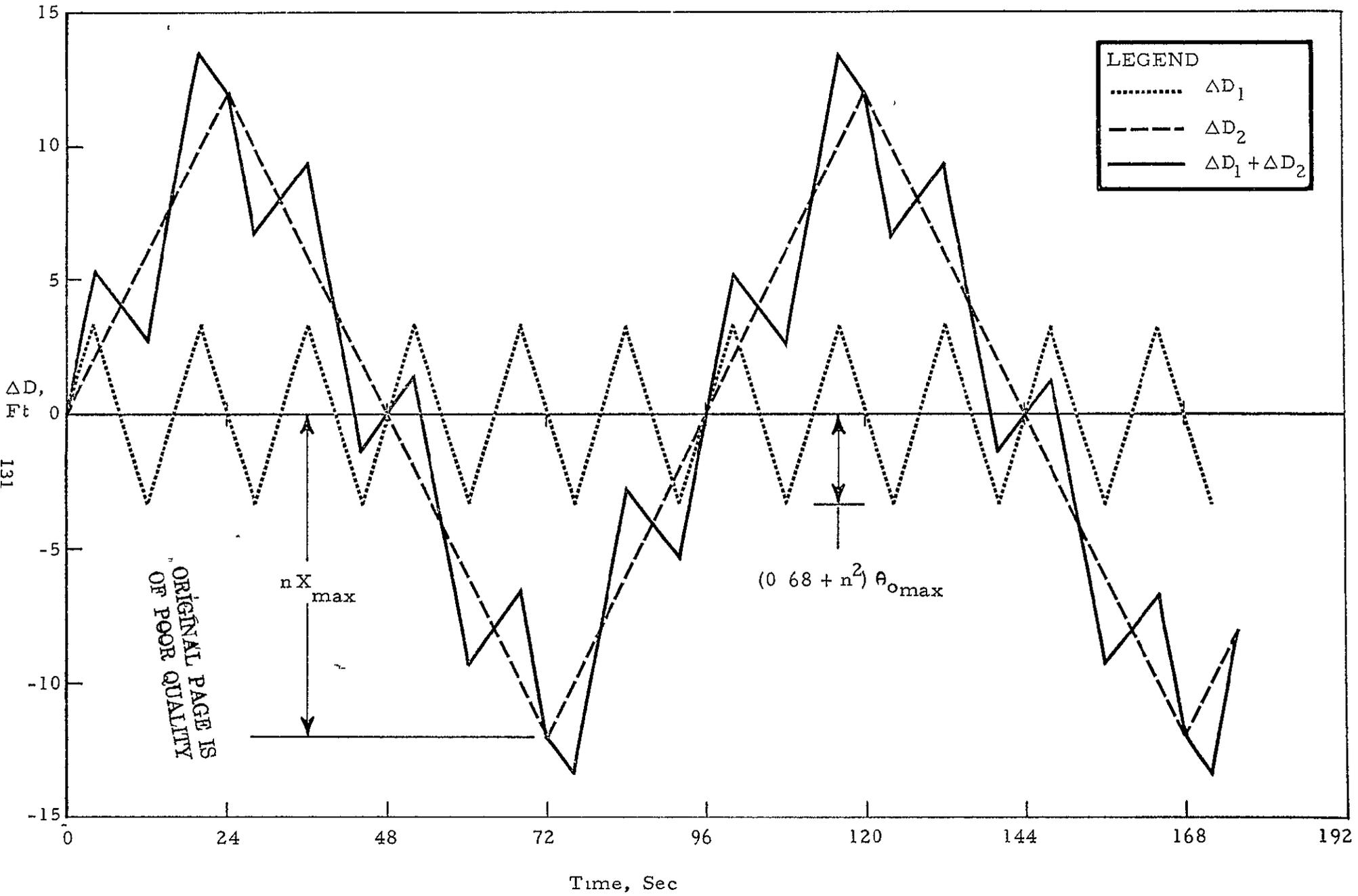
Figure 17-2.- Aft CCTV Image Noise, ΔD
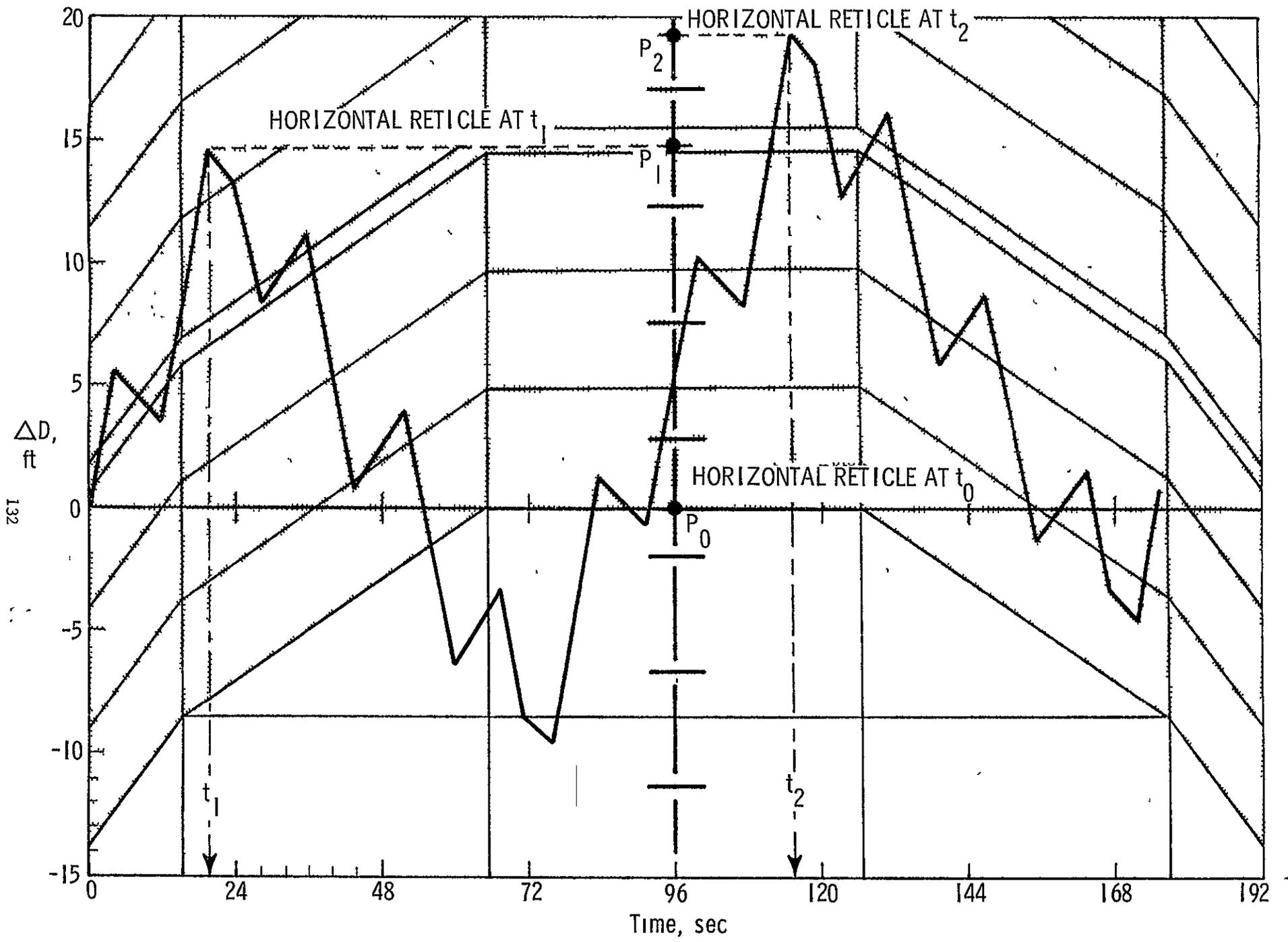
Figure 17-3 - Image Noise, ΔD, Superimposed on LDEF at a Range of 224 Feet

LDEF or point P_2. Point P_2, in this case, is situated 4.8 feet higher

than P_1, which corresponds to a mean motion of 0.05 fps (closing) over

the interval $t_2 - t_1$, or 96 seconds. Ideally the pilot's detection of

this position difference is all that is required to establish some true

range rate.

In order to better appreciate the pilot's task, some "snapshots"

of the CCTV monitor screen have been created. They are presented in

figures 17-4a through 17-4d. The snapshot at t = o can be considered

the set-up orientation in which the CCTV LOS is directed at the lower

facing edge of LDEF. Exact positioning is not very important. The

subsequent snapshots depict the image position at major positive or

negative peaks in the motion. The scenes at 20 seconds and 116 seconds

are those which must be compared to test the mean value. The screen is

sized to comply with the latest available CCTV specification. In

addition, all scenes are presented with maximum camera zoom, which gives

a diagonal field of view of 9 degrees.

Heretofore, only the technique of testing the mean value has been

discussed. The reader at this point is probably asking, "What are the

constraints and uncertainties of the test, and are they acceptable?"

The answer to the last question is apparently yes, since successful $\bar{R}$

approaches have been accomplished in the Shuttle Engineering Simulator

at JSC. But because flight simulation activities are far from being

complete, specific answers to the first question are not available. A

paper analysis would be quite involved and may never truly reflect what

the pilot is capable of accomplishing. For example, by controlling his
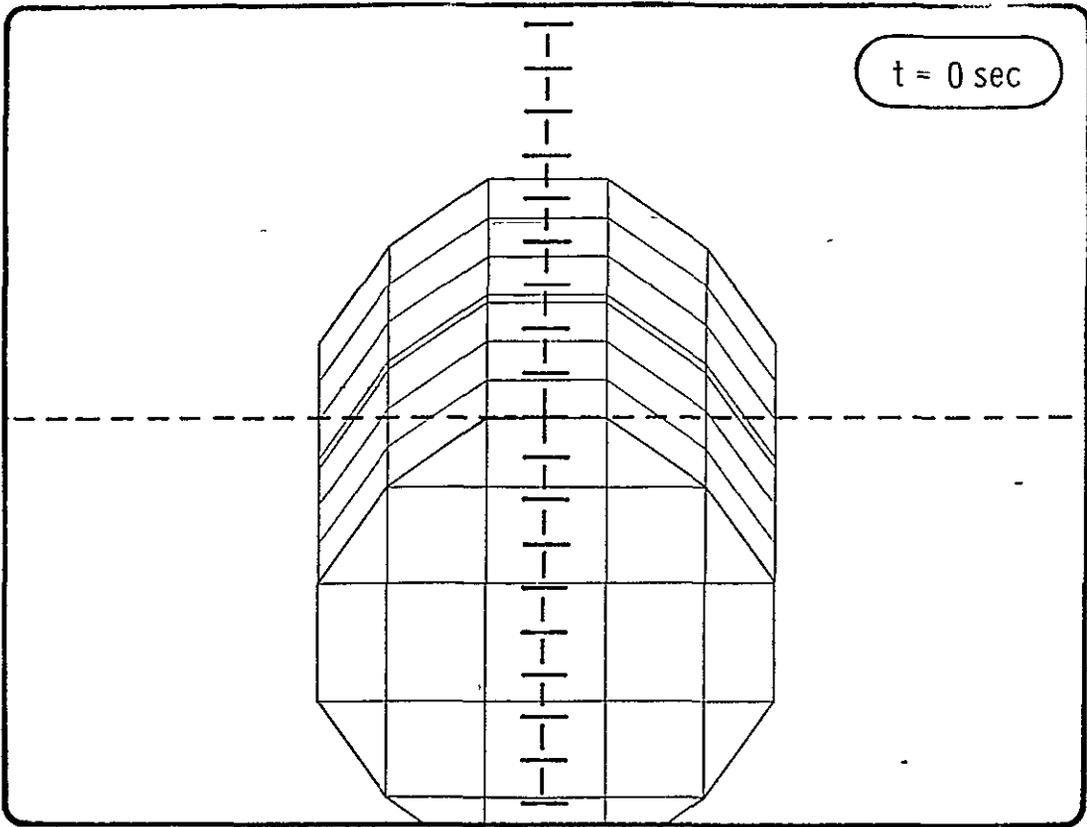
Figure 17-4a.- Initial CCTV Alinement at 224 feet
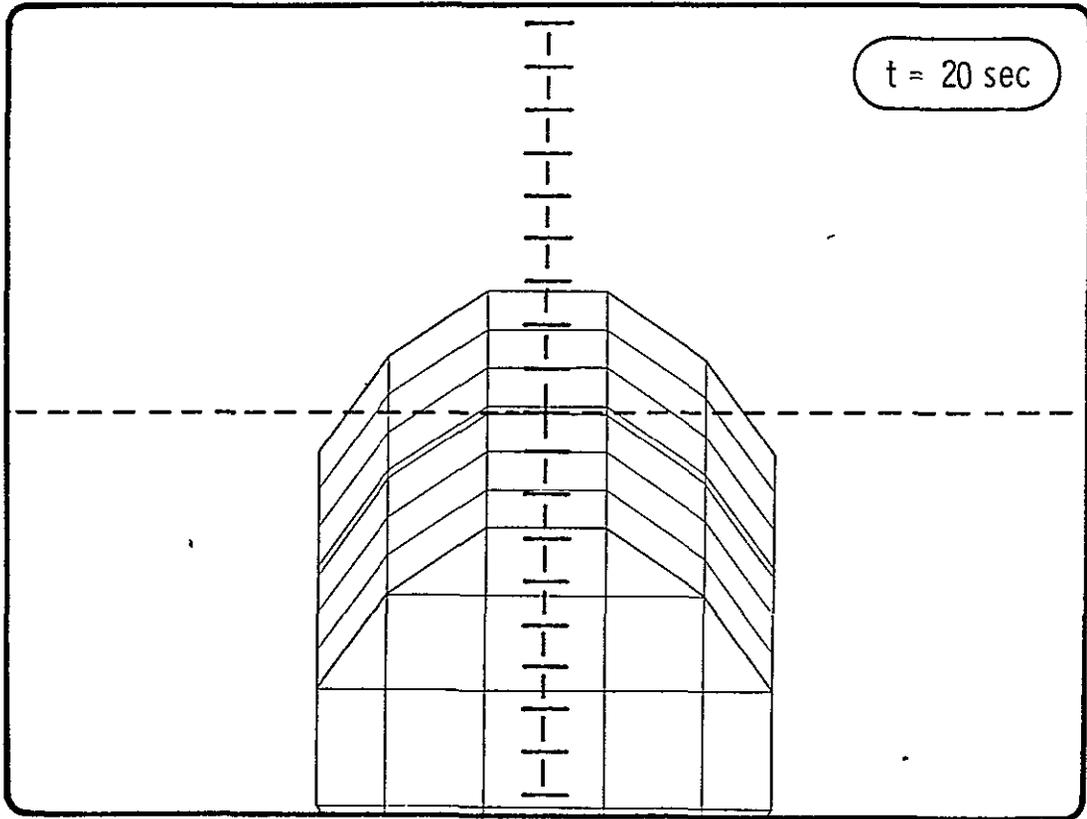
Figure 17-4b.- The first major positive peak at 224 feet
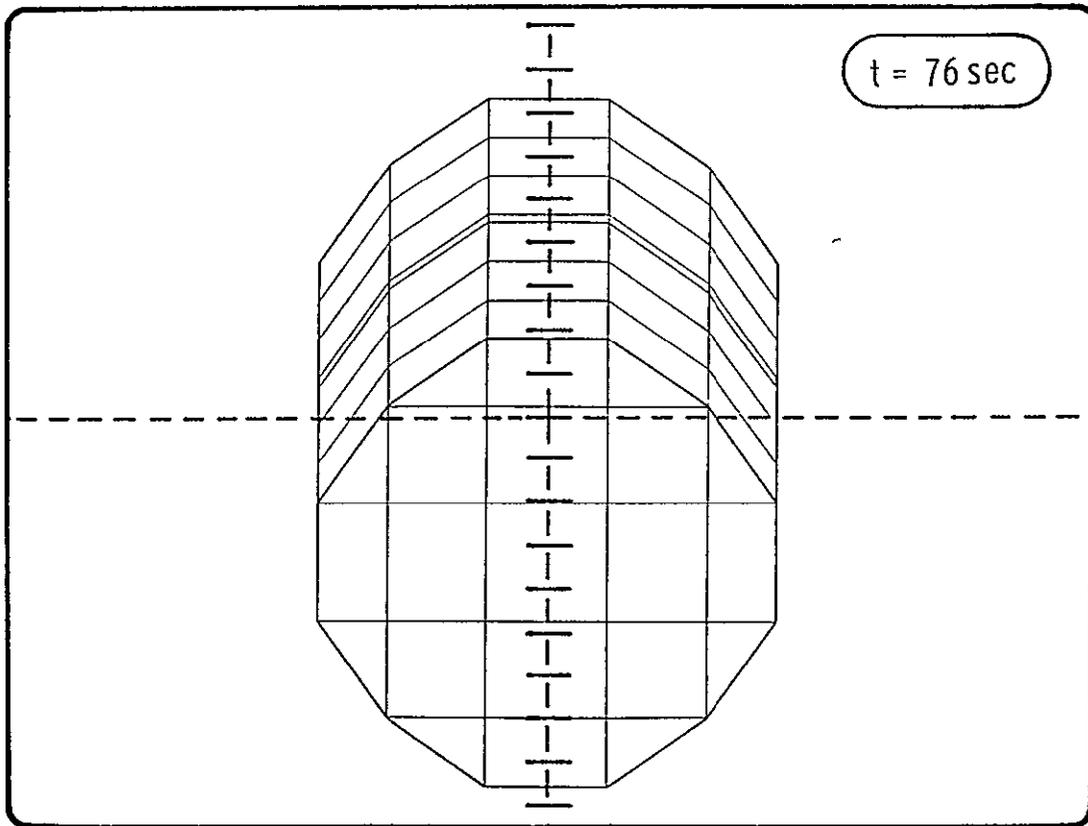
Figure 17-4c.- The first major negative peak at 224 feet
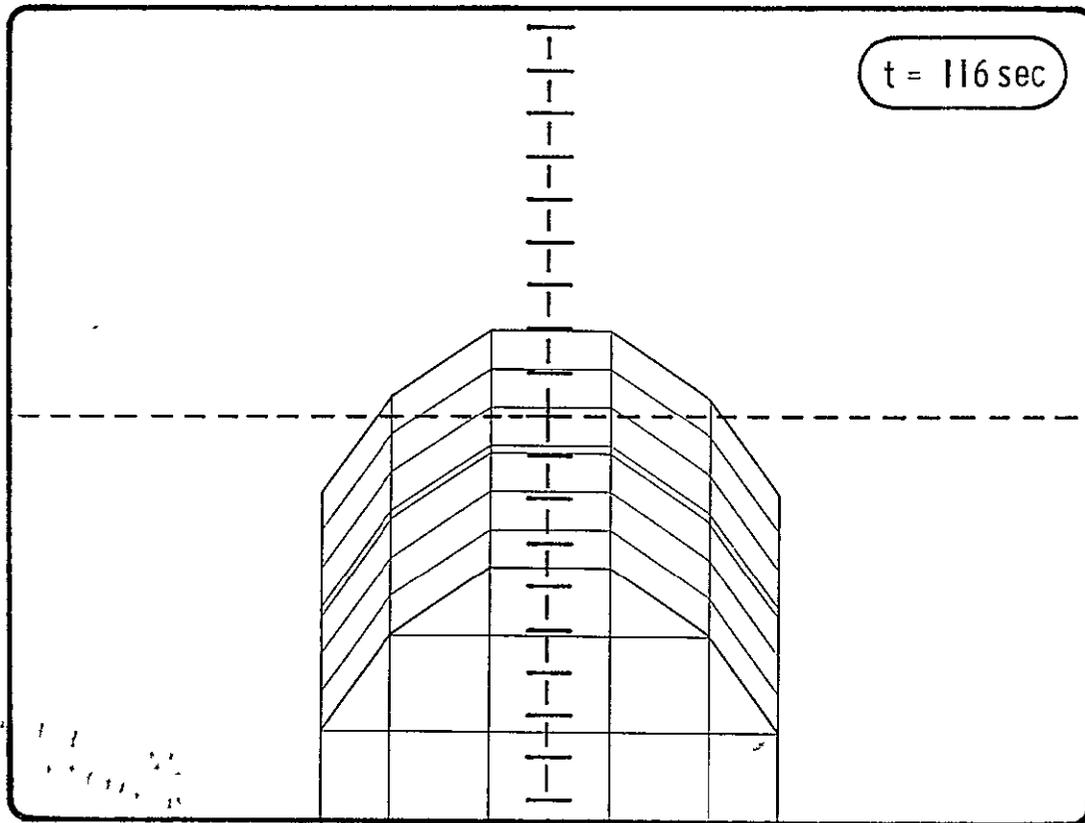
Figure 17-4d.- The second major positive peak at 224 feet

135

position error beneath LDEF, the pilot is actually controlling the peak

value of ΔD_2. From observing LDEF in the COAS, he knows when ΔD_2 will

be at its peaks; therefore, he may anticipate and mentally prepare for a

CCTV observation. On the other hand, it is not difficult to see from

analysis that the results of the mean value test are sensitive to incon-

sistent boundaries on X. Normally,

$$T = \frac{4 \, X}{\dot{X}}$$

where　　　　　T = period between positive peaks in ΔD_2

X_{max} = desired boundary on X

$\dot{X}$ = velocity along X

But if upon nearing the completion of a position cycle the pilot

reverses the motion at some ΔX short of X_{max}, the period between

positive peaks in ΔD_2 changes to T' where

$$T' = \frac{4 \, X_{max} - \Delta X}{\dot{X}}$$

In addition, ΔD_2 will fall short of its previous reference peak by $n\Delta X$.

The combined effect (ignoring changes in the phasing between ΔD_1 and

ΔD_2) is a mean value error of

$$E_{mean} = \frac{n\Delta X}{T'} = \frac{n \, \dot{X}}{\frac{4X_{max}}{\Delta X} - 1}$$

To illustrate, let

$n = 4$ (for $R = 224$ ft.)

136

$$X_{max} = \pm 3 \text{ ft.}$$

$$\Delta X = 1 \text{ ft.}$$

$$\dot{X} = 0.125 \text{ fps}$$

Then,

$$E_{mean} = 0.045 \text{ fps}$$

On the surface 0.045 fps appears small. But referring to the section on $\bar{R}$ approach sensitivity only 0.07 fps in excess of the approach asymptote at 224 feet requires 0.25 fps of braking when the station keeping range at 20 feet is reached.

Without doubt the Aft CCTV System of establishing zero range rate is superior to using the COAS. At 224 feet, for example, 0.07 fps of closing range rate causes the 14 foot LDEF target image to change approximately 0.11 degrees[1] over a 96 second interval. For an X_{max} of ± 3 feet and an $\dot{X}$ of 0.125 fps, the pilot would have to detect the 0.11 degree change in the presence of a 1.53 degree[2] peak-to-peak lateral image movement. The lateral movement would demand that the 0.11 degree change be determined by reading the edges of the image twice. Thus the 0.11 degrees would be derived from four COAS readings, each with a resolution error of less than

---

[1] $\Delta\theta = \dot{SR}\Delta t$
$$= -0.017 \ (-0.07)(96)$$
$$= 0.11 \text{ degrees}$$

[2] $1.53 \text{ deg.} = 2 \ (\frac{3}{224}) (\frac{180}{\pi})$

$$\sigma = \frac{0.11}{6} = 0.018 \text{ degrees}$$

This is obviously an unrealistic requirement to place on the pilot.

18.0 A Specific $\bar{R}$ Approach Strategy

A specific $\bar{R}$ approach strategy is best illustrated by two categories of "decision graphs".* One category covers the portion of the approach when only radar data is used; these graphs are presented in figures 18-1a through 18-1d. The second category covers the situations where range rate is permitted to decay to zero before inserting the appropriate range rate; these graphs are presented in figures 18-2a through 18-2c.

The development of the decision graphs is straightforward. For the first category

$$\text{True } \dot{R}_{max} = m \ (R_T^2 - R_S^2)^{1/2}$$

where

R_T = true range

R_S = station keeping range or 20 feet

m = slope of the hyperbolic asymptote or 1.96×10^{-3} sec^{-1} at 190 n. miles

This equation is represented by the solid line and is the allowable range rate based on perfect state knowledge. However, the pilot is reading indicated range from the radar. This can be represented by

$$R = R_T + \delta R$$

---

*The decision graphs developed in this section were not used during the PDRS III simulation runs at JSC. However, the writer believes that they reduce a description of the approach strategy to its fundamentals.

138
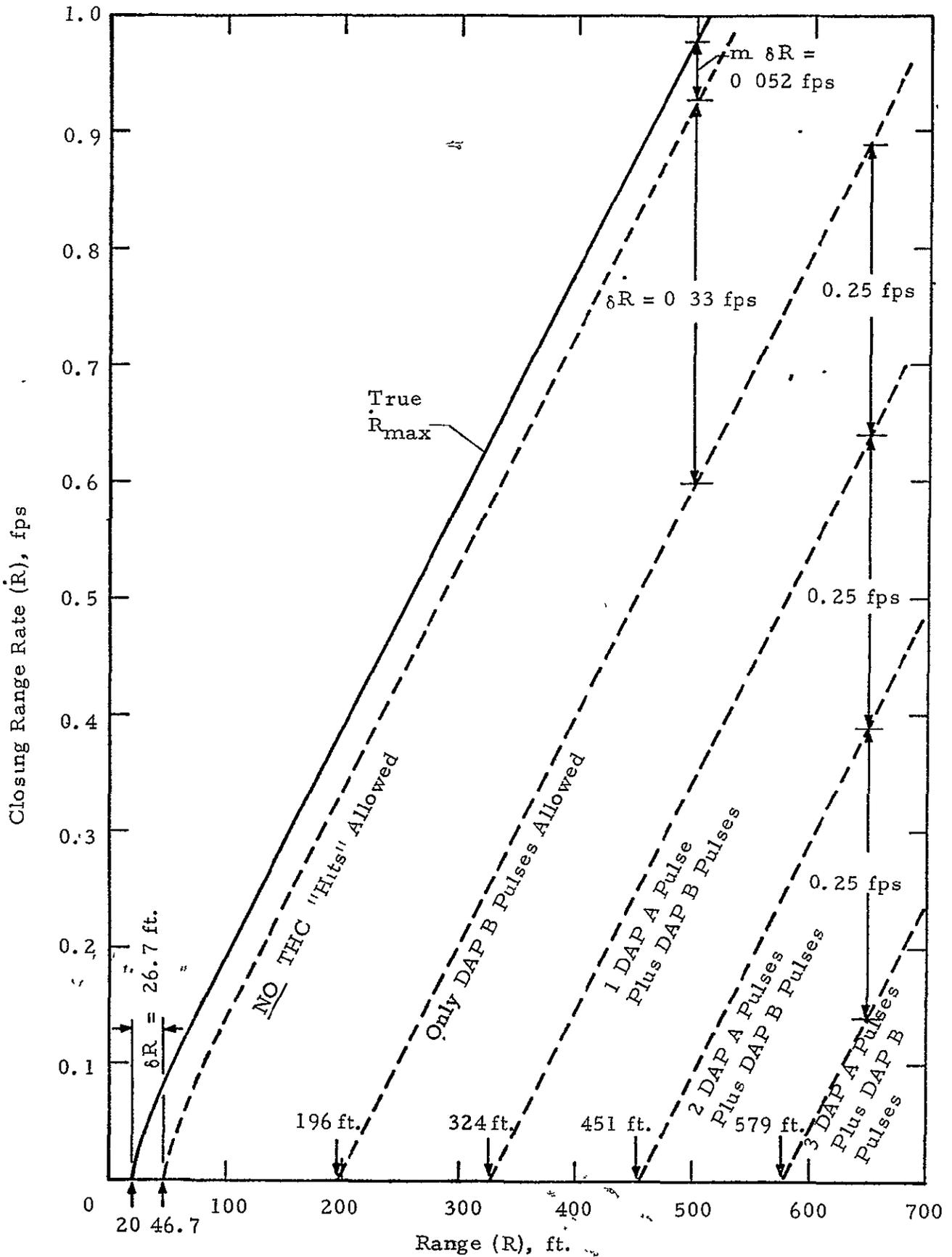
Figure 18-1a.- Burn Constraints When Utilizing Only Radar Data

139
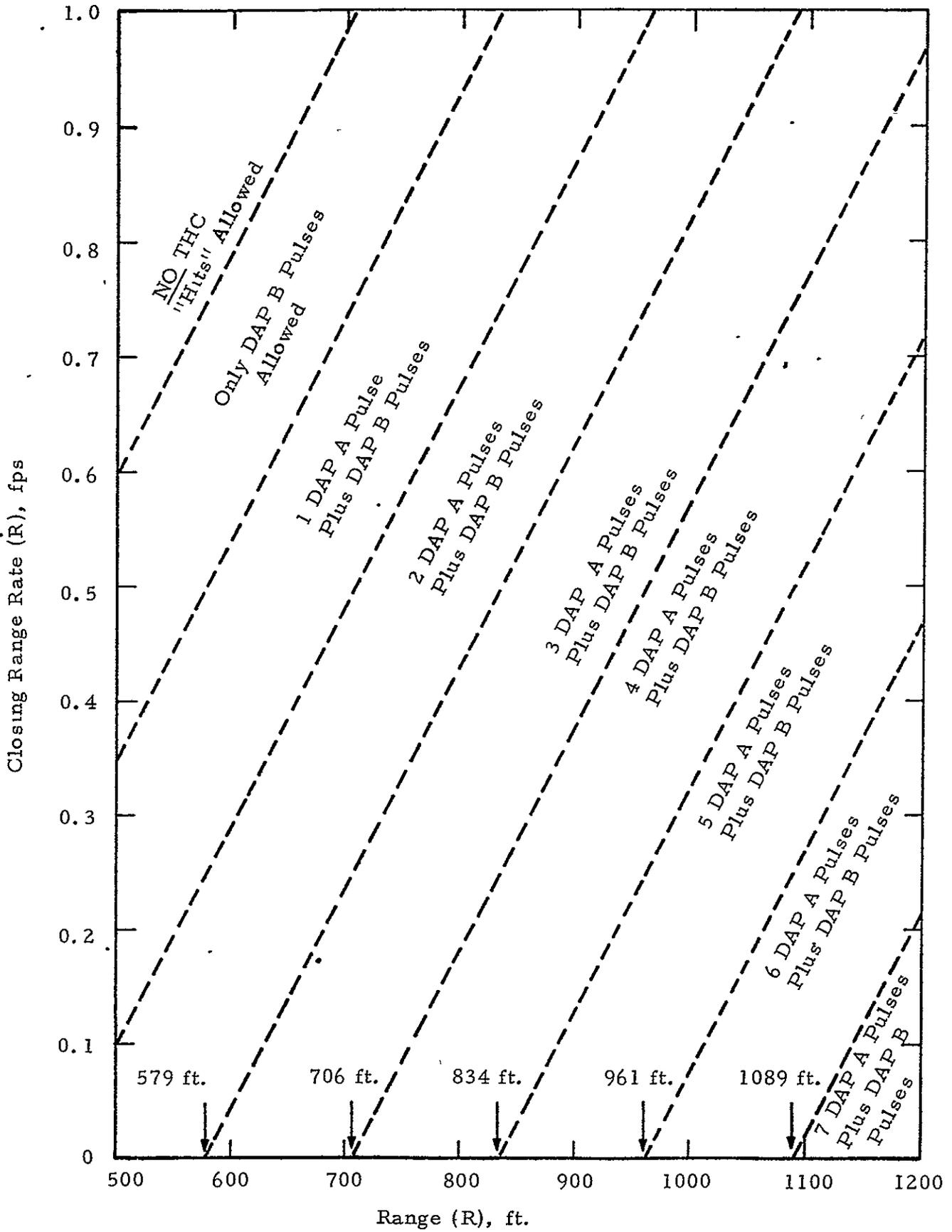
Figure 18-1b.- Burn Constraints When Utilizing Only Radar Data

140
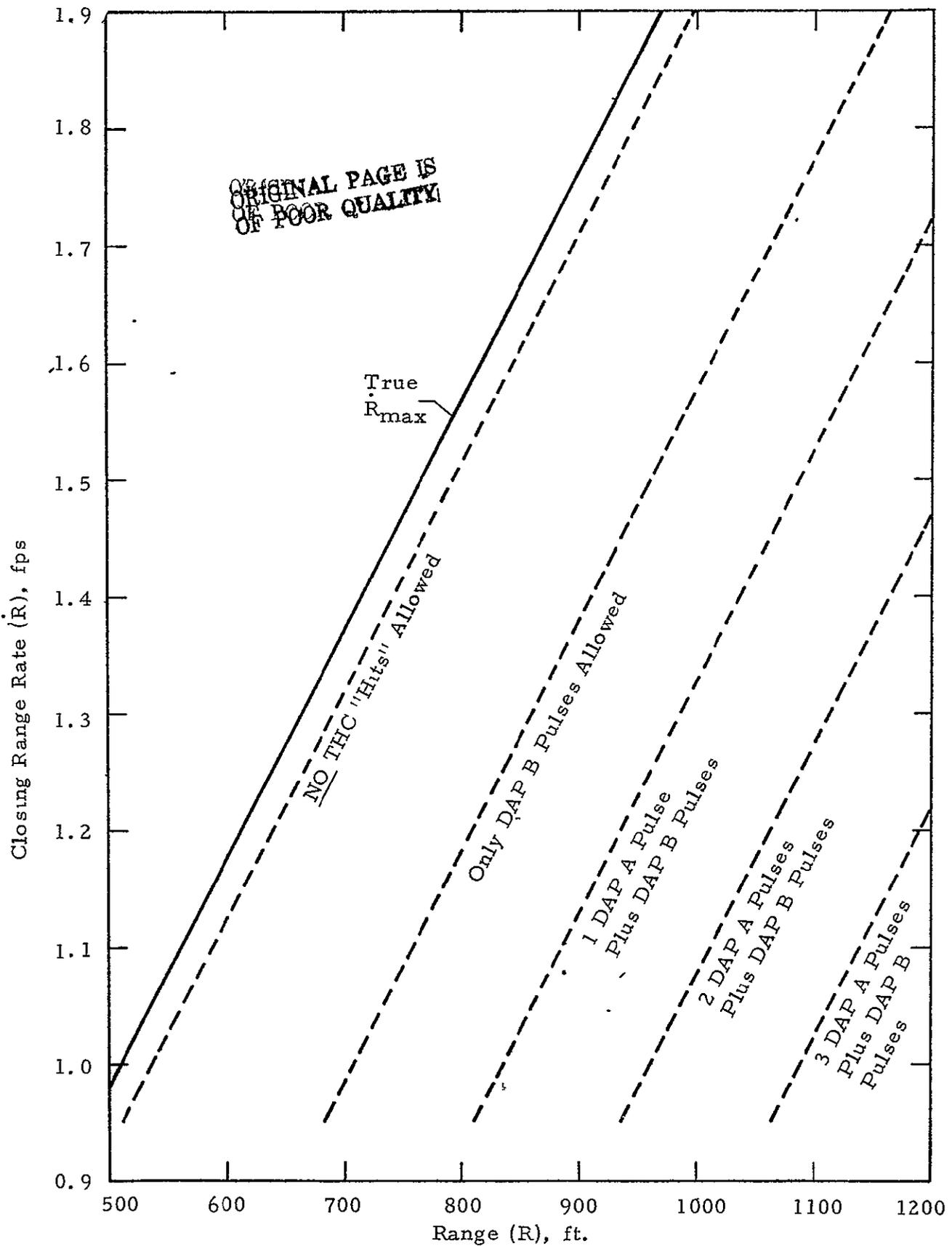
Figure 18-1c.- Burn Constraints When Utilizing Only Radar Data

141
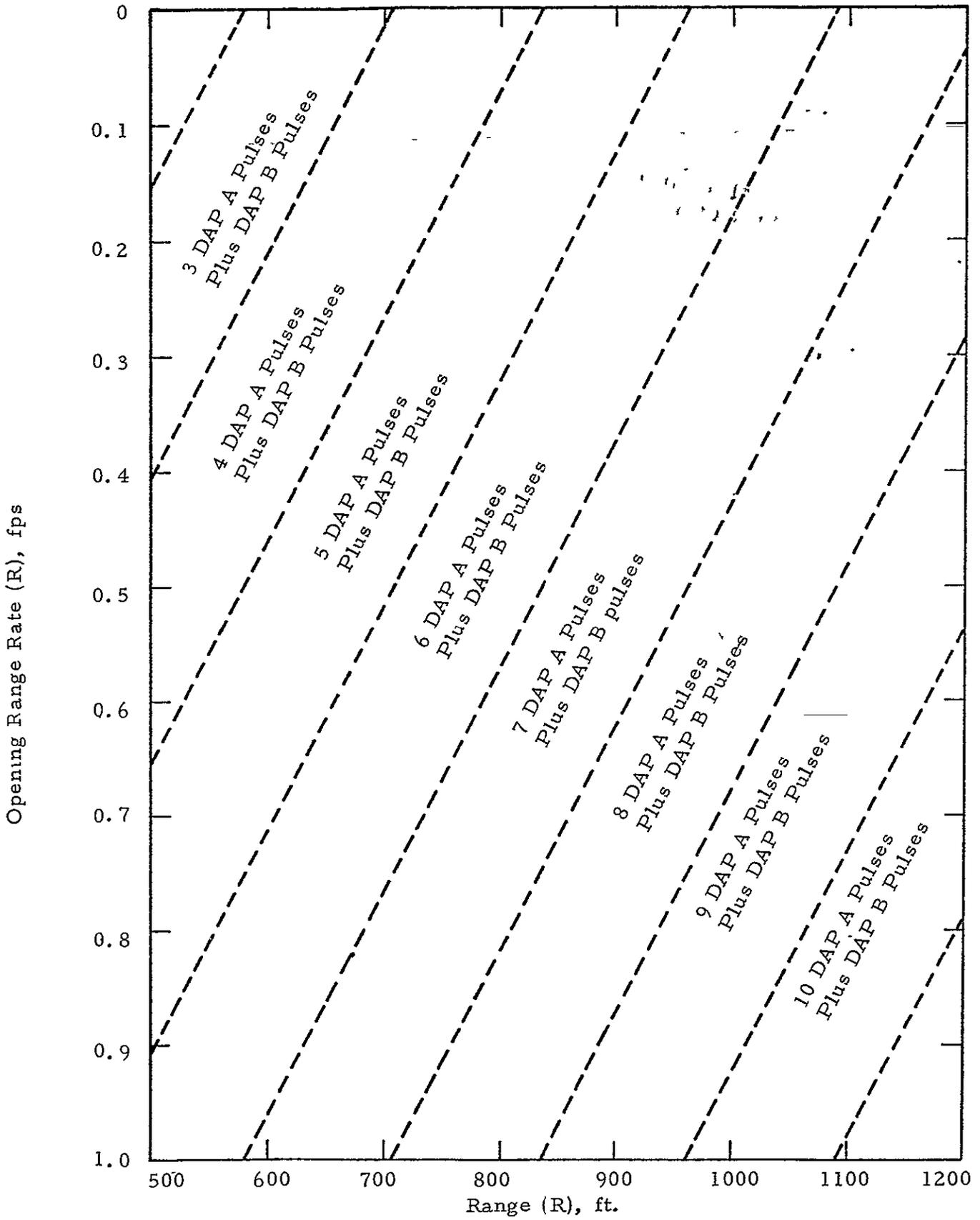
Figure 18-1d.- Burn Constraints When Utilizing Only Radar Data

where R = indicated range

δR = radar range uncertainty or $\pm \frac{80}{3}$ ft. 3σ (based on

PDRS III simulation findings)

Rearranging,

$$R_T = R - \delta R$$

Substituting this expression for R_T into $\dot{R}_{max}$ gives,

$$\dot{R}_{max} = m \left[(R - \delta R)^2 - R_S^2 \right]^{1/2}$$

Assuming that δR is always $+ 26.7$ feet, this equation is represented as

the first dashed line beneath true $\dot{R}_{max}$. Correcting further for a

possible radar range rate error, $\delta \dot{R}$, gives

$$\dot{R}_{max} = m \left[(R - \delta R)^2 - R_S^2 \right]^{1/2} + \delta \dot{R}$$

Assuming that $\delta \dot{R}$ is always -0.33 fps, the last equation is represented

by the second dashed line below true $\dot{R}_{max}$. A very conservative approach

allows no THC "hits" if the indicated range and range rate coordinates

fall above this line. In essence $\dot{R}_{max}$ has been transformed from the <u>true</u>

$\dot{R}$ versus R domain to the <u>indicated</u> $\dot{R}$ versus R domain. All subsequent

dashed lines are in increments of 0.25 fps, the equivalent of one DAP A

pulse.[1] For example, if at the start of the $\bar{R}$ approach radar indicates

an opening $\dot{R}$ of 0.20 fps and an R of 1000 feet, the pilot may introduce

7 DAP A pulses without any reasonable probability of exceeding the true

---

[1] Each increment of 0.25 fps may be subdivided into 8 DAP B pulses of 0.03
fps each. But, the scatter in range rate data makes the merits of such
subdivision questionable.

$\dot{R}_{max}$. Similarly, all subsequent burn decisions are made on the basis of where the indicated range and range rate coordinates fall on the decision graphs.

For the second category of decision graphs, the range rate is always assumed to be zero.* Thus, the allowable $\dot{R}_{max}$ is adjusted to accommodate only range uncertainty. Once again,

$$R_T = R - \delta R$$

But when the COAS is used,

$$\delta R = \left\{ \frac{-1 + (1 - \frac{R_T}{k}) \cos \psi}{1 + \frac{R_T}{k} \cos \psi} \right\} R_T$$

Substituting and solving for R_T in terms of R gives,

$$R_T = \frac{1}{(\frac{1}{R} - \frac{1}{k}) \cos \psi}$$

where $\qquad k = \frac{W}{\delta \theta} (\frac{180}{\pi})$

ψ = yaw skew angle

Therefore,

$$\dot{R}_{max} = m \left\{ \left[\frac{1}{(\frac{1}{R} - \frac{1}{k}) \cos \psi} \right]^2 - R_S^2 \right\}^{1/2}$$

---

*As stated in the preceding section, a quantitative assessment of the errors in determining zero range rate does not exist.
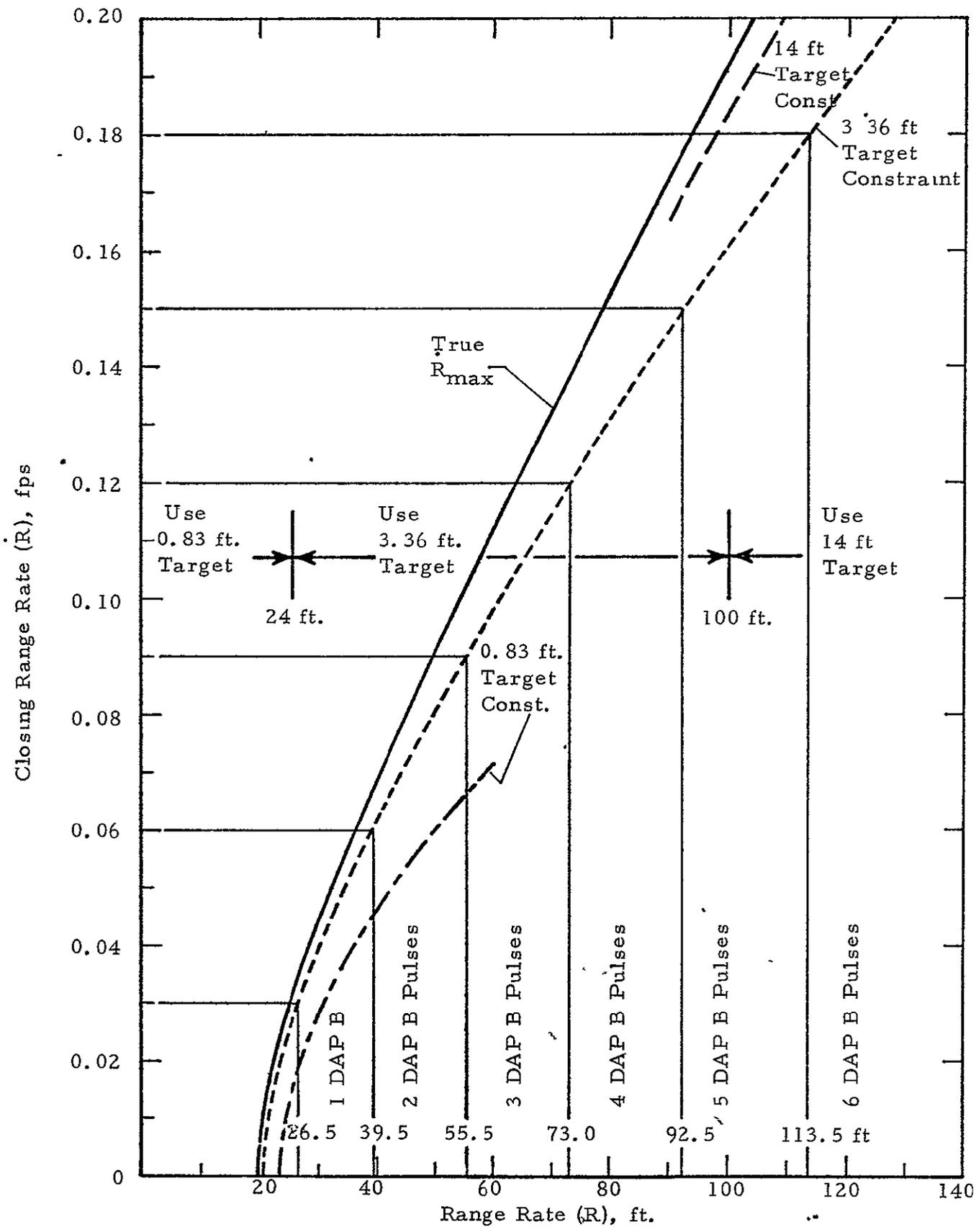
Figure 18-2a.- Burn Constraints When Range Rate is Known to be ZERO

145
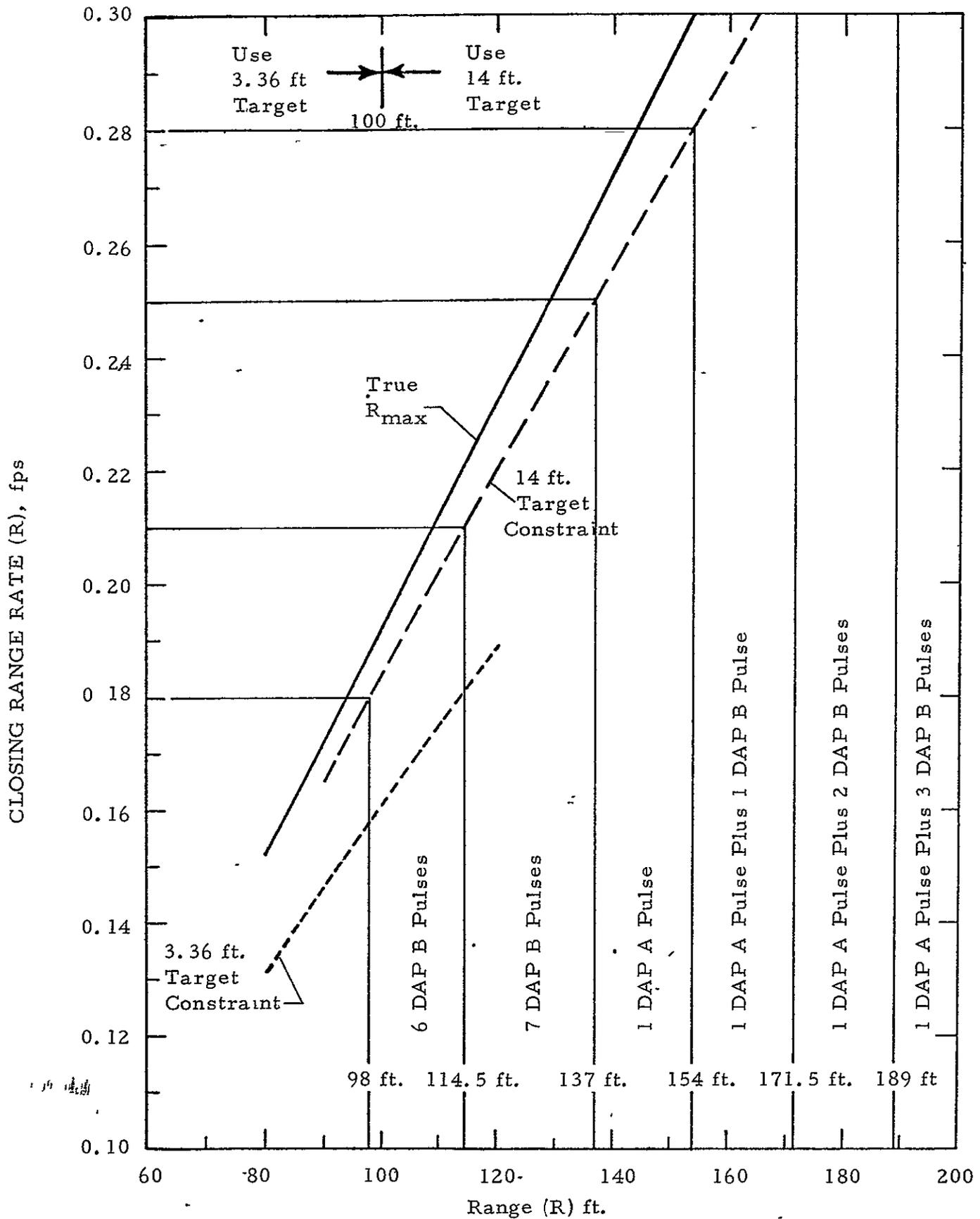
Figure 18-2b.- Burn Constraints When Range Rate is Known to be ZERO
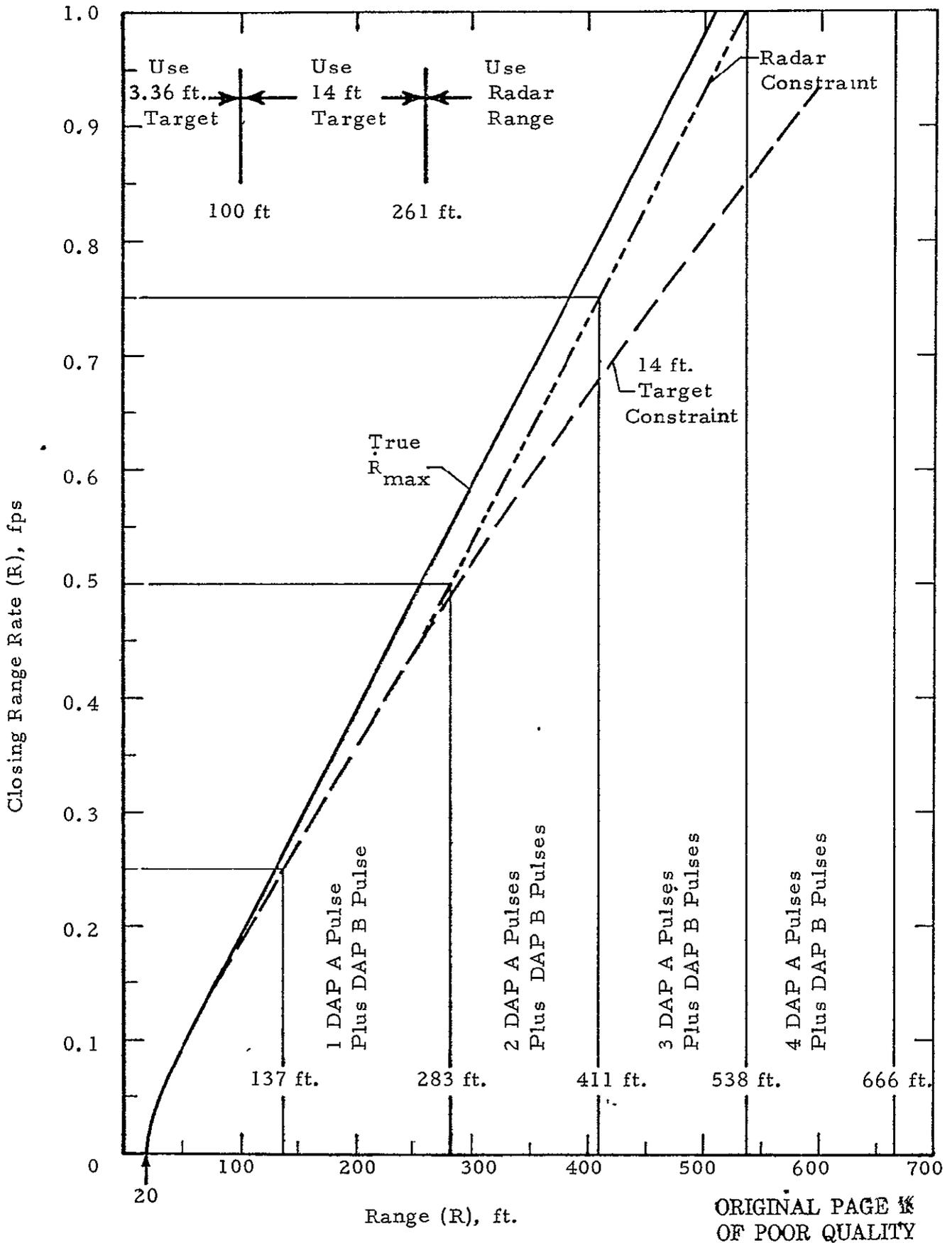
Figure 18-2c.– Burn Constraints When Range Rate is Known to be <u>ZERO</u>

147

The conservative approach assumes that the indicated range is always greater than the actual; accordingly, $\delta\theta$ is assumed to be -0.35 degrees. Figures 18-2a through 18-2c present plots of the adjusted $\dot{R}_{max}$ for each of the three targets and the radar. A yaw skew of zero degrees is assumed when using the 0.83 and 3.36 foot targets. Hand over from radar occurs ideally at 261 feet where the error associated with the 14 foot target is equivalent to the radar error. The hand over range from one target to the next is based on a θ_a (available field of view) of 8 degrees. The allowable number of THC hits at any range is determined as follows:

$$n_A = \text{number of DAP A pulses}$$
$$= \text{integral part of } \frac{\dot{R}_{max}}{0.25}$$

$$n_B = \text{number of DAP B pulses}$$
$$= \text{integral part of } \frac{R_{max} - n_A\,(0.25)}{0.03}$$

This process is graphically shown by the series of horizontal lines starting from zero in increments of 0.03 fps and then 0.25 fps. The ranges at which the horizontal lines intercept $\dot{R}_{max}$ represent points in the approach where integral numbers of DAP B and/or DAP A pulses may be introduced.

19.0 Applying the Approach Strategy - An Example

Assume that after initializing on the LDEF $\bar{R}$ the radar indications are.

Range = 1000 feet

Range Rate = 0.2 fps, opening

The decision graphs (see figure 19-1a) would allow the pilot to insert 7 DAP A pulses or a $\Delta\dot{R}$ of 1.75 fps. Because the initial radar readings would be subject to errors, the true range rate after the burn would be anywhere between 1.22 fps and 1.88 fps closing. Thus, the Orbiter could be on coasting $\bar{R}$ trajectories which, if allowed to continue, would stop anywhere from 817 feet to 163 feet from LDEF. Since the radar readings would continue to be affected by errors, it becomes apparent that the pilot's action after the first burn would have many possibilities. In order to continue illustrating the approach strategy, it is clear, therefore, that some simplifying assumption about the radar errors is required. The writer has chosen to assume that the pilot's interpretation of the radar readings reflects the actual range and range rate. The pilot, of course, would not be aware of such a situation.

Continuing with the example, the radar would indicate a range rate of 1.55 fps after the initial burn. This rate would cause the Orbiter to stop at 612 feet from LDEF. But as shown by the trajectory in figure 19-1c another DAP A pulse could be inserted at 742 feet where the range rate fell to 0.822 fps. The closing range rate would then jump to 1.072 fps and the Orbiter would be on a new trajectory which would stop at 501 feet. But when the range collapsed to 551 feet, the radar would indicate 0.448 fps and another DAP A pulse could be inserted.

This repetitive process (i.e., inserting DAP pulses, observing the trajectory on the decision graphs, and inserting additional pulses when allowed) would be continued until the desired station keeping range

149
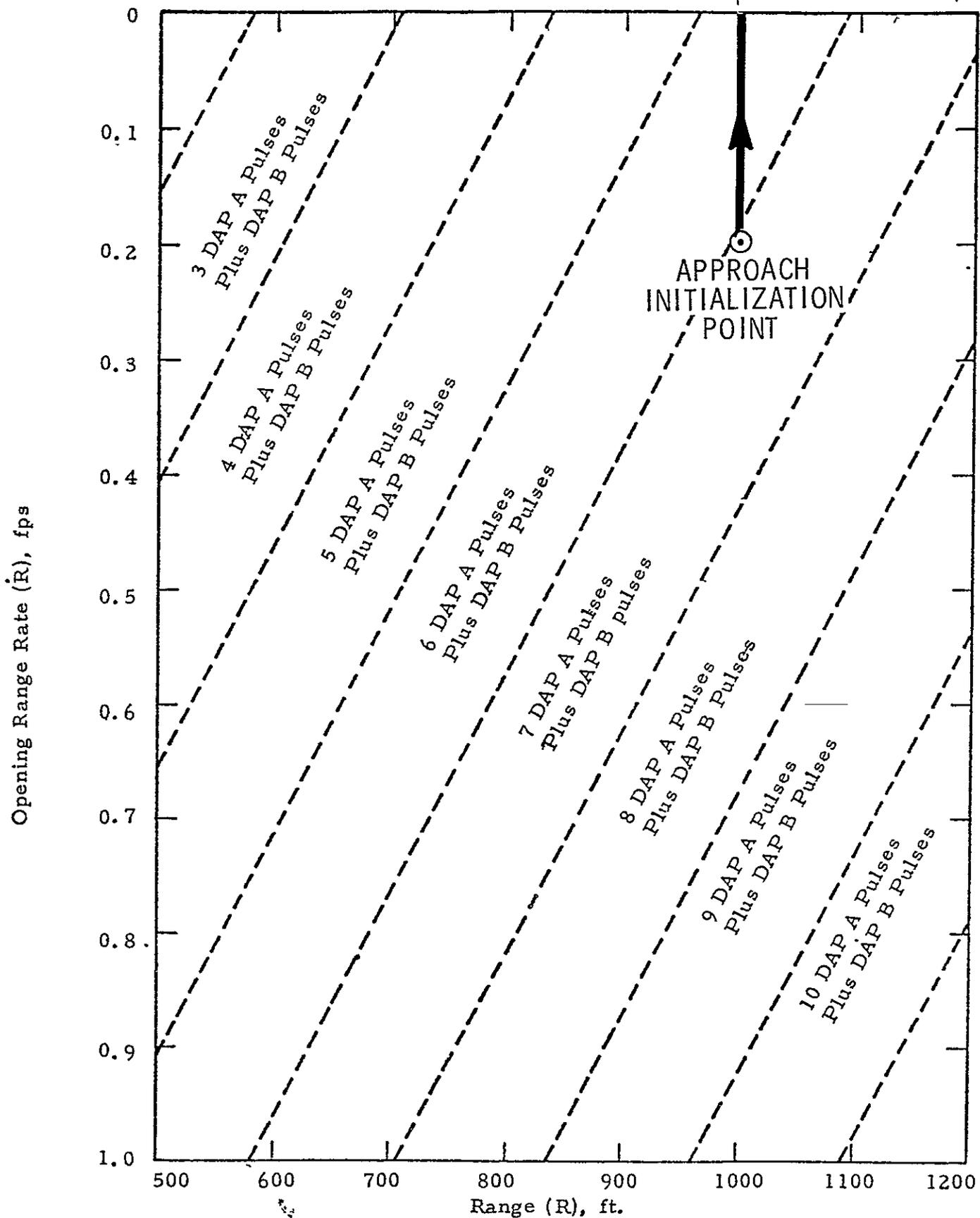
Figure 19-1a.- Plotting the Approach Example on the Decision Graphs

150
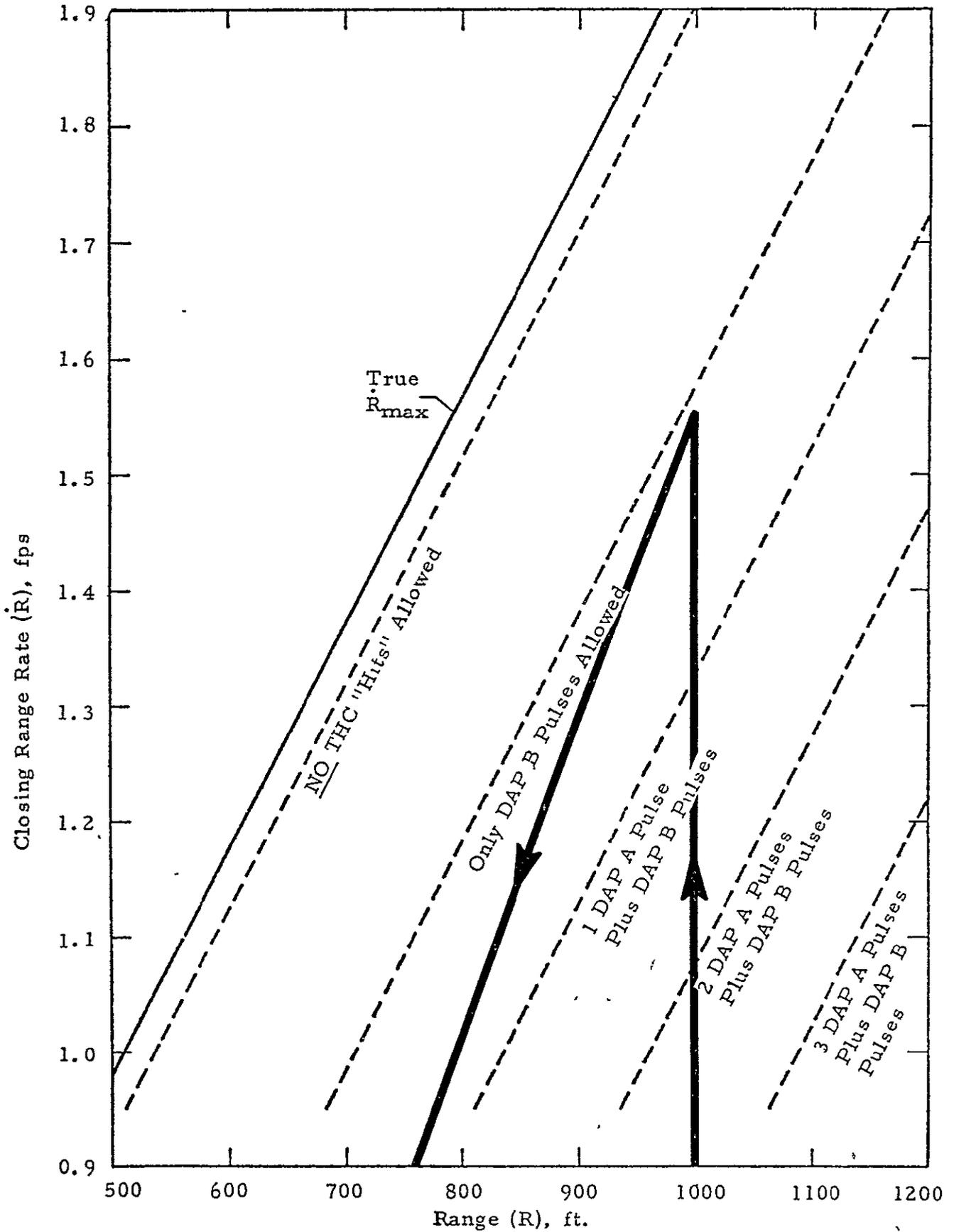
Figure 19-1b.— Plotting the Approach Example on the Decision Graphs

151
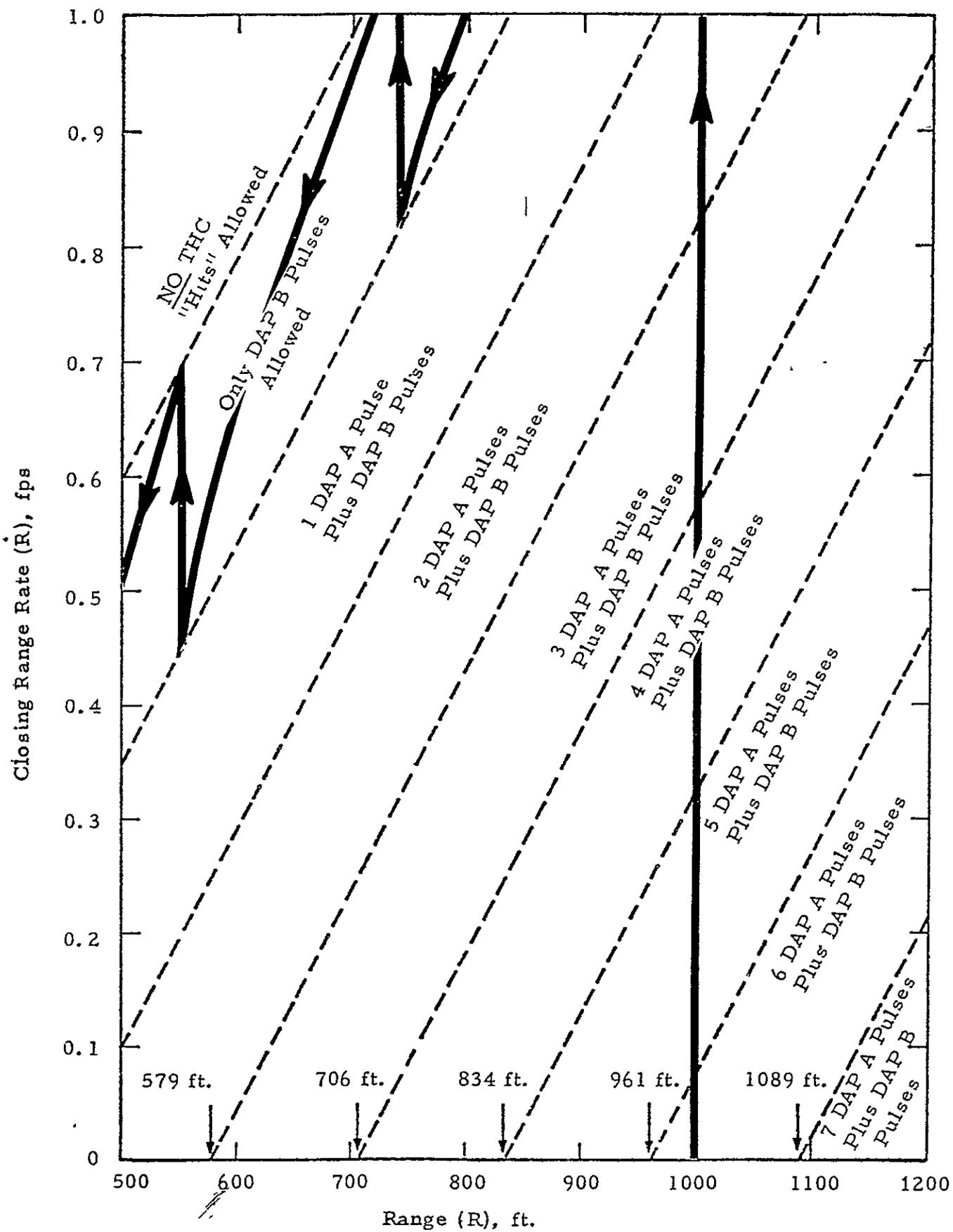
Figure 19-1c.- Plotting the Approach Example on the Decision Graphs
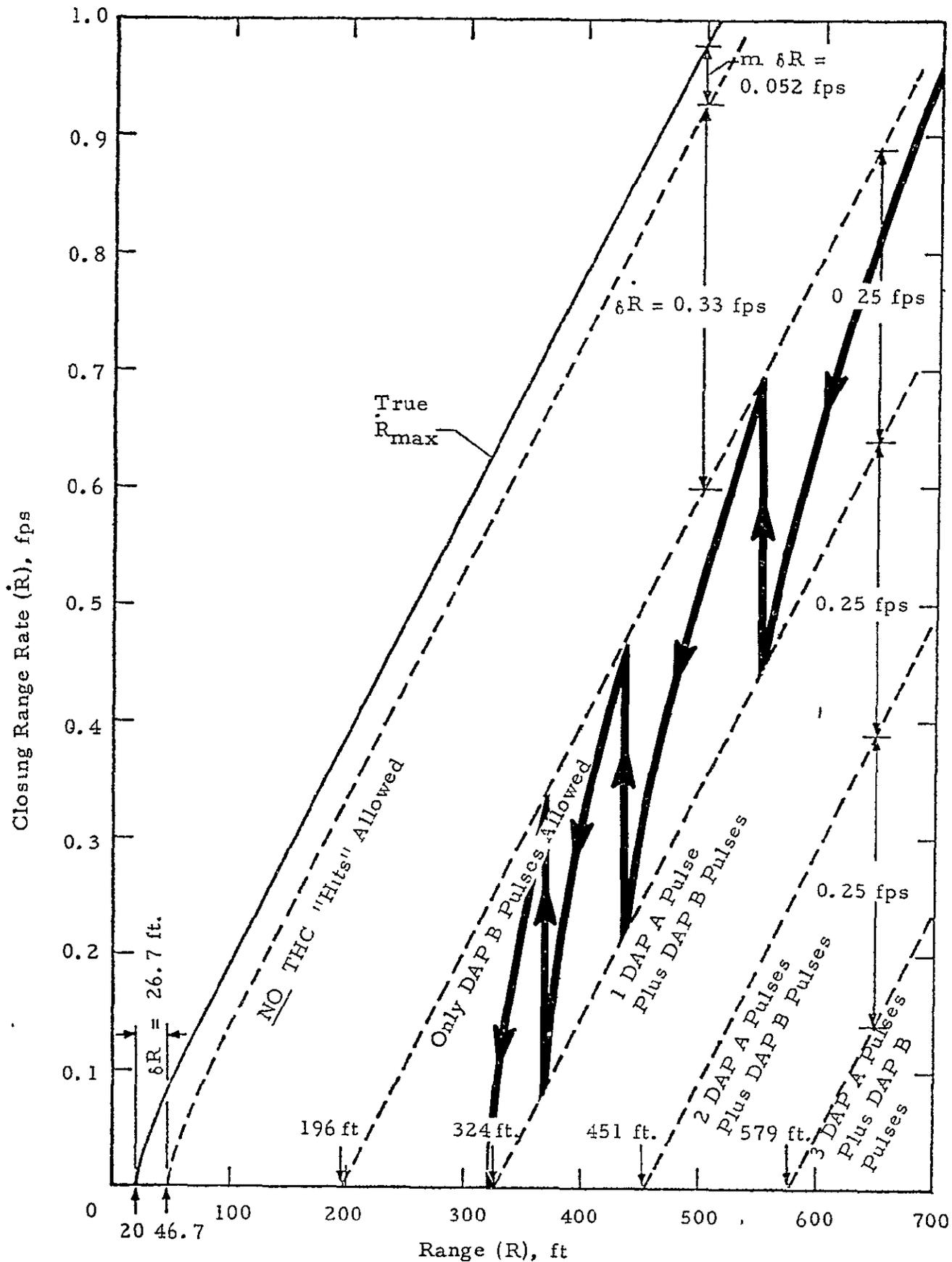
Figure 19-1d.- Plotting the Approach Example on the Decision Graphs

153
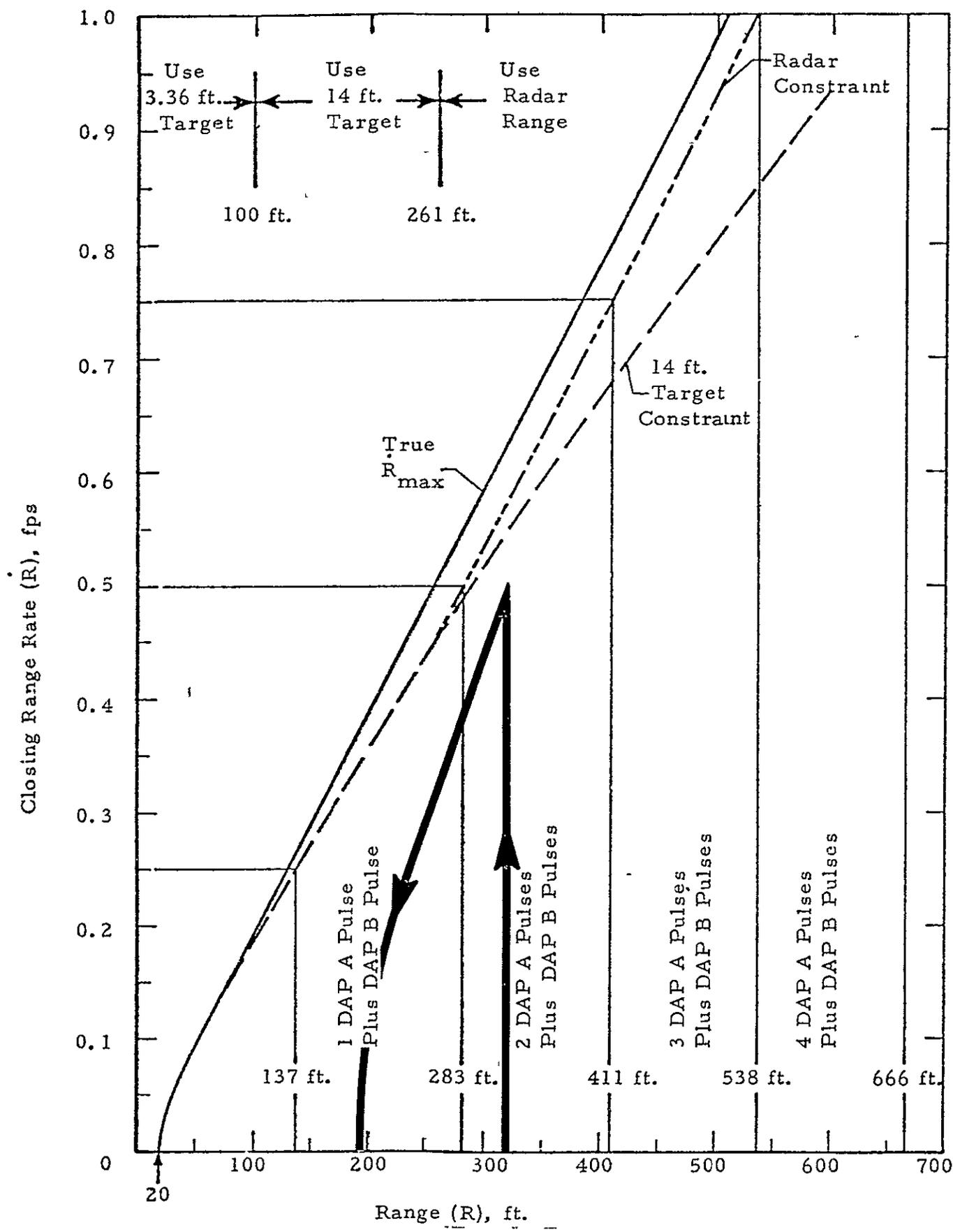
Figure 19-1e.- Plotting the Approach Example on the Decision Graphs

154
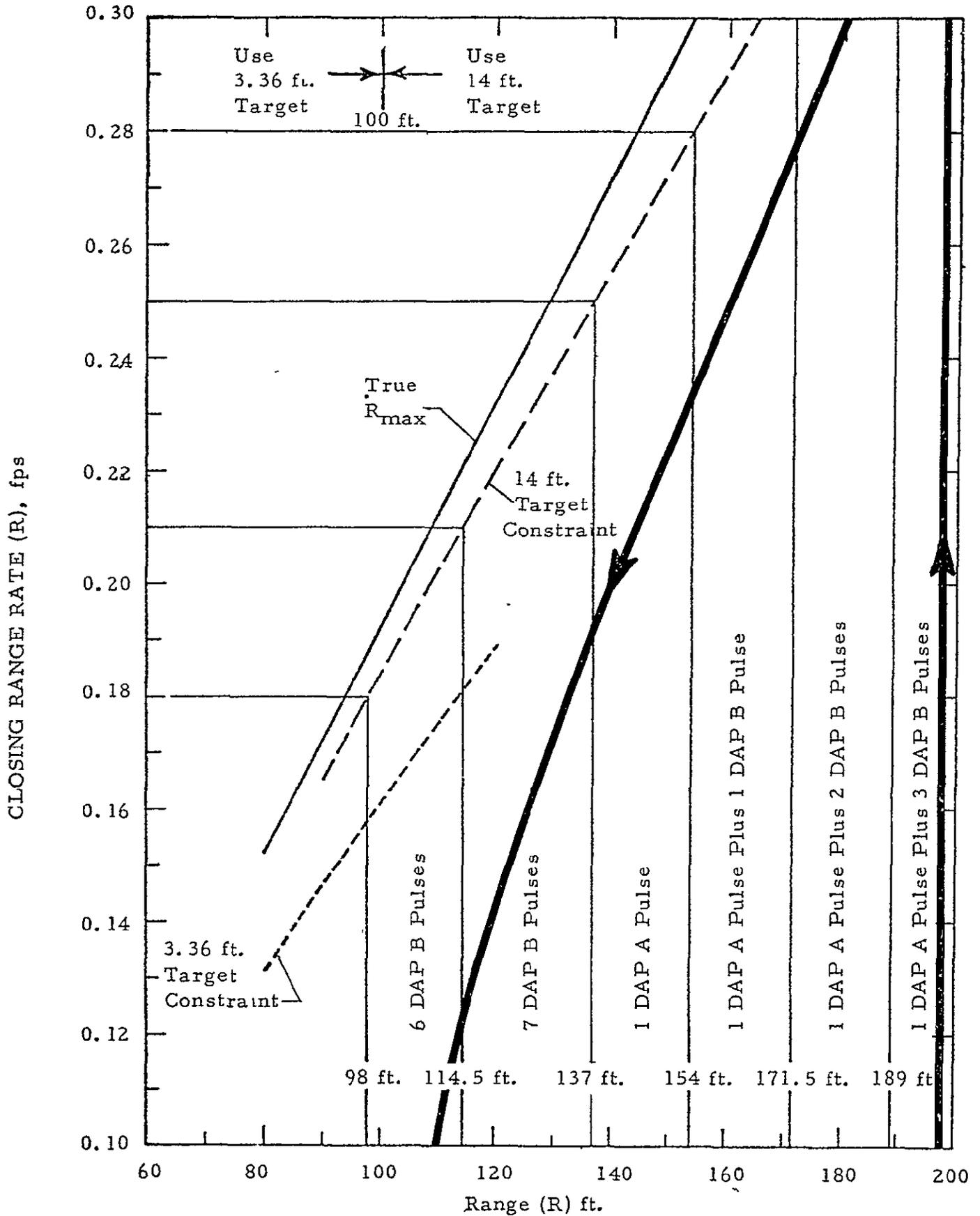
Figure 19-1f.— Plotting the Approach Example on the Decision Graphs

155
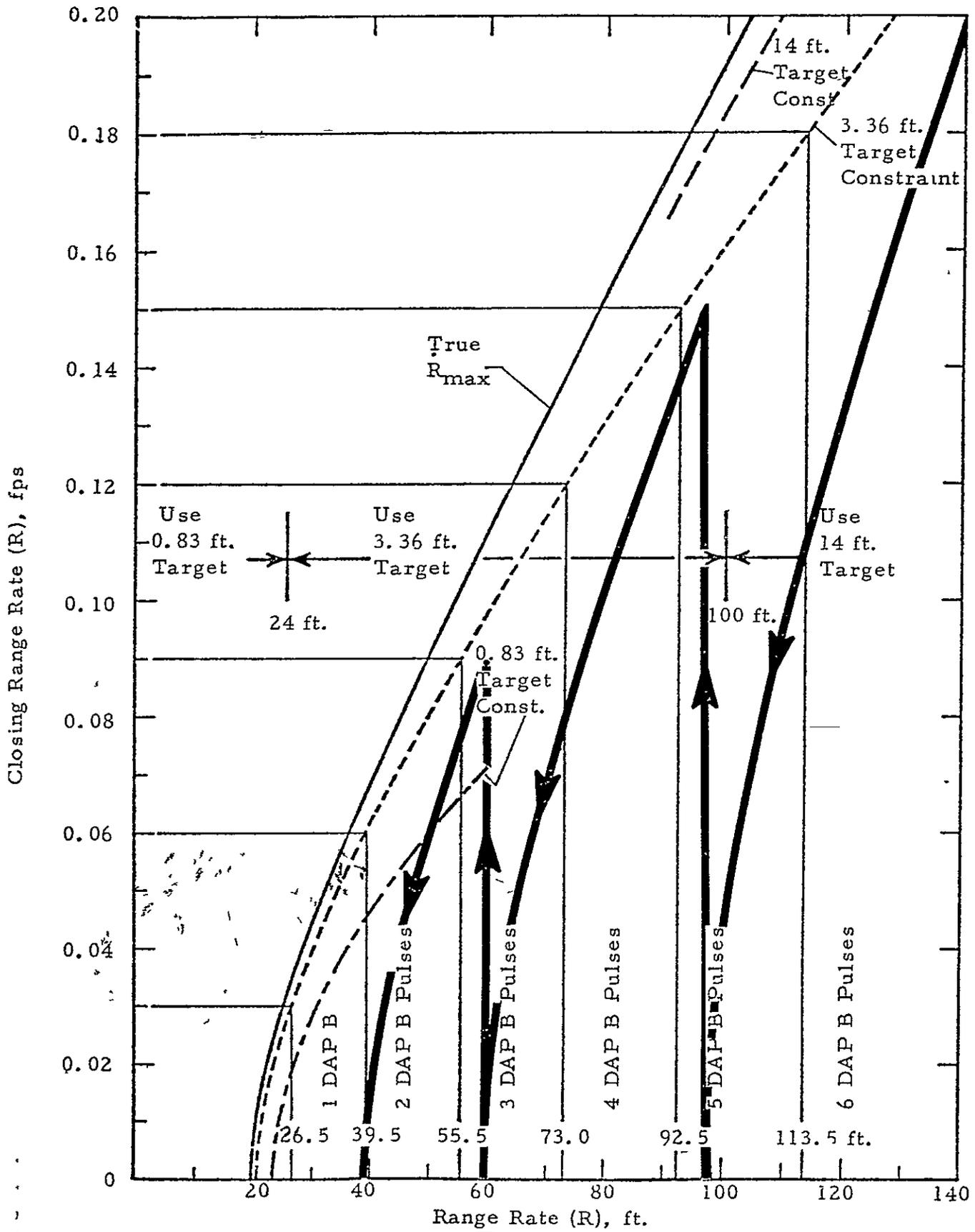
Figure 19-1g.- Plotting the Approach Example on the Decision Graphs

TABLE 19-1. An Approach Trajectory Example

Δt (sec)	t (sec)	R (ft)	$\dot{R}$ (fps)	R_S^* (ft)	ΔR (ft)
–	0	1000.0	-0.200	–	–
	0	(insert 7 DAP A pulses)			
221	0	1000.0	1.550	612.0	258
–	221	742.0	0.822	612.0	–
	221	(insert 1 DAP A pulse)			
257	221	742.0	1.072	501.4	191
–	478	551.0	0.448	501.4	–
259	478	(insert 1 DAP A pulse)			
	478	551.0	0.6980	420.4	116
–	737	435.0	0.2187	420.4	–
	737	(insert 1 DAP A pulse)			
254	737	435.0	0.4687	363.4	69
–	991	366.0	0.0858	363.4	–
	991	(insert 1 DAP A pulse)			
260					42.6
	991	366.0	0.3358	323.4	
–	1251	323.4	0	323.4	–
	1251	(insert 2 DAP A pulses)			124.6
545	1251	323.4	0.5000	198.8	
–	1796	198.8	0	198.8	–
	1796	(insert 1 DAP A + 3 DAP B pulses)			
686	1796	198.0	0.3400	97.13	101.7
–	2482	97.13	0	97.13	–
	2482	(insert 5 DAP B pulses)			
544	2482	97.13	0.1500	59.8	37.3
–	3026	59.8	0	59.8	–
	3026	(insert 3 DAP B pulses)			
519	3026	59.8	.0900	38.3	21.5
–	3545	38.3	0	38.3	–
	3545	(insert 2 DAP B pulses)			
558	3545	38.3	.06	23.1	15.2
–	4103	23.1	0	23.1	–

TOTAL TIME = 4103 seconds = 68.38 minutes

TOTAL PULSES:
14 DAP A = 3.50 fps
13 DAP B = 0.39 fps

TOTAL ΔV = 3.89 fps

ORIGINAL PAGE IS OF POOR QUALITY

*R_S is the destination of the present trajectory if $\dot{R}$ is permitted to decay to zero.

157

was achieved. The complete sequence of approach trajectories is over-layed on the decision graphs shown in figures 19-1a through 19-1g. In addition, table 19-1 lists the entire process in the time domain.

The most interesting point in the approach occurs when the radar range rate data becomes unmeaningful to burn decisions and a transition to establishing a zero range rate condition must be made. In the example this point occurred at 323.4 feet. The graphs allowed almost a whole DAP A pulse at 323.4 feet, but such action would have taken the Orbiter to only 297.2 feet before stopping – a gain of just 26.2 feet. Instead, it was assumed that a zero range rate condition could be accurately established at 323.4 feet. This assumption permitted at least two DAP A pulses (and, in addition, perhaps two DAP B pulses) to be inserted. Thus, the Orbiter moved to a range of 198.8 feet – a gain of 124.6 feet.

Was the assumption of 323.4 feet correct? Only man-in-the-loop simulations of the specific circumstances can provide an undisputable answer. Certainly the margin for error is still very small; at 323.4 feet only 0.048 fps above $\dot{R}_{max}$ will produce a braking requirement of 0.25 fps at 20 feet. If the aft CCTV is utilized,

$$n = \frac{323.4}{56} = 5.78$$

Consequently, if the mean value test is not applied, the Orbiter motion must be very quiet. Specifically,

$$\dot{X} \leq \frac{\dot{D}_1}{n} = \frac{0.048}{5.78} = 0.008 \text{ fps}$$

158

or,

$$\dot{\theta}_o \leq \frac{\dot{D}_2}{0.68 + n^2} = \frac{0.048}{34.09} = 0.001 \text{ deg/sec}$$

If the mean value test is applied, the image motion may be quite large. For example, if the pilot is holding the Orbiter within a one degree half cone angle about the LDEF $\bar{R}$,

$$\Delta D_1 = nX_{max} = 5.78 \ (323.4) \ (\frac{\pi}{180})$$

$$= \pm \ 32.6 \text{ feet}$$

Thus, the peak-to-peak amplitude of this component alone can be more than twice the length of LDEF. The remaining component, which is not controlled by the pilot, would be

$$\Delta D_2 = \theta_{o_{max}} (0.68 + n^2)$$
$$= 0.2 \ (34.09) = \pm \ 6.8 \text{ feet}$$

Unfortunately, the period of ΔD_1 becomes more and more critical at large ranges. In this case the shortest ΔD_1 period would be 180.6 seconds. If the Orbiter were released at 323.4 feet with zero initial range rate, it would fall 20.5 feet in 180.6 seconds. In other words, at large ranges Orbiter acceleration is a significant source of error[1] in the mean value test.

The change in the COAS reading is another source of information for the pilot. But the sensitivity of the 14 foot target is only 0.008 deg/ft at 323.4 feet. If 0.048 fps is the allowable error, the rate of

---

[1]This error source was previously introduced in the section entitled "Determining Range Rate with the COAS."

159

change in the COAS reading would be

$$\dot{\theta} = 0.008 \ (0.048) = 0.0004 \ deg/sec$$

Thus, ignoring the acceleration error source, the subtended angle would

change less than 0.07 degrees in 180 seconds.

The third source of information lies in the radar range indicator.

If after filtering the readouts the true 3σ uncertainty is 26.7 feet,

the 3σ error in the difference between any two readings should be 38.8

feet. Again, ignoring the acceleration error source, the derived range

rate error over 180 seconds would be 0.210 fps.

In the final analysis (and as previously stated) only man-in-the-loop

simulations can provide an undisputable answer to the assumption made

at 323.4 feet. Perhaps only one DAP A pulse would actually be inserted.

But the situation wouldn't improve much at 297 feet. Note that if the

pilot waits until he "senses" an opening rate before inserting two DAP A

pulses, the net effect could very well approach that of inserting one

pulse at zero range rate.

The total time of the approach, 4103 seconds or 68.38 minutes,

merits some discussion. For comparison, the time of an optimum approach

from 1000 feet to 23.1 feet may be computed. Referring to the section

entitled "The $\overline{R}$ Approach",

$$\frac{R}{R_o} = \frac{1000}{23.1} = 43.29$$

Thus, 4.461 time constants or 37.93 minutes is required for a perfect

approach. The difference between the optimum and actual trajectories

is, therefore, 30.45 minutes. It is convenient, for analysis purposes,

to apportion this additional time between the two phases of the approach. For the phase covering 323.4 feet into 23.1 feet,

$$\frac{R}{R_o} = \frac{323.4}{23.1} = 14$$

Therefore, 3.331 τ is optimally required over the last approach phase, and the remainder, 4.461τ - 3.331τ, or 1.130τ, is optimally required over the first phase. In tabular form, the comparisons are:

Range Interval (ft)	Duration (mins)		
	Actual	Optimal	Difference
1000 to 323.4	20.85	9.61	+11.24
323.3 to 23.1	47.55	28.32	+19.23
TOTAL	68.4	37.9	+30.5

The time differences represent the penalties for having imperfect state knowledge and for not allowing any Orbiter braking in the approach strategy.

To be sure, some payloads may be capable of withstanding some braking plume impingement, both from a dynamic viewpoint and from a contamination viewpoint. It is appropriate, therefore, to assess the benefits of some braking allowance as the station-keeping range is achieved.

In essence, any braking allowance has the effect of raising by some $\Delta \dot{R}$ the true $\dot{R}_{max}$ line on the decision graphs. This produces one or two benefits. First, if the additional $\dot{R}$ is inserted during the approach, the approach time may be reduced. Or second, if the additional $\dot{R}$ is not inserted, more margin for error will exist in the decision graphs. Clearly, either benefit is insignificant during the first phase of the

161

approach. As pointed out 0.25 fps of braking allows an additional range

rate of only 0.048 fps at 323.4 feet. And, of course, the allowance

for additional range rate diminishes with increasing range.[1]

Braking allowances become much more meaningful in the second phase

of the approach. If, for example, 0.25 fps of braking is allowed at 20

feet, $\dot{R}_{max}$ may be increased by the following amounts:

R_T (ft)[2]	$\Delta \dot{R}_{max}$ (fps)
323.4	0.048
198.8	0.074
97.1	0.125
59.8	0.163
38.3	0.194
23.1	0.228

Since a good assessment of the aft CCTV errors does not exist, it might

be argued that the additional $\dot{R}_{max}$ should be "saved" for added margin.

Unfortunately, the added margin diminishes rapidly with range while the

CCTV uncertainties grow with range. But this also implies that there

is some point where the additional $\dot{R}_{max}$ is more than adequate to protect

against the aft CCTV system errors. At that point, some or all of the

additional $\dot{R}_{max}$ may be used to reduce the approach time.

Due to the sensitivity of the $\bar{R}$ approach, any addition to $\dot{R}_{max}$

---

[1] See the section entitled "$\bar{R}$ Approach Sensitivity."

[2] The values for R_T correspond to the decision points in the example.

usually causes dramatic changes in the time domain. In the approach

example, 2307 seconds or 38.45 minutes was required to travel from

198.8 feet to the station keeping range of 23.1 feet. Suppose that the

approach strategy had allowed 0.25 fps of braking at 20 feet. Further

assume that the additional $\dot{R}_{max}$ could be fully utilized because a

perfect zero rate condition could be established at 198.8 feet. How

would the approach time change? The original decision graph (which

assumed a zero rate condition) allowed one DAP A pulse plus "3+" DAP B

pulses to be inserted for a total $\dot{R}$ of 0.34 + fps. The braking

allowance would add another 0.074 fps at 198.8 feet such that one DAP A

pulse plus 6 DAP B pulses or 0.43 fps could be inserted. Referring to

the section entitled "The $\bar{R}$ Approach,"

$$R = \frac{1}{2} (R_o + \tau \dot{R}_o) e^{t/\tau} + \frac{1}{2} (R_o - \tau \dot{R}_o) e^{-t/\tau}$$

where, in this case,

$$R_o = 198.8 \text{ ft}$$
$$\dot{R}_o = -0.43 \text{ fps}$$
$$\tau = 510.2 \text{ sec}$$

When t/τ equaled 1.259, R would equal 23.1 ft., the station keeping

range in the original example. Thus, only a single burn would be

required and the time would be cut from 38.45 minutes to only 10.71

minutes, a reduction of 27.7 minutes. The braking requirement at 23.1

feet would be opposite in sign but equal in magnitude to

$$\dot{R} = \frac{1}{2} (\frac{R_o}{\tau} + \dot{R}_o) e^{t/\tau} - (\frac{R_o}{\tau} - \dot{R}_o) e^{-t/\tau}$$

where $\qquad R_o \equiv 198.8$ ft.

$\dot{R}_o = -0.43$ fps

$\tau = 510.2$ sec

$t/\tau = 1.259$

Or, $\dot{R}$ would be -0.187 fps.[1]

In conclusion, the reader should remember that some simplifying assumptions had to be made to proceed through the $\bar{R}$ approach example. These included.

1. Ignoring Orbiter RCS interaction with the orbital mechanics forces along $\bar{R}_L$, which can corrupt the "pure" trajectories used in the example.

2. Ignoring the scatter in interpreting the radar data, which can randomly increase or decrease the progress of an approach or even eliminate (on a random basis) a messy transition point.

3. Predicting pilot response in a robot fashion, perhaps the most questionable assumption of all.

But these are the areas which should be pursued in a man-in-the-loop simulator. The purpose of this section was to bring to the desk of the reader a basic understanding of:

1. Approach strategy and tactics.

2. The significance of Orbiter state uncertainties.

3. The benefits of braking allowances.

---

[1] The braking requirement is not closer to 0.25 fps because the decision graphs are still providing margin for range measurement errors.

A by-product may be an appreciation of the pilot and co-pilot's tasks during the approach.

20.0 The Rationale for Two LDEF Grapple Fixtures and Station Keeping

   Targets

As stated previously there is some uncertainty in predicting the yaw attitude of LDEF when rendezvous operations begin. In addition, it has been pointed out that there are advantages to maintaining the Orbiter's X axis in the orbital plane during an $\bar{R}$ approach. This raises the question of how the various Orbiter/LDEF yaw attitudes are accommodated during grappling operations.

The RMS reach capability for grappling is very dependent on the relative positioning of the LDEF and Orbiter. Therefore, some early and perhaps preliminary positioning constraints have been established. These are:

   1.   The LDEF 0.83 foot target must be observable in the COAS.

        This permits the pilot to establish a desired station keeping

        range while nulling relative motion along the X and Y axes.

        The aft CCTV is used to null motion along the Z axis.

   2.   The grappling operation must be observable by both the pilot

        and RMS operator.

The 0.83 foot LDEF target has been designed to aid the pilot in

establishing the proper position. See Figure 20-1. Note that an

abbreviated target cross exists to locate the grapple fixture. If the

pilot centers the COAS cross hairs on the point representing the base

$$90° \leq \psi \leq 180°$$
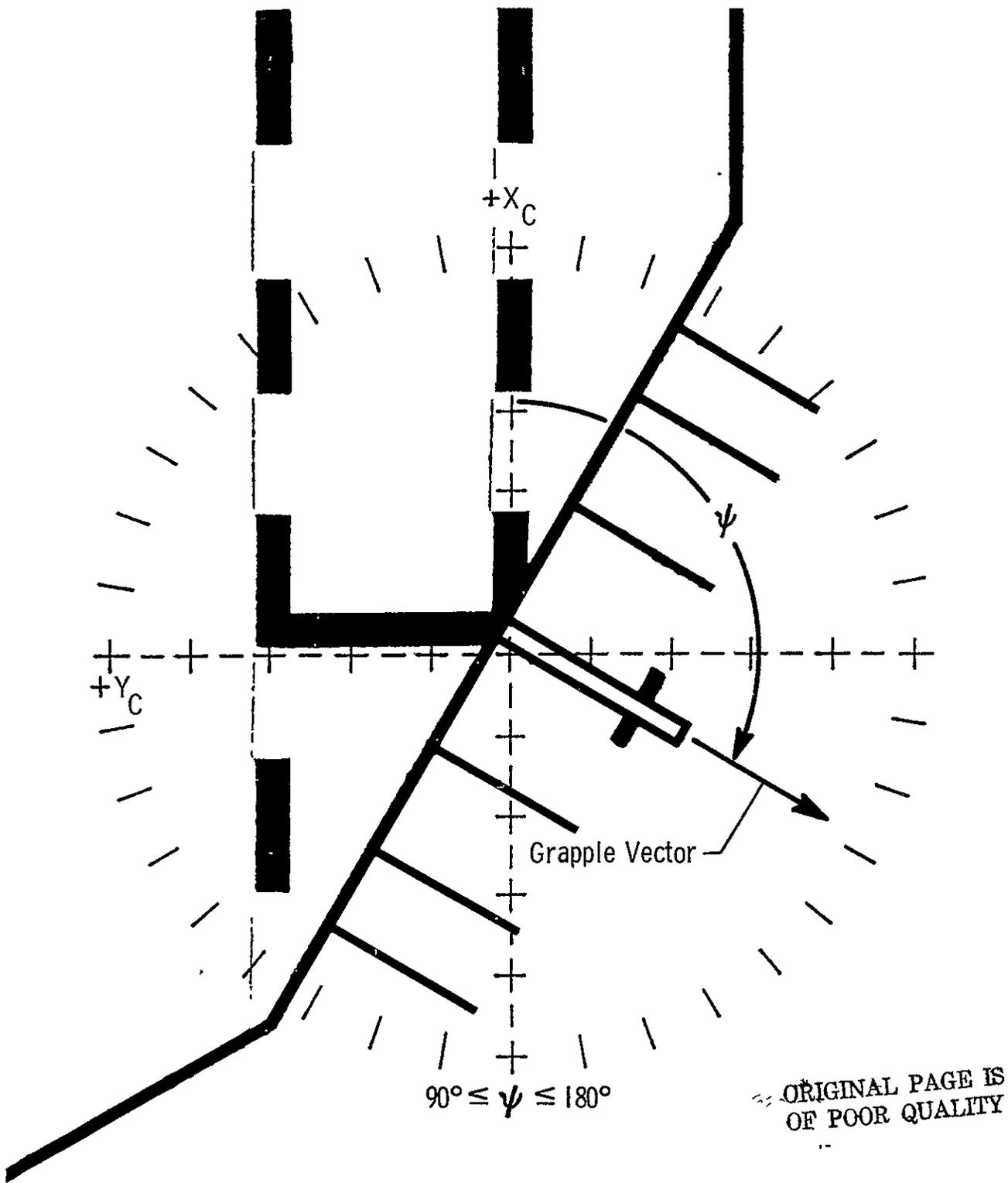
Figure 20-1.- Defining Grappling Operation Limits in the COAS

166

of the grapple, he can perform his station keeping operations while

observing the grappling operation. It will be recalled that the pilot's

view is not bounded by the COAS combining glass but by his much larger

upper window. Thus he will observe the RMS end effector's approach well

before contact with the grapple fixture.

If a port side RMS is used for grappling operations, grappling may

be accomplished if the relative yaw attitude of the Orbiter and LDEF

satisfies the following criteria:

Assume that the COAS cross hairs define a set of axis, X_C and Y_C,

which are parallel to the Orbiter's body axes X_B and Y_B, respectively.

Also define a grapple fixture vector which emanates from the

grapple's base and passes out its tip. Then grappling may be

accomplished if and only if the projection of the grapple vector

onto the X_C - Y_C plane has a positive clock angle between 90° and

180° with respect to $+X_C$ as viewed along $-Z_B$, or the COAS LOS.

If the 0.83 foot target is centered in the COAS (as shown in figure 20-1),

the yaw attitude constraint essentially means that the grapple fixture

will be observed to reside in the COAS quadrant defined by $-X_C$ and $-Y_C$.

Since the Orbiter crew has the option of initializing the $\bar{R}$

approach with the Orbiter's X axis directed along or against $\bar{V}$,

grappling may occur if the LDEF grapple vector lies in either of two

LVLH frame quadrants, specifically, that defined by $-\bar{V}$ and $-\bar{H}$ or that

defined by $+\bar{V}$ and $+\bar{H}$. To assure that this situation will always exist,

a second LDEF grapple fixture is mounted 90 degrees to the first. The

complete coverage provided by the two grapples and the Orbiter attitude
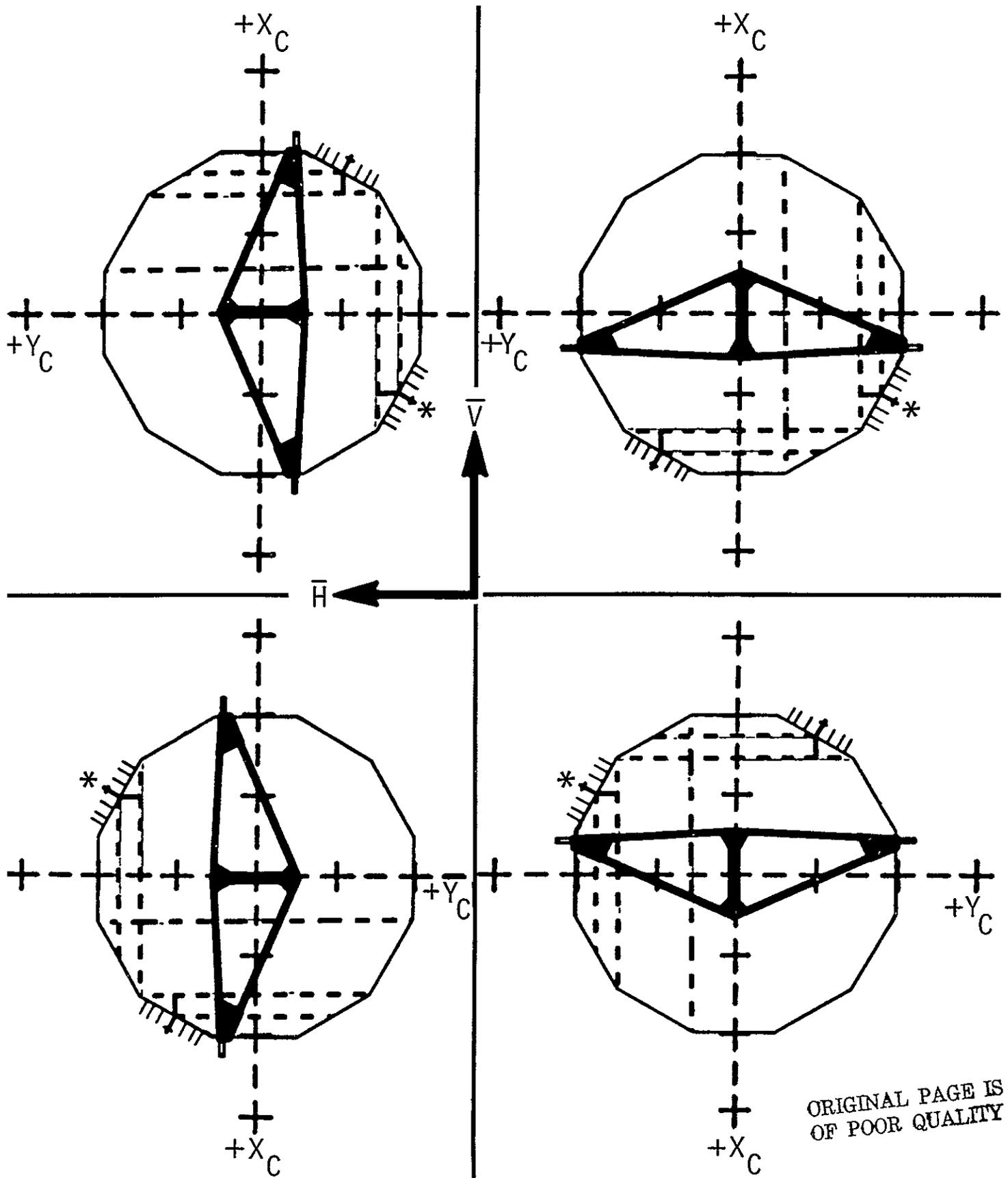
* Available Grapple

Figure 20-2. Accommodating the Various LDEF Yaw Attitudes for Grappling Operations
(All views are through the COAS)

168

attitude options is depicted in figure 20-2.

For reasons previously mentioned, a separate station keeping target is provided for each grapple. In addition, a total set of targets, approach and station keeping, are duplicated on the opposite end of LDEF to accommodate a tumbled LDEF condition.

1 Report No NASA TM-78668	2 Government Accession No	3 Recipient's Catalog No
4 Title and Subtitle AN INTRODUCTION TO SHUTTLE/LDEF RETRIEVAL OPERATIONS: THE R-BAR APPROACH OPTION		5 Report Date February 1978
		6 Performing Organization Code
7 Author(s) William M. Hall		8 Performing Organization Report No
		10 Work Unit No 750-02-01-02
9 Performing Organization Name and Address NASA Langley Research Center Hampton, VA 23665		
		11 Contract or Grant No
		13 Type of Report and Period Covered Technical Memorandum
12 Sponsoring Agency Name and Address National Aeronautics and Space Administration Washington, DC 20546		
		14 Sponsoring Agency Code

15 Supplementary Notes

The use of SI Units, as the primary unit of measurement, has been waived for this report. U.S Customary Units were used to make the principal measurements and calculations contained in this report. A table for unit conversion has been added.

16 Abstract

Simulated Orbiter direct approaches during Long Duration Exposure Facility (LDEF) retrieval operations have revealed that the resultant Orbiter jet plume fields can significantly disturb LDEF. This paper discusses one of the more promising alternate approaches being studied at the Johnson Space Center, namely, the "R-bar approach." This new approach technique utilizes orbital mechanics forces in lieu of jets to brake the final Orbiter/LDEF relative motion during the final approach.

First, the paper gives the reader a basic background in rendezvous operations from the terminal phase initiation burn through braking at some standoff distance from LDEF. The background acquaints the reader with pilot and copilot activities, the cockpit instrumentation employed, and a convenient coordinate frame for studying the relative motion between two orbiting bodies. Second, the reader is introduced to the basic equations of motion for operating on the LDEF radius vector and why orbital mechanics forces are always acting to separate the Orbiter from LDEF. The paper then concentrates on the practical considerations of implementing an R-bar approach, namely, Orbiter/LDEF relative state uncertainties and Orbiter control system limitations. Finally, a possible R-bar approach strategy is developed and used in an example.

17 Key Words (Suggested by Author(s)) Long Duration Exposure Facility (LDEF) Rendezvous Trajectory Shuttle Orbiter Retrieval R-bar approach	18 Distribution Statement Unclassified - Unlimited 16 Subject Category 31
19 Security Classif (of this report) Unclassified	20 Security Classif (of this page) Unclassified	21 No of Pages 178	22 Price* $7 50

* For sale by the National Technical Information Service Springfield Virginia 22161